

# **EVALUATION OF THE STRUCTURAL INTEGRITY OF AN AIRCRAFT LOADING WALKWAY UNDER SEVERE FUEL-SPILL FIRE CONDITIONS**

George B. Geyer

Lawrence M. Neri

Charles H. Urban



**OCTOBER 1973**

**FINAL REPORT**

Document is available to the public through  
the National Technical Information Service,  
Springfield, Virginia 22151

**Prepared for**

**DEPARTMENT OF TRANSPORTATION**

**FEDERAL AVIATION ADMINISTRATION**

**Systems Research & Development Service**

**Washington D. C., 20590**

**AIR TRANSPORT ASSOCIATION OF AMERICA**

**Washington, D.C. 20006**

FSS 000161 R



1. Report No. FAA-RD-73-144		2. Government Accession No.		3. Recipient's Catalog No.	
4. Title and Subtitle EVALUATION OF THE STRUCTURAL INTEGRITY OF AN AIRCRAFT LOADING WALKWAY UNDER SEVERE FUEL-SPILL FIRE CONDITIONS				5. Report Date October 1973	
				6. Performing Organization Code	
7. Author(s) George B. Geyer, Lawrence M. Neri, Charles H. Urban				8. Performing Organization Report No. FAA-NA-73-79	
9. Performing Organization Name and Address Federal Aviation Administration National Aviation Facilities Experimental Center Atlantic City, New Jersey 08405				10. Work Unit No. (TRAIS)	
				11. Contract or Grant No. 081-431-040	
12. Sponsoring Agency Name and Address Department of Transportation Federal Aviation Administration Systems Research and Development Service Washington, D. C. 20590				13. Type of Report and Period Covered Final December 1972-October 1973	
				14. Sponsoring Agency Code	
15. Supplementary Notes This project was a joint effort of the Federal Aviation Administration and the Air Transport Association of America, Washington, D. C. 20006.					
16. Abstract A full-scale fire test was conducted to determine the capability of an aircraft loading walkway to provide a safe emergency egress route for passengers from an aircraft when it is exposed to severe fuel-spill fire conditions in terms of structural integrity and of maintaining survivable environmental conditions within the structure. Fire exposure of the walkway indicated that the structural integrity of the walkway maintained throughout the 10 minute fire exposure period and that the most serious problem confronting passengers passing through the tunnel would be caused by smoke and the pyrolysis of the underside of the plywood flooring adjacent to the corrugated steel shell. Small-scale laboratory tests of modified floor panels indicated that by employing thermally stable load-bearing materials the quantity of pyrolysis products and smoke can be controlled within the walkway.					
17. Key Words Liquid Fuel Fires Suppression of Aircraft Fires			18. Distribution Statement Document is available to the public through the National Technical Information Service, Springfield, Virginia 22151		
19. Security Classif. (of this report) Unclassified		20. Security Classif. (of this page) Unclassified		21. No. of Pages 105	
				22. Price	



## PREFACE

This project was a joint effort of the Federal Aviation Administration (FAA) and the Air Transport Association of America (ATA). The ATA furnished the aircraft loading walkway, technical assistance, and logistic support. The FAA provided the facilities, conducted the test at the National Aviation Facilities Experimental Center (NAFEC), and prepared the report.



## TABLE OF CONTENTS

	Page
INTRODUCTION	1
Purpose	1
Background	1
DISCUSSION	1
Description of the Fire Test Bed	1
Instrumentation	2
General	2
Exterior Radiometer Locations	8
Fire Pit Thermocouple Positions	8
Exterior Steel Thermocouple Positions	8
Enclosed Airspace Thermocouple Positions	8
Interior Surface Thermocouple Positions	8
Interior Air Thermocouple Positions	8
Tunnel Overlap Thermocouple Positions	14
Smoke Evaluation Methods	14
Manikin Positions	14
Interior Radiometer Locations	14
Aluminum Panel Positions	14
Fire Test Procedure	21
Fire Test Results	21
Test Conditions	21
Fuel Flame Temperatures	21
Thermal Effects on the Walkway	25
Analysis of the Interior Smoke Data	25
Interior Radiometer Data	29
Floor Ramp Fire	29
Fire Damage to the Walls and Ceiling	29
Damage to the Service Entrance Door	34
Metallurgical Examination of the Exterior Steel Shell of the Walkway After Fire Exposure	34
Thermal Effects on the Aluminum Panels	37
Small-Scale Panel Tests	37
Test No. 1 - Sidewall Panel	37
Test No. 2 - Floor Panel Sections	41
Test No. 3 - Flexible Closure Canopy	41
Floor Structure Modifications	46
SUMMARY OF RESULTS	53
CONCLUSIONS	55
RECOMMENDATIONS	56
REFERENCES	57

## TABLE OF CONTENTS (continued)

### APPENDICES

- A - Ancillary Construction Components of the Aircraft  
Loading Walkway
- B - Instrumentation Thermocouple Positions of the Aircraft  
Loading Walkway
- C - Time-Temperature Thermocouple Profiles
- D - Metallurgical Examination of the Aircraft Loading  
Walkway Material
- E - Small-Scale Fire Tests on Aircraft Loading Walkway  
Panel Sections
- F - Modified Floor Panel Configurations and Fire Test Results

## LIST OF ILLUSTRATIONS

Figure		Page
1	Plan View of the Fire Test Bed (Not to Scale)	3
2	Elevation View of the Aircraft Loading Walkway, Fuselage Section, and Fire Pit (Not to Scale)	4
3	Portable Blowers Showing the Installation of the Insulated Air Conduits and Instrumentation Cable	5
4	Exterior View of the Fuselage Section With the Passenger Loading Walkway in Position and the Radiometer and Thermocouple Locations	6
5	Floor Loading Plan of the Aircraft Loading Walkway	7
6	Elevation View of the Aircraft Loading Walkway Showing the Location of the Instrumentation Positions	9
7	Typical Thermocouple Installation on the Inside of the Exterior Metal Wall Surfaces	10
8	Typical Thermocouple Installation on the Interior Metal and Plywood Floor Decking	11
9	Typical Thermocouple Installation on the Surface of the Plywood Flooring	12
10	Typical Installation Showing a Thermocouple Embedded in the Carpet Over the Configuration Shown in Figure 9	13
11	Aircraft Loading Walkway Thermocouple Positions Within the Overlapping Section Between Tunnels B and C	15
12	Optical Array of "Exit" Signs and Clock for Estimating the Visual Obscuration Times by Smoke and Organic Pyrolysis Products	16
13	Interior Floodlight and Camera Positions	17
14	Photometric Smoke Density Meter Installation	18
15	Instrumented Manikin Showing Several Air Thermocouple Locations	19
16	Position of the Aluminum Panel on the Fuselage Section Relative to the Fire Pit and Loading Walkway	20

# LIST OF ILLUSTRATIONS (continued)

Figure		Page
17	Typical Free-Burning Pool-Fire Conditions	22
18	Critical Phases During the Firefighting Operation	23
19	Exterior Radiometer Profiles Showing Heat Flux as a Function of Time After Fuel Ignition	24
20	Summary of the Time-Temperature Data Obtained for the Aircraft Loading Walkway During Fire Exposure	26
21	Obscuration of the Walkway Interior by Pyrolysis Products and Smoke	28
22	Walkway Interior Heat Flux as a Function of Time After Fuel Ignition	30
23	Effects of Fire in the Floor Ramp Section Between Tunnels B and C	31
24	Cross Section Through Tunnels B and C Indicating the Effects of Fire Exposure on the Weather Stripping	32
25	Ceiling and Wall Fire Damage in Tunnel C	33
26	"Exit" Sign Array Showing Evidence of Smoke Penetration and Discoloration	35
27	Visual Condition of the Manikins After Fire Exposure of the Walkway	36
28	The Effects of Flame Impingement on The Aluminum Panels	38
29	Thermal Effects on a Representative Wall Panel Section Where the Corrugated Metal and Asbestos-Cement Board are Separated by an Airspace	39
30	Smoke Generated From a Wall Panel Section as a Function of Fire Exposure Time	40
31	Thermal Effects on a Representative Walkway Floor Panel Where the Corrugated Metal and Plywood are Adjacent to One Another	42



# LIST OF ILLUSTRATIONS (continued)

Figure		Page
32	Thermal Effects on a Representative Walkway Floor Panel Where the Corrugated Metal and Plywood Flooring are Separated by an Airspace	43
33	Charring of the Plywood Flooring Separated From the Corrugated Metal by an Airspace	44
34	Flexible Walkway Closure Canopy Before Flame Exposure	45
35	Thermal Effects on the Walkway Closure Canopy as a Function of Fire Exposure Time	47
36	Damage to the Walkway Closure Canopy Caused by Fire Exposure	48
37	Exterior Configuration of the Modified Floor Test Panels	49
38	Typical Thermal and Structural Damage to the Asbestos-Cement Board Modified Floor Panels	50
39	Summary of the Smoke Data for the Modified Floor Sample Configurations	52
B-1	Aircraft Loading Walkway Thermocouple Positions at Station W	B-1
B-2	Aircraft Loading Walkway Thermocouple Positions at Station X	B-2
B-3	Aircraft Loading Walkway Thermocouple Positions at Station Y and Y'	B-3
B-4	Aircraft Loading Walkway Thermocouple Positions at Station Z	B-4
C-1	Fire Pit Flame Temperatures as a Function of Time After Fuel Ignition	C-1
C-2	Internal Wall Surface Temperature as a Function of Time After Fuel Ignition	C-2

# LIST OF ILLUSTRATIONS (continued)

Figure		Page
C-3	Temperature on the Left Side Exterior Metal Surface of the Aircraft Loading Walkway	C-3
C-4	Enclosed Floor and Wall Airspace Temperatures of the Aircraft Loading Walkway	C-4
C-5	Interior Air Temperature as a Function of Time After Fuel Ignition	C-5
C-6	Exterior Metal Floor Temperature as a Function of Time After Fuel Ignition	C-6
C-7	Internal Wood and Carpet Floor Temperatures	C-7
C-8	Temperature on the Right Side Exterior Metal Surface of the Aircraft Loading Walkway	C-8
C-9	Air Temperature as a Function of Time After Fuel Ignition in the Overlap Section Between Tunnels B and C	C-9
D-1	Average Mechanical Properties of the Corrugated Steel as Functions of Temperature	D-5
D-2	Tensile Strength of Welded Seams as a Function of Temperature	D-6
E-1	Fire Test Setup for Evaluation of Aircraft Loading Walkway Panels	E-2
F-1	Test 1 - Floor Panel Configuration and Thermal Profiles	F-1
F-2	Test 2 - Floor Panel Configuration and Thermal Profiles	F-2
F-3	Test 3 - Floor Panel Configuration and Thermal Profiles	F-3
F-4	Test 4 - Floor Panel Configuration and Thermal Profiles	F-4

# LIST OF TABLES

Table		Page
1	Visual Obscuration of the "Exit" Sign Array by Smoke	27
2	Visual Obscuration of the Manikins by Smoke	29
D-1	Corrugated Sheet Metal Mechanical Tests	D-3
D-2	Corrugated Sheet Metal Welds	D-4
D-3	Steel Structural Members	D-4
D-4	Tunnel B, Mechanical Properties of the Corrugated Steel (Right Side)	D-7
D-5	Tunnel B, Mechanical Properties of the Corrugated Steel (Left Side)	D-7
D-6	Tunnel B, Mechanical Properties of the Corrugated Steel (Bottom)	D-8
D-7	Tunnel C, Mechanical Properties of the Corrugated Steel (Right Side)	D-8
D-8	Tunnel C, Mechanical Properties of the Corrugated Steel (Left Side)	D-9
D-9	Tunnel C, Mechanical Properties of the Corrugated Steel (Bottom)	D-9
D-10	Tunnel C, Mechanical Properties of the Corrugated Steel (Right Side)	D-10
D-11	Tunnel C, Mechanical Properties of the Corrugated Steel (Left Side)	D-10
D-12	Tunnel C, Mechanical Properties of the Corrugated Steel (Bottom)	D-11
D-13	Tunnel C, Mechanical Properties of the Corrugated Steel (Right Side)	D-11
D-14	Tunnel C, Mechanical Properties of the Corrugated Steel (Left Side)	D-12
D-15	Tunnel C, Mechanical Properties of the Corrugated Steel (Bottom)	D-12

LIST OF TABLES (continued)

Table		Page
D-16	Tunnel C, Mechanical Properties of the Corrugated Steel (Structural Members)	D-13

## INTRODUCTION

### PURPOSE.

The objective of this effort was to determine the capability of an aircraft loading walkway to provide a safe emergency egress route for passengers from an aircraft when it is exposed to severe fuel-spill fire conditions in terms of structural integrity and of maintaining human survivable environmental conditions within the structure.

### BACKGROUND.

According to the National Fire Protection Association (Reference 1) the current construction of aircraft loading walkways consists basically of a fully enclosed steel-shelled tunnel with no windows other than those essential for operator vision and a minimum number of other openings such as joints and diaphragms. The flexible closures and diaphragms are designed to minimize the entrance of air, smoke, and heat from the exterior. The primary load-bearing structural elements are fabricated of steel.

Interior surfaces of floors, roof, and walls are constructed of noncombustible materials. When in use, walkway interiors are maintained at a low positive pressure with the source of pressurizing air from either the interior of the terminal building or from another area which would normally be a source of uncontaminated air during a ramp or aircraft fire emergency.

Based upon the best available data, each aircraft loading walkway is designed to provide a safe fire egress route from aircraft for a minimum of 5 minutes (Reference 1) under severe fire exposure conditions. However, to date, design data for aircraft loading walkway structures has been based primarily upon information developed from the performance of small unit components of structure. Therefore, this task was designed to provide information which would bridge the gap between the theoretical survival time of the walkway based upon small unit tests and the full-scale structure exposed to severe free-burning pool-fire conditions.

## DISCUSSION

### DESCRIPTION OF THE FIRE TEST BED.

The fire test bed comprised a 40-foot cabin section of a four-engine commercial jet aircraft and an aircraft loading walkway positioned over a fire pit. The aircraft section was completely covered externally with an 0.5-inch-thick layer of ceramic fiber insulation over which was bolted sheets of 0.031-inch-thick, type-304 stainless steel. This configuration was employed to protect the fuselage from destruction during the prolonged fire-exposure period. The aircraft loading walkway was positioned on the upwind side in the approximate

center and at right angles to the stainless-steel-covered fuselage section at an elevation of 7 feet above the surface of a simulated fuel spill and the closure made in the usual way. The opposite end of the extended walkway was elevated 10 feet above ground level to duplicate the height at the entrance to a terminal building.

A plan of the fire test facility is presented in Figure 1 and an elevation view of the aircraft loading walkway, fuselage section, and fire pit are shown in Figure 2.

The walkway consisted of a terminal entrance (Tunnel A) designed for rigid attachment to a finger or an airport terminal building and two telescoping steel sections (Tunnels B and C). A rubber composition gasket material was provided around the telescoping end of Tunnel C which acted as weather stripping or seal between the two tunnel sections. The exterior shell of the walkway was fabricated of 16-gauge corrugated steel and all of the glass in the windows (Reference 1) had been removed and steel plates welded over the openings. A description of the ancillary materials employed in the fabrication of the walkway is given in Appendix A.

The interior of the walkway was maintained at very low positive pressure by providing 1,500 cubic feet per minute of approximately 70°F air delivered through flexible conduits from two blowers discharging at ceiling level through baffles positioned in the terminal end of the walkway. The two 750 cubic-feet-per-minute portable blowers and the asbestos insulated conduits are shown in Figure 3.

Figure 4 shows the position of the fuselage section and the aircraft loading walkway relative to the fire pit location. The walkway is shown supported by two insulated steel structures forming a predetermined angle with the fuselage section. The four steel window closures on the right side of the walkway, and the main instrumentation trunk line emerging from the rear of the walkway at floor level are also visible.

A static floor loading of 40 pounds-per-square foot was provided by distributing a layer of 32-pound Waylite blocks and 5-pound fire bricks uniformly over the entire floor area of Tunnels B and C. The floor dimensions and loading pattern are indicated schematically in Figure 5.

#### INSTRUMENTATION.

GENERAL. The thermal effects of the fire on the walkway were determined principally by means of thermocouples located strategically on and within the structure. Additional instrumentation and tests included internal and external radiometers, smoke meters, instrumentation cameras, and a physical metallurgical analysis of steel samples taken from the exterior metal surfaces after fire exposure.

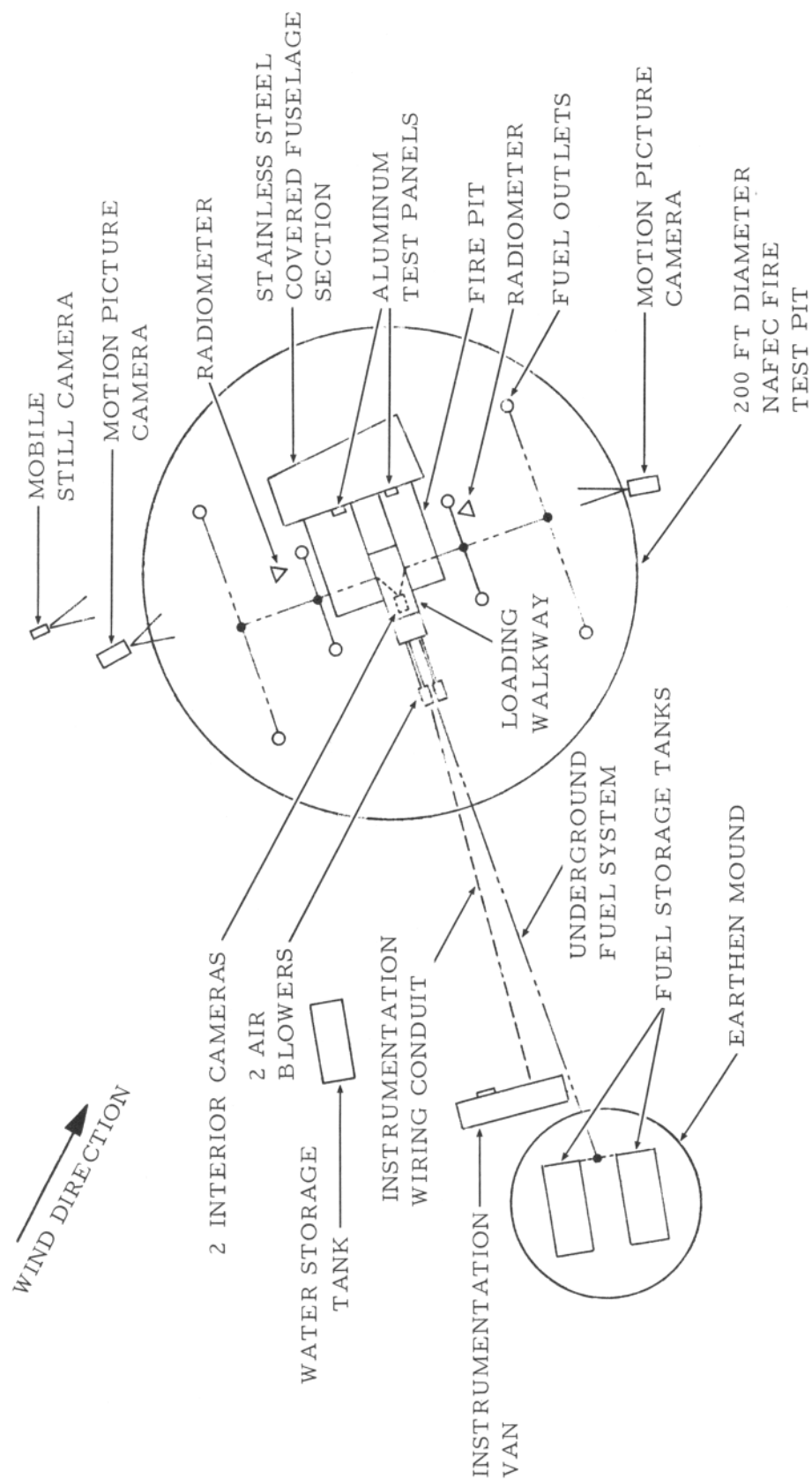


FIGURE 1. PLAN VIEW OF THE FIRE TEST BED (NOT TO SCALE)

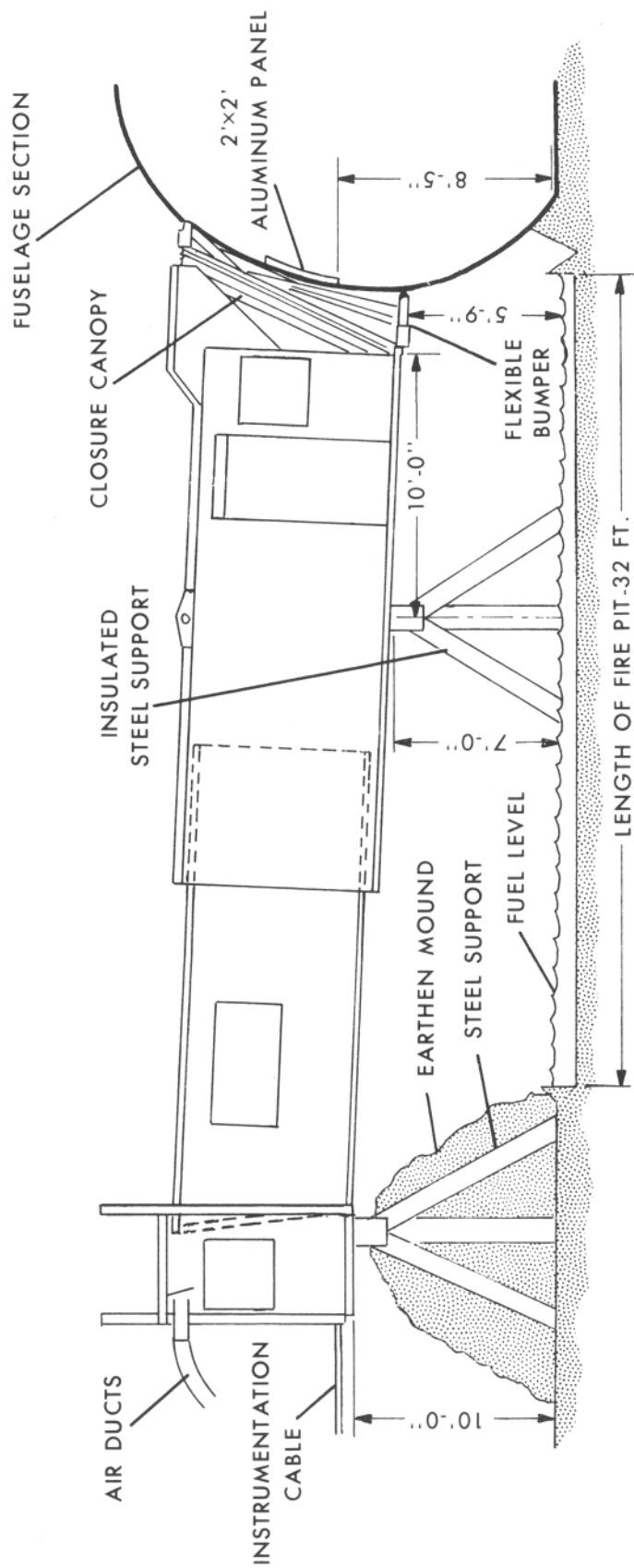


FIGURE 2. ELEVATION VIEW OF THE AIRCRAFT LOADING WALKWAY, FUSELAGE SECTION, AND FIRE PIT (NOT TO SCALE)





FIGURE 3. PORTABLE BLOWERS SHOWING THE INSTALLATION OF THE INSULATED AIR CONDUITS AND INSTRUMENTATION CABLE

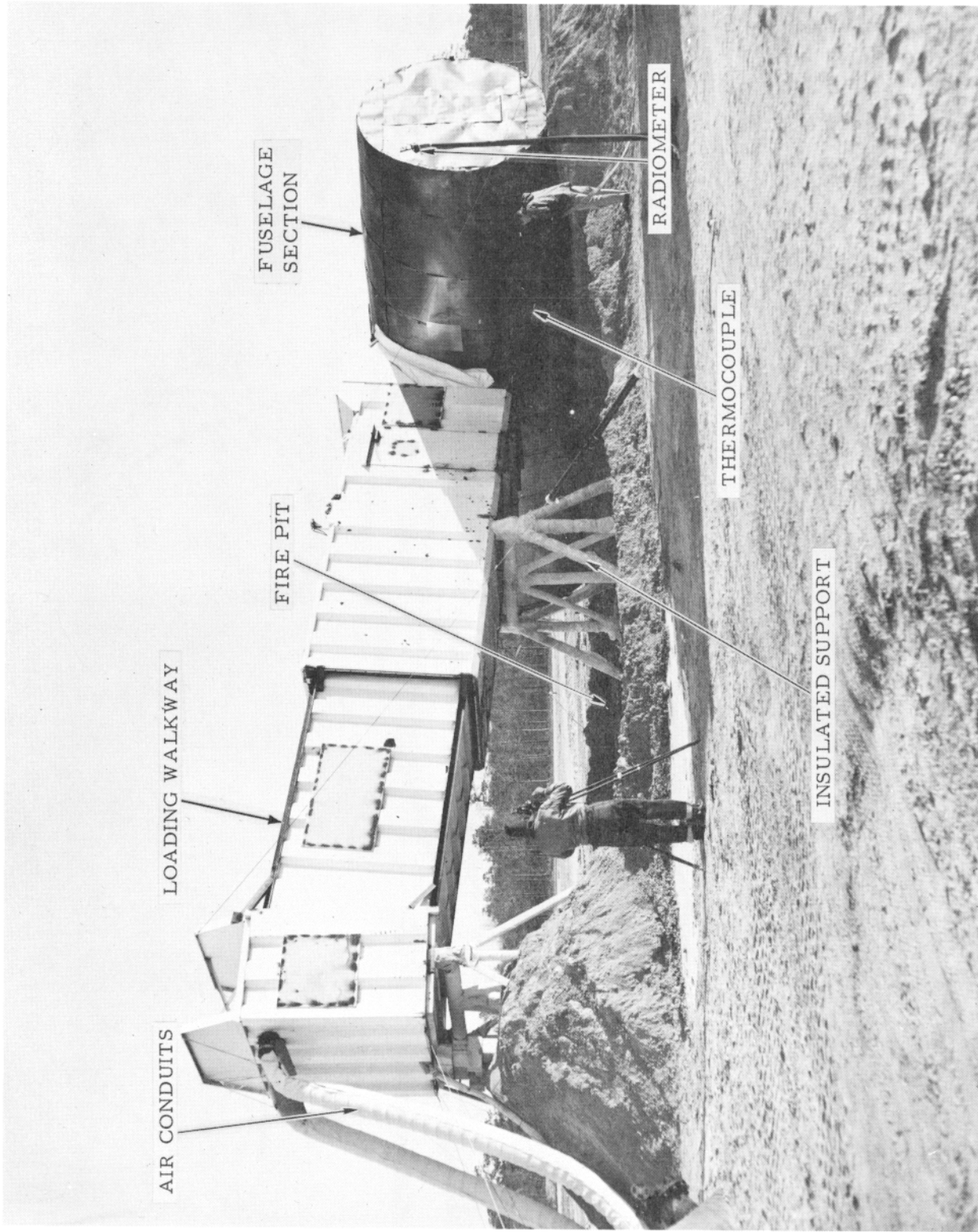
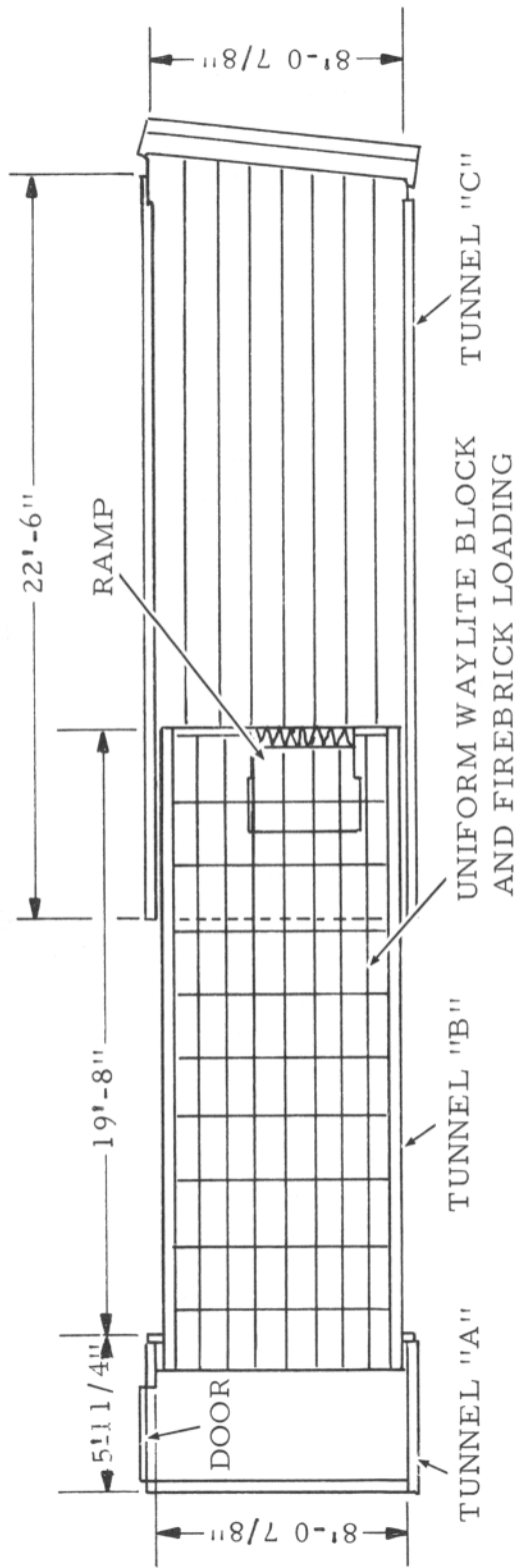
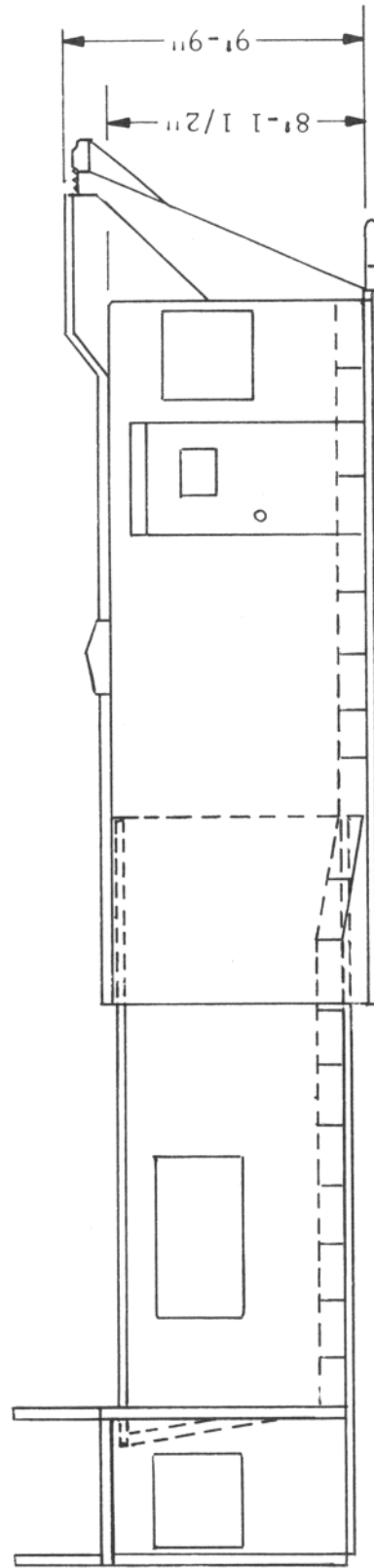


FIGURE 4. EXTERIOR VIEW OF THE FUSELAGE SECTION WITH THE PASSENGER LOADING WALKWAY IN POSITION AND THE RADIOMETER AND THERMOCOUPLE LOCATIONS



PLAN VIEW OF WALKWAY LOADING (NOT TO SCALE)



ELEVATION VIEW OF WALKWAY LOADING (NOT TO SCALE)

FIGURE 5. FLOOR LOADING PLAN OF THE AIRCRAFT LOADING WALKWAY

The thermocouples were positioned on, within, and beneath the walkway in cross sections on stations indicated by the letters W, X, Y, Y', and Z in Figure 6. Detailed sketches showing the installation points of each thermocouple at these stations are presented in Appendix B.

The instrumentation of the test bed including the aircraft loading walkway, the stainless-steel-covered fuselage section, and fire pit comprised the following elements:

Exterior Radiometer Locations. One radiometer was positioned on each side of the fire pit to determine the time required for the fire to reach the equilibrium burning-rate condition to provide a realistic and definitive starting time for measuring the subsequent sequence of events.

Fire Pit Thermocouple Positions. The flame temperature configuration of the free-burning pool fire was monitored by positioning thermocouples beneath the walkway along the longitudinal centerline 4 feet above the fuel level at points 2 feet 7 inches (Station Z) and 14 feet 10 inches (Station X) from the aircraft fuselage. Two additional heat sensors were located 3 feet above the fuel surface, 1 foot from the fuselage section, and 4 feet to the left and right sidewalls of the walkway.

Exterior Steel Thermocouple Positions. Thermocouples were welded to the inside surfaces of the metal skin at the longitudinal centerlines of both wall surfaces above the fire pit thermocouple positions. A typical wall thermocouple installation is shown in Figure 7. Three additional sensors were welded to the inside surface of the steel floor at points 7 feet 10 inches, 13 feet 10 inches, and 23 feet 3 inches from the fuselage section. One thermocouple installation is shown in Figure 8 where the flooring had been reinforced by a double layer of plywood.

Enclosed Airspace Thermocouple Positions. As a result of the steel corrugations, a series of airspaces was alternately formed between the metal skin and the interior surfaces of the walkway. To determine the temperatures developed within these spaces, thermocouples were positioned 7 feet 10 inches and 14 feet 10 inches from the fuselage section. These positions are shown in detail in Appendix B.

Interior Surface Thermocouple Positions. Heat sensors were bonded to the inside wall and floor surfaces of the walkway at points corresponding to the positions of the exterior metal surface thermocouples. Figure 9 illustrates a typical thermocouple installation in the plywood flooring, and Figure 10 shows a thermocouple embedded in the carpet covering over the installation shown in Figure 9.

Interior Air Thermocouple Positions. Thermocouples were positioned in the airspaces within the walkway at points 2 feet 7 inches, 7 feet 10 inches, 14 feet 10 inches, and 23 feet 4 inches from the fuselage section along the centerline of the floor at points 3 feet 5 inches and 6 feet 6 inches above floor level with the exception of two thermocouple positions which were 23 feet 4 inches and 2 feet 7 inches from the fuselage where thermocouples were positioned 3 feet and 6 feet 6 inches above floor level.

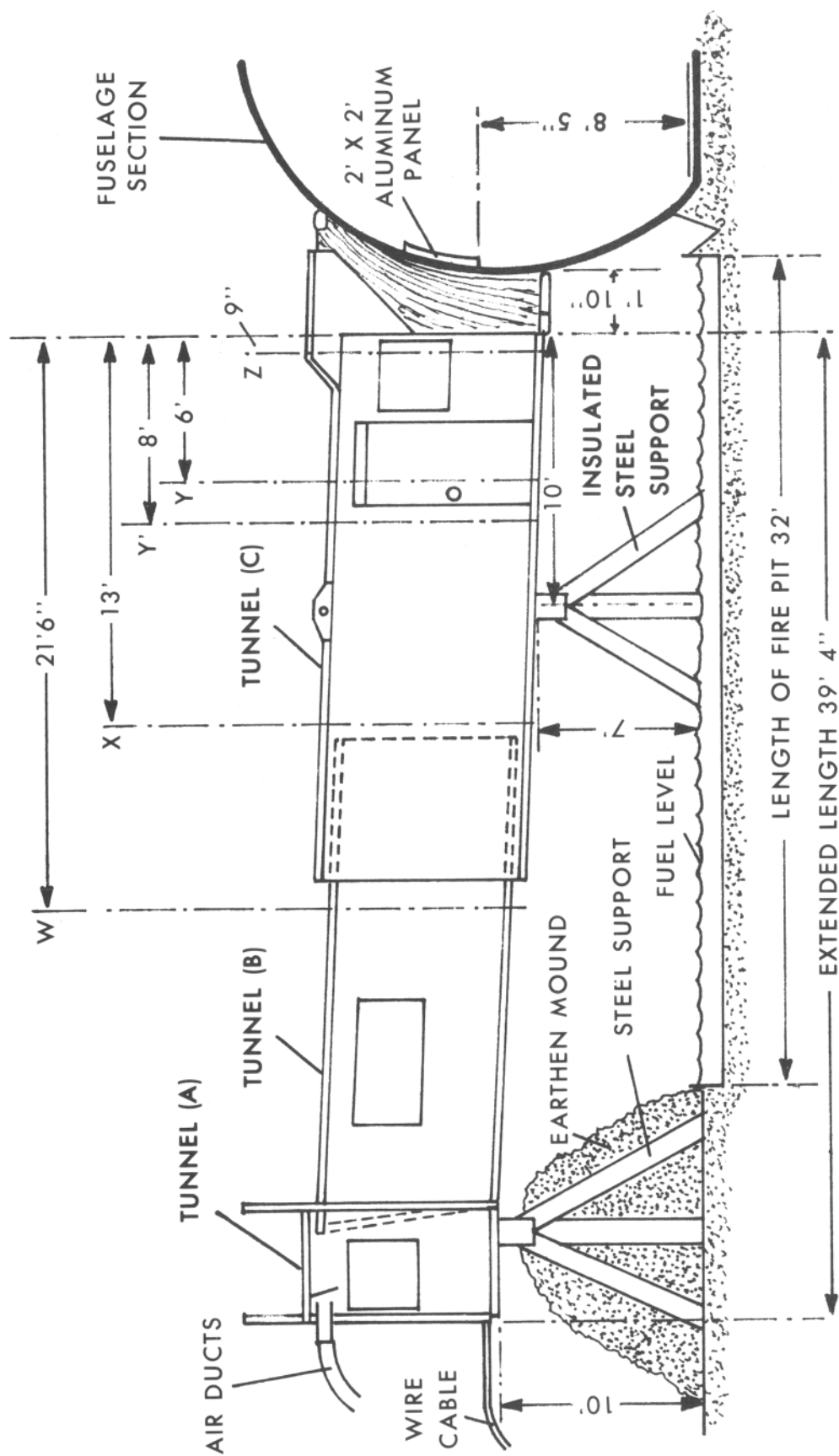


FIGURE 6. ELEVATION VIEW OF THE AIRCRAFT LOADING WALKWAY SHOWING THE LOCATION OF THE INSTRUMENTATION POSITIONS



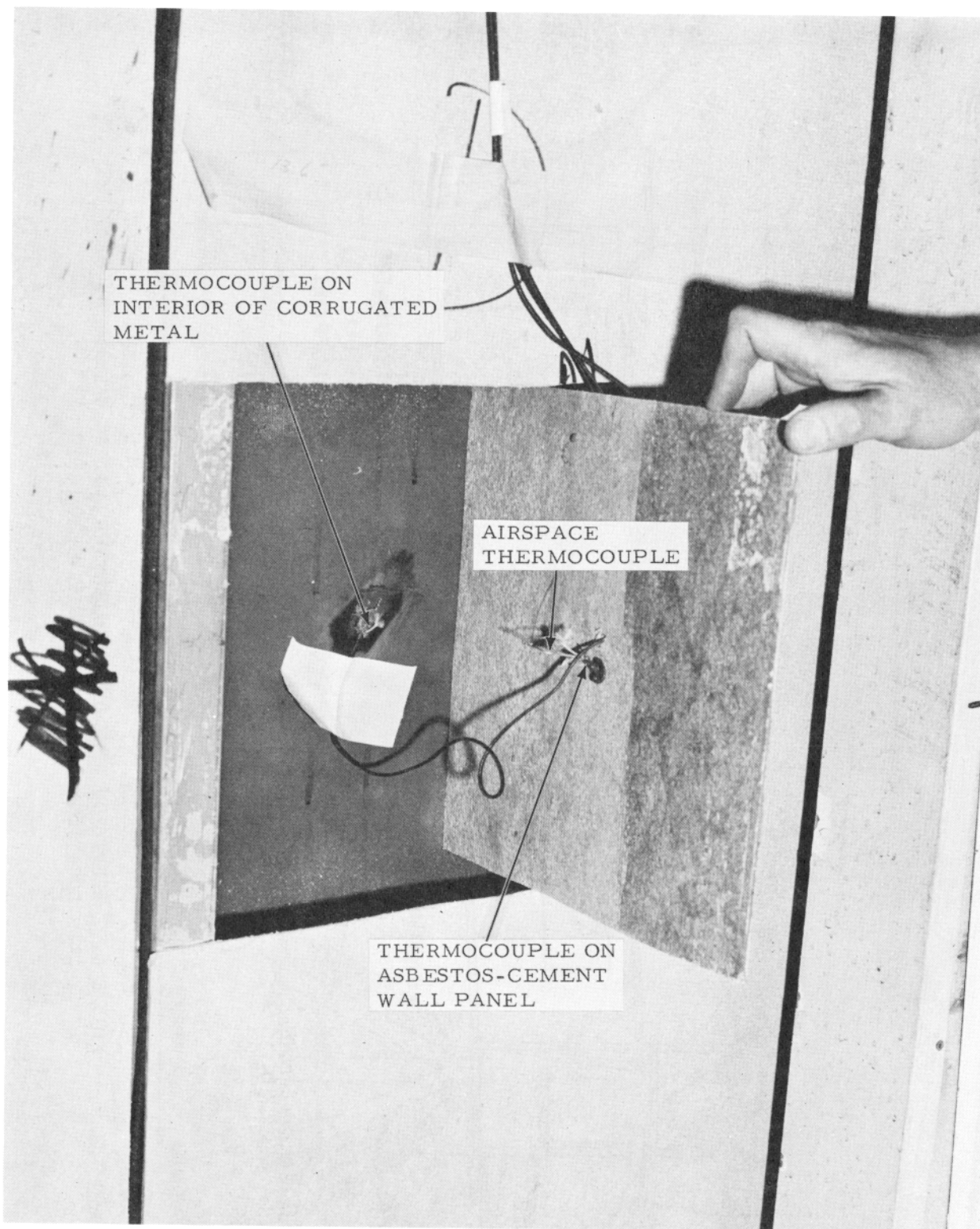


FIGURE 7. TYPICAL THERMOCOUPLE INSTALLATION ON THE INSIDE OF THE EXTERIOR METAL WALL SURFACES

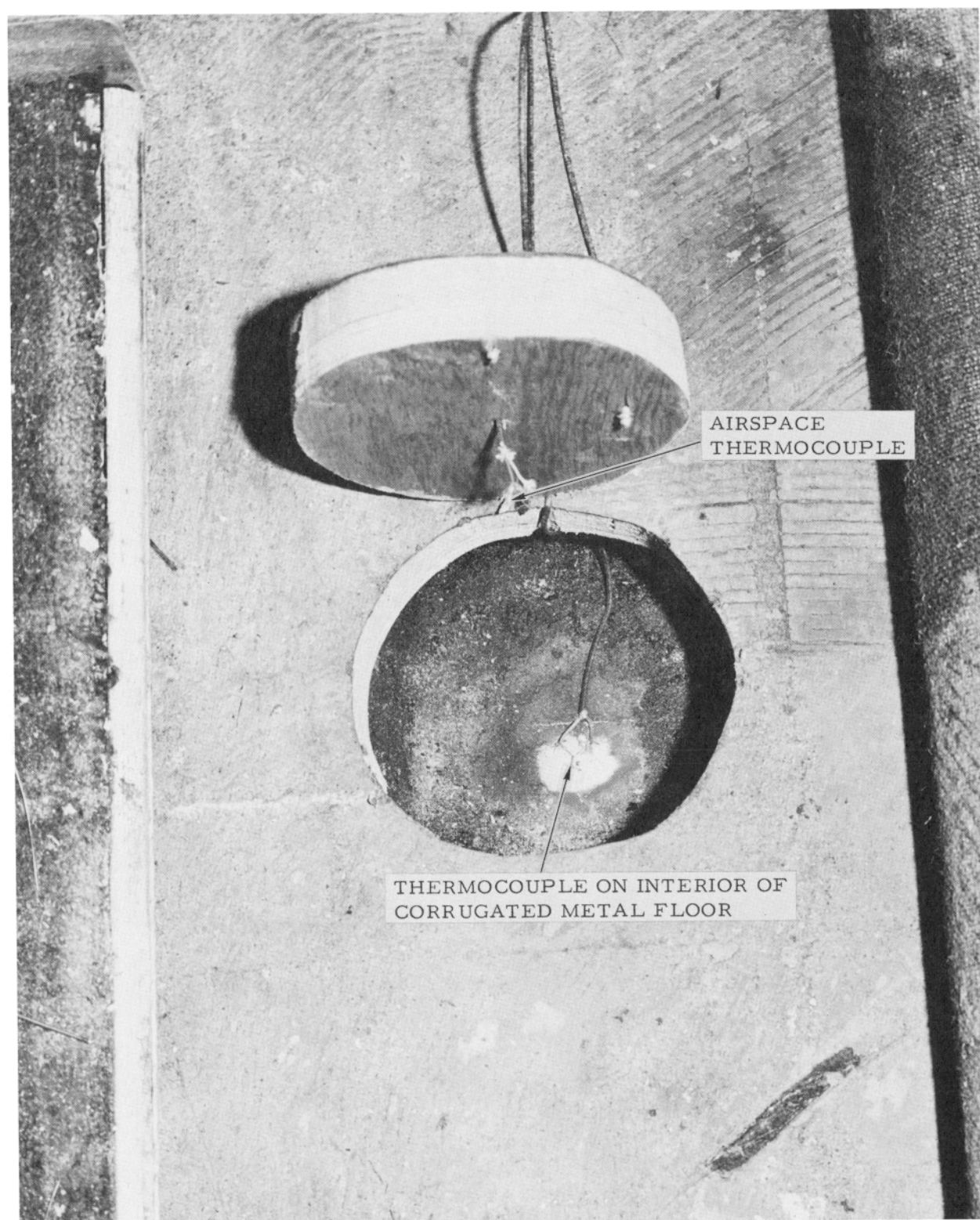


FIGURE 8. TYPICAL THERMOCOUPLE INSTALLATION ON THE INTERIOR METAL AND PLYWOOD FLOOR DECKING

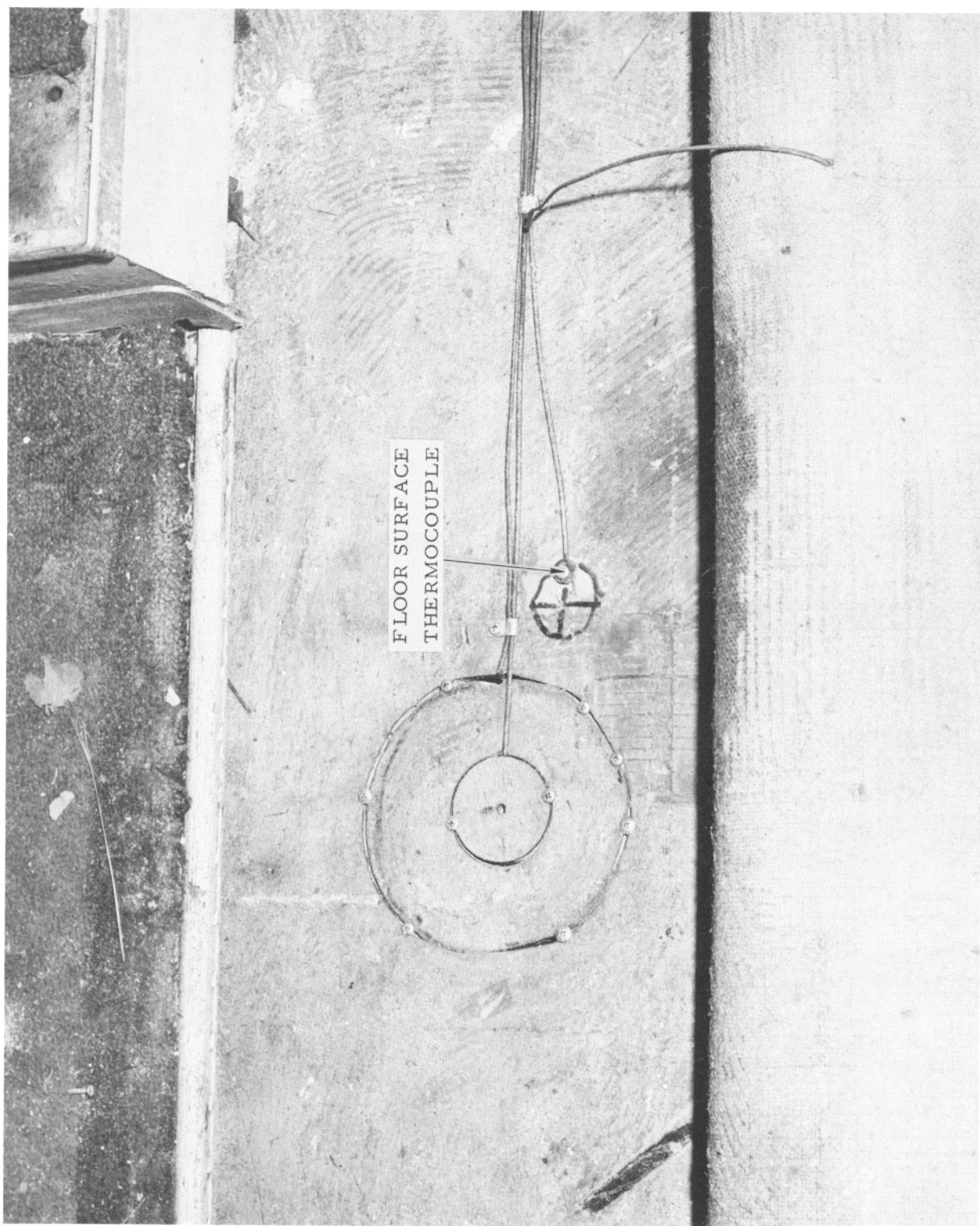


FIGURE 9. TYPICAL THERMOCOUPLE INSTALLATION ON THE SURFACE OF THE PLYWOOD FLOORING



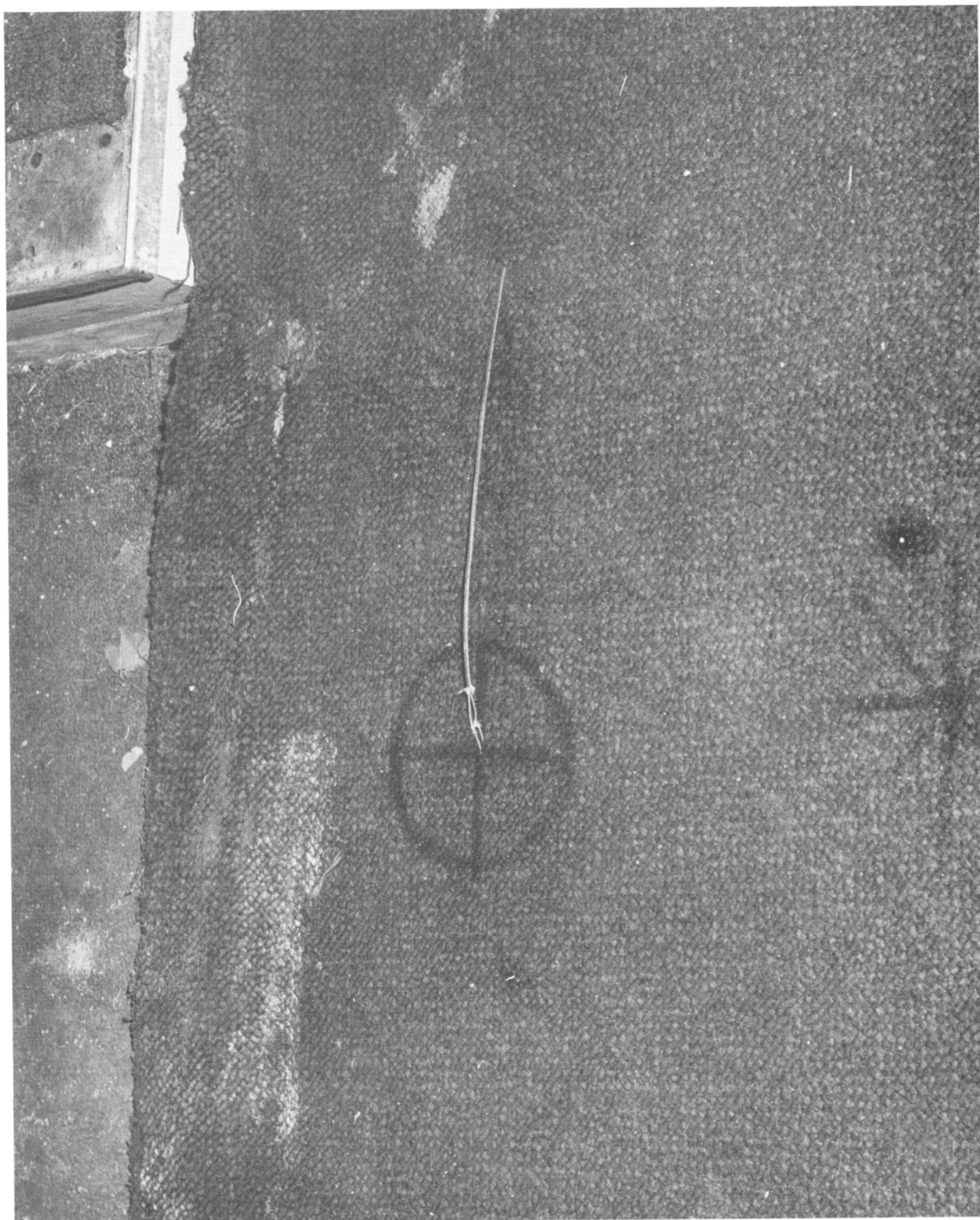


FIGURE 10. TYPICAL INSTALLATION SHOWING A THERMOCOUPLE EMBEDDED IN THE CARPET OVER THE CONFIGURATION SHOWN IN FIGURE 9

Tunnel Overlap Thermocouple Positions. Thermocouples were positioned in the overlapping section of Tunnels B and C between the ceiling and sidewalls. Heat sensors were also located above the water drain holes in Tunnel B as indicated in Figure 11.

Smoke Evaluation Methods. Three illuminated "EXIT" signs and an electric clock with a sweep-second hand were established in a vertical array (Figure 12) within the optical range of two instrumentation-type motion picture cameras, at the fuselage end of the walkway, to provide a visual display for estimating the obscuration time through the walkway caused by any pyrolysis products and/or smoke generated during fire exposure.

The two instrumentation motion-picture cameras exposing 16 mm color film at 24 frames per second were mounted inside thermally insulated steel boxes and positioned in Tunnel B of the walkway 21 feet 4 inches from the "EXIT" sign array to obtain a visual recording of events as they occurred during fire exposure. Adequate interior lighting of the walkway was provided by six 500-watt photoflood lamps to obtain proper film exposure. To establish the starting time of photographic coverage a photoflash bulb was mounted on the "EXIT" sign array within range of the cameras and synchronized with the ignition of the exterior fuel by a remote-controlled switch. The cameras and floodlight positions are shown in Figure 13.

In addition, two photocell smoke density meters were positioned along the longitudinal centerline of the walkway 6 feet 6 inches above floor level. One was 23 feet 4 inches from the fuselage and the other 14 feet 10 inches from the fuselage. A typical smoke meter installation is shown in Figure 14.

Manikin Positions. Three clothed manikins were positioned within the walkway at 23 feet 4 inches, 14 feet 10 inches, and 7 feet 10 inches from the fuselage section to provide a visual means for estimating the time of smoke obscuration of the walkway interior by passengers during egress from aircraft. The manikins also provided a means of support for some of the thermocouples measuring the internal air temperature of the walkway as shown in Figure 15.

Interior Radiometer Locations. One radiometer was positioned in Tunnel B of the walkway in an attempt to detect any heat flux emanating from flame penetration into the interior as a consequence of the failure of the aircraft closure curtain and bumper or of the weather stripping between Tunnels B and C.

Aluminum Panel Positions. To estimate the thermal effects of the pool fire on the fuselage section in the vicinity of the aircraft loading door, two 2-foot-square aluminum panels backed by 3/16-inch thick asbestos insulation were bolted to the fuselage section at a distance of 20 inches from each side of the walkway and 8 feet 5 inches above the fuel level in the pit. One thermocouple was bonded to the center of the backside of each aluminum panel.

The position of the aluminum panel on the fuselage section to the left of the walkway is shown in Figure 16. A similar panel was placed in position on the fuselage to the right of the walkway closure.

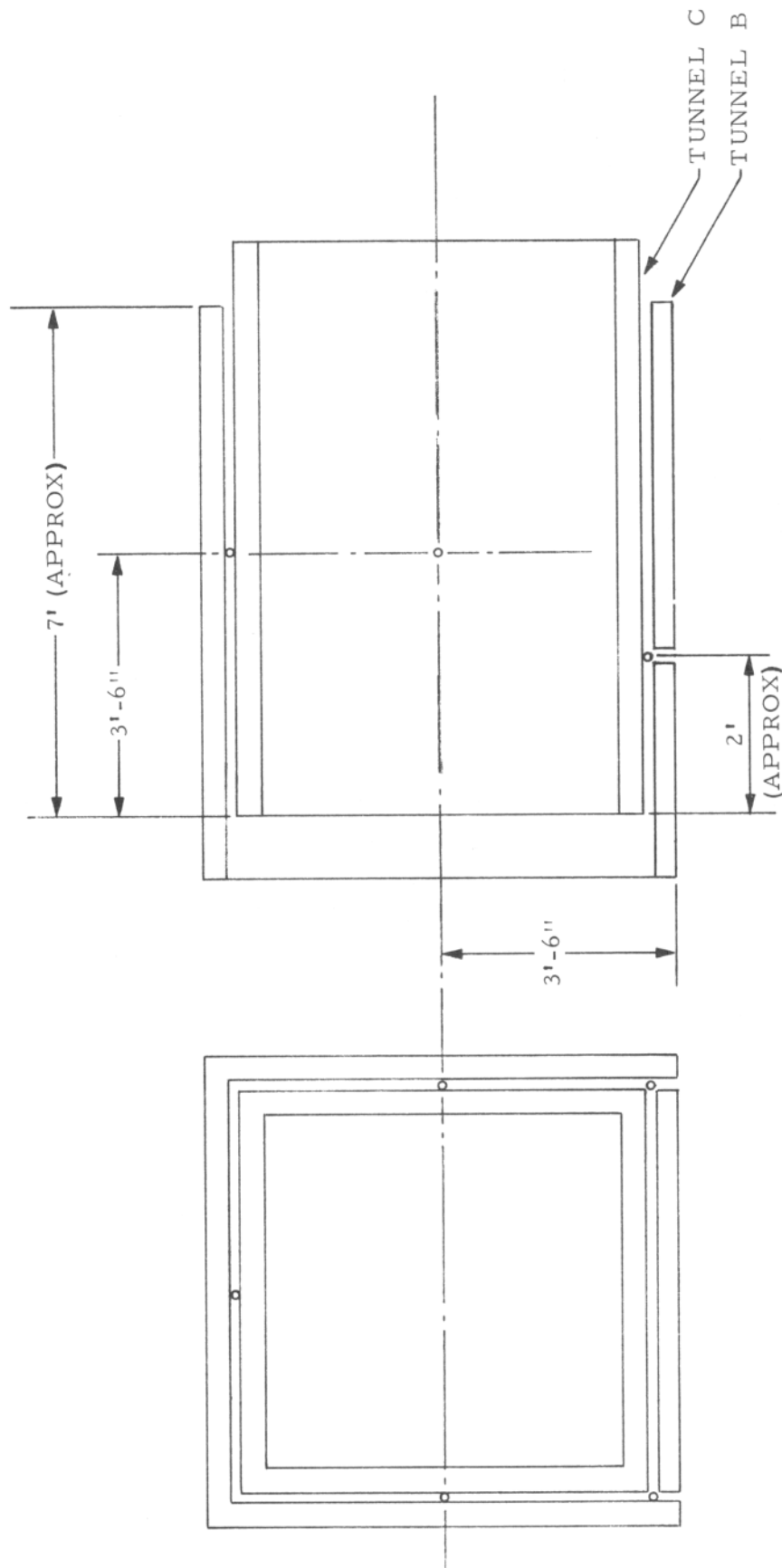


FIGURE 11. AIRCRAFT LOADING WALKWAY THERMOCOUPLE POSITIONS WITHIN THE OVERLAPPING SECTION BETWEEN TUNNELS B AND C



FIGURE 12. OPTICAL ARRAY OF "EXIT" SIGNS AND CLOCK FOR ESTIMATING THE VISUAL OBSCURATION TIMES BY SMOKE AND ORGANIC PYROLYSIS PRODUCTS





FIGURE 13. INTERIOR FLOODLIGHT AND CAMERA POSITIONS

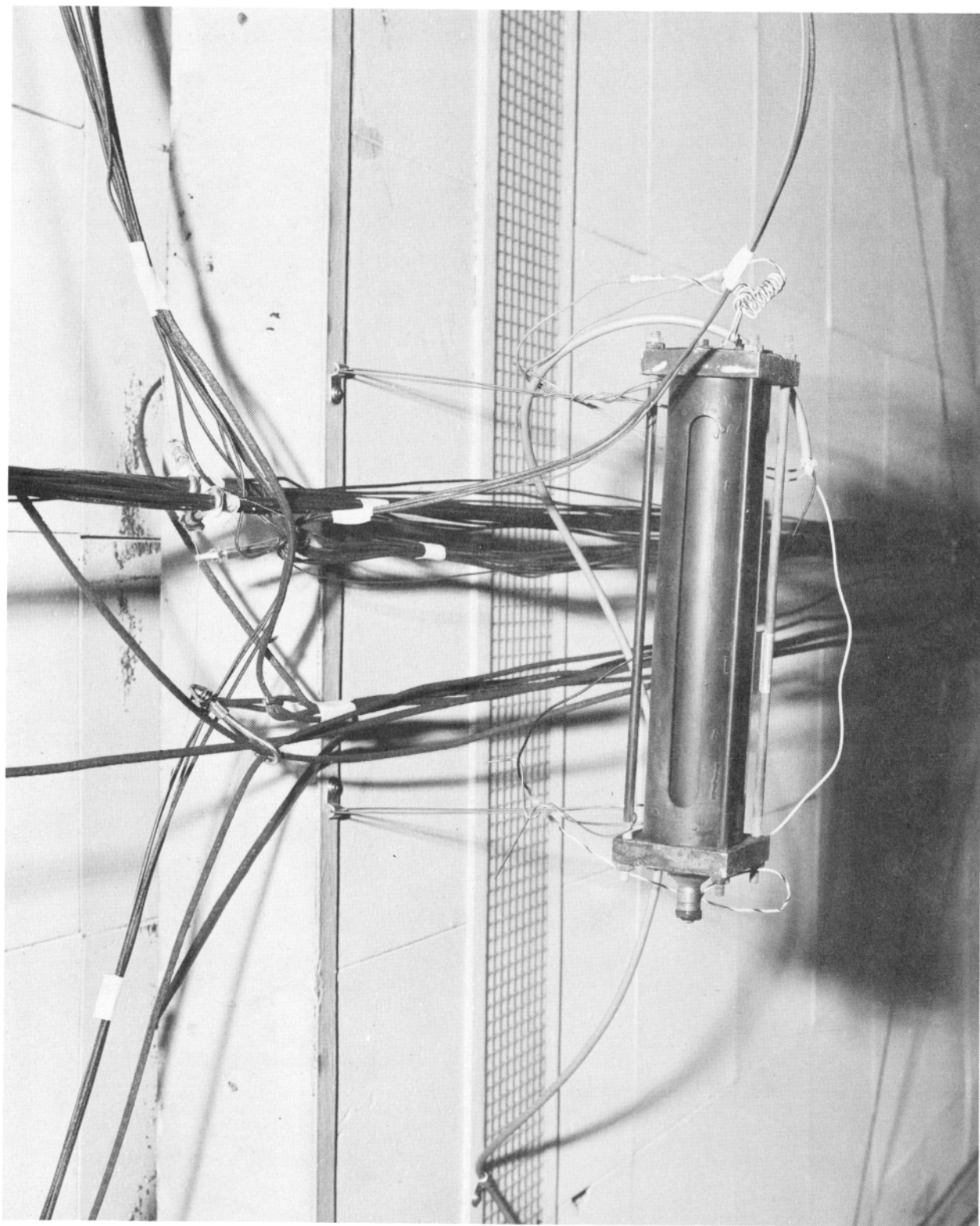


FIGURE 14. PHOTOMETRIC SMOKE DENSITY METER INSTALLATION

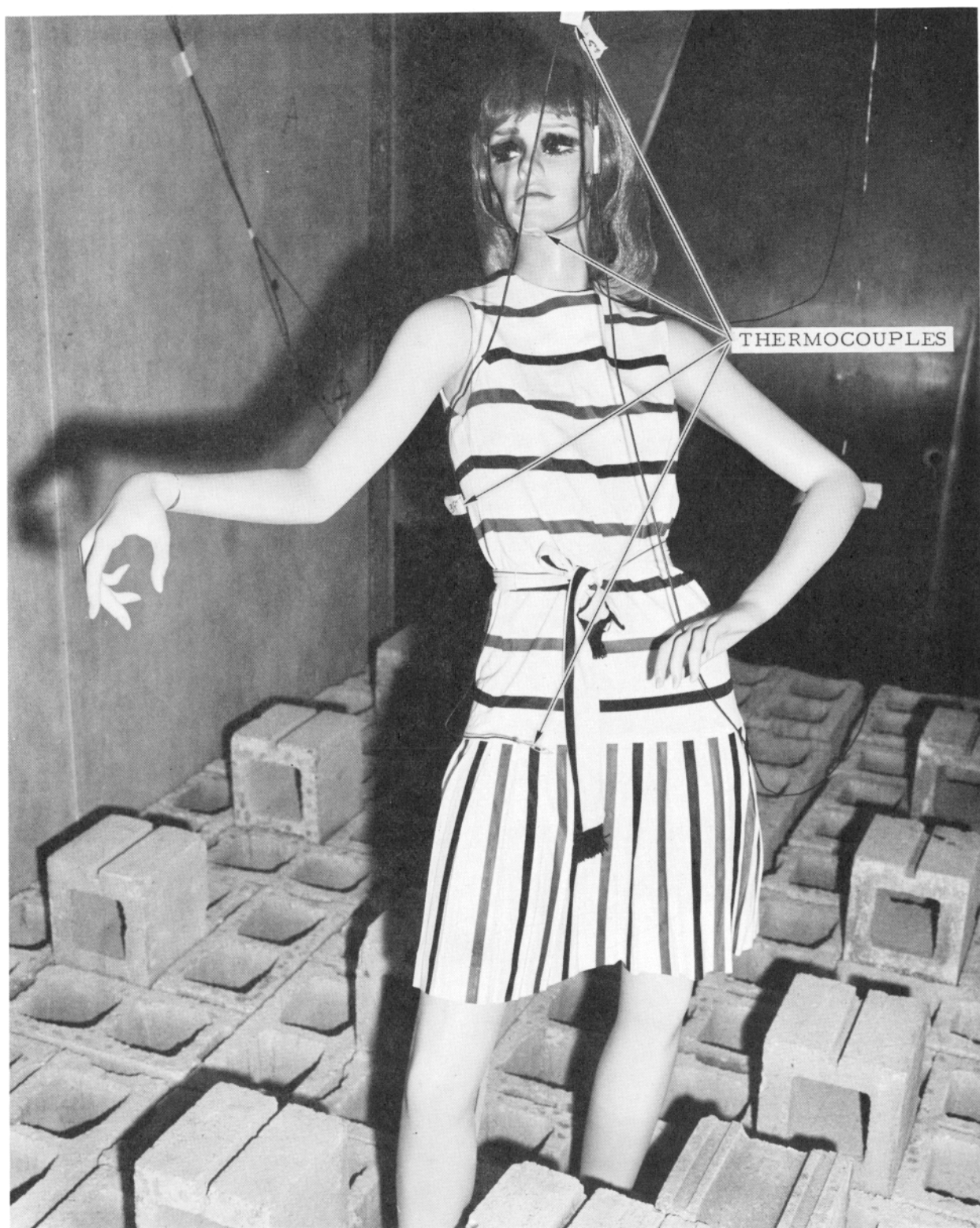


FIGURE 15. INSTRUMENTED MANIKIN SHOWING SEVERAL AIR THERMOCOUPLE LOCATIONS





FIGURE 16. POSITION OF THE ALUMINUM PANEL ON THE FUSELAGE SECTION RELATIVE TO THE FIRE PIT AND LOADING WALKWAY



## FIRE TEST PROCEDURE.

The experiment was initiated by igniting the JP-4 aviation fuel from the upwind side of the pit by means of two torches soaked in fuel. The pit was then permitted to burn freely for 10 minutes after which it was extinguished by two handlines each discharging Aqueous-Film-Forming Foam (AFFF) at a solution rate of 60 gallons per minute (0.125 gallons per minute per square foot of fire area). Under these conditions fire control was obtained in 45 seconds (90-percent reduction in heat flux) and extinguished within approximately 65 seconds. A typical view of the free-burning pool fire conditions is shown in Figure 17.

Two phases in the firefighting operation are presented in Figure 18. Figure 18A shows the initial foam discharge employing both handline nozzles using the fully dispersed foam pattern and Figure 18B shows the quality of the AFFF blanket after fire extinguishment.

## FIRE TEST RESULTS.

TEST CONDITIONS. The test was conducted on January 9, 1973, at 9:45 a.m. at which time the ambient air temperature was 20°F and the barometric pressure 30.27 inches of mercury with a relative humidity of 35 percent.

At the time of fuel ignition and throughout the burning period the wind was blowing and gusting at approximately 14 knots toward the fuselage section forming an angle between 45° and 55° with the centerline of the walkway and the overall thermal effects on the test bed tend to reflect this condition.

As a consequence of this diagonal wind direction, the flame plume was intermittently swept under the walkway which resulted in a lower heat flux recording on the radiometer on the upwind side of the fire pit.

The profiles in Figure 19 show the heat flux as a function of time after fuel ignition and indicate that the time required to reach equilibrium burning conditions was approximately 75 seconds.

FUEL FLAME TEMPERATURES. The flame temperature profiles obtained from the thermocouples positioned in the fire plume, approximately 4 feet above the fuel surface, are presented in Appendix C, Figure C-1, where temperature is plotted as a function of time after fuel ignition.

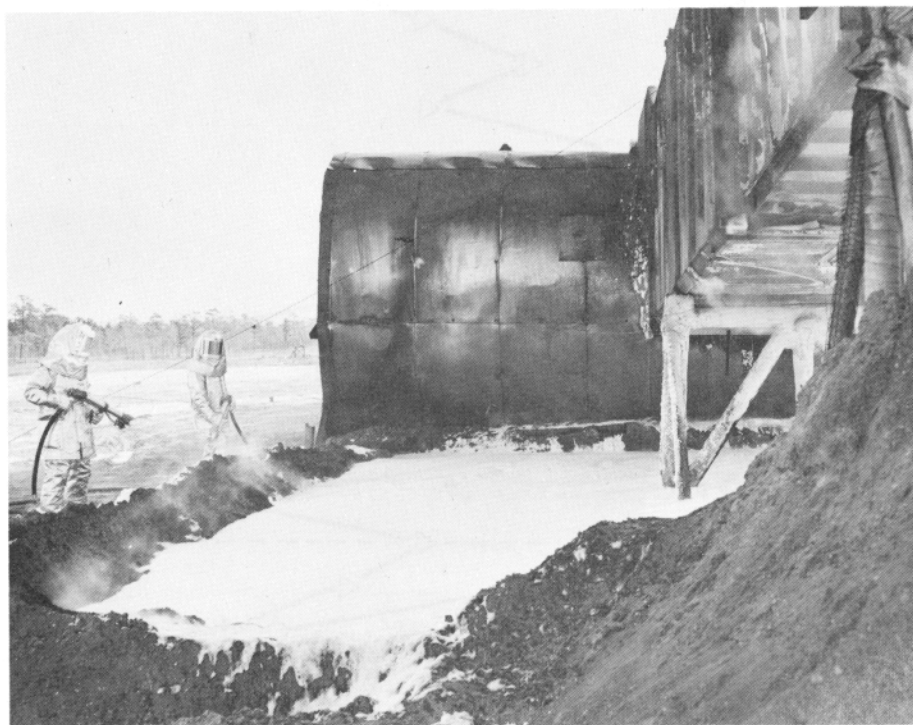
The thermocouple at Station X, which was below the centerline of the walkway and 14 feet 10 inches from the fuselage, showed a minimum and maximum variation from 1,050° to 2,200°F with an estimated average temperature of 1,625°F. The flame temperature at Station Z, which was also under the centerline of the walkway and 2 feet 7 inches from the fuselage, indicated a minimum and maximum variation of 500° to 1,500°F with an approximate average temperature of 1,000°F.



FIGURE 17. TYPICAL FREE-BURNING POOL-FIRE CONDITIONS



a. Initial Attack With Foam/Water Handlines.



b. AFFF Blanket After Fire Extinguishment.

FIGURE 18. CRITICAL PHASES DURING THE FIREFIGHTING OPERATION

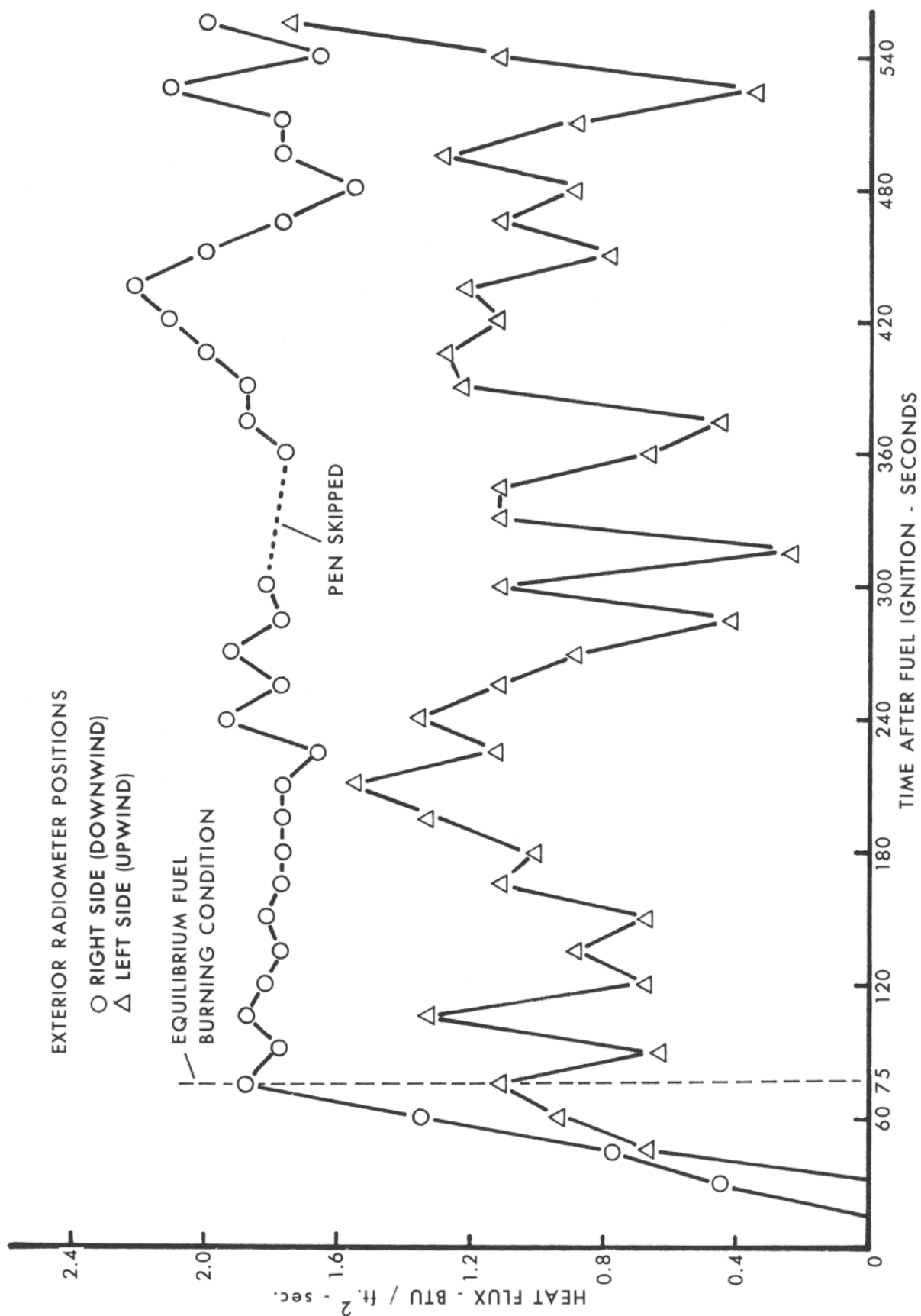


FIGURE 19. EXTERIOR RADIOMETER PROFILES SHOWING HEAT FLUX AS A FUNCTION OF TIME AFTER FUEL IGNITION

Of the two thermocouples positioned 1 foot from the fuselage and 4 feet on either side of the walkway, only the one on the right or downwind side was operational. The temperature on this heat sensor indicated a fluctuation between 700° and 1,900°F with an approximate average of 1,300°F.

THERMAL EFFECTS ON THE WALKWAY. The data obtained from each thermocouple position within and on the walkway structure are indicated by the profiles presented in Appendix C.

The overall thermal effects on the walkway are summarized in the envelopes presented in Figure 20 in which temperature is plotted as a function of time after fuel ignition.

The top envelope encloses all of the time-temperature data developed for the exterior steel floor during fire exposure. The horizontal dashed lines at 900° and 1,200°F were drawn to indicate the melting range for aircraft aluminum which may be considered critical temperatures in any aircraft environment involving fire. The envelope shows that the steel reached the incipient melting temperature for aluminum of 900°F in approximately 45 seconds after equilibrium burning conditions were established which closely approximates the value developed in a previous project under free-burning pool fire conditions (Reference 2).

The middle hatched envelope is a composite made up of two individual time-temperature envelopes developed for the sides of the walkway. The uppermost envelope contains all of the time-temperature values obtained on the right or downwind side of the walkway, while the lower envelope shows the values obtained on the left or upwind side of the walkway. From these data it is apparent that the maximum temperature obtained on the downwind side of the walkway was approximately 950°F after 390 seconds and that the temperature on the left or upwind side did not exceed 900°F during fire exposure.

The bottom envelope encloses all of the time-temperature data obtained at the interior air thermocouple positions. The maximum air temperature after equilibrium burning conditions were established was 245°F at 465 seconds and 220°F within 300 seconds.

Based upon data provided in the U.S. Air Force "Flight Surgeon's Manual" for proficient human performance at elevated air and wall temperatures in equilibrium, it was estimated that the maximum limits of exposure to temperatures of 220°F and 245°F would be approximately 15 minutes and 13 minutes, respectively. Since it was determined that it required approximately 13 seconds to traverse the walkway at a normal walking stride, it is apparent that the environmental air temperature alone would not be a limiting factor in providing a safe egress route.

ANALYSIS OF THE INTERIOR SMOKE DATA. The parameter limiting the safe egress of passengers through the walkway was the early release of excessive amounts of smoke and organic pyrolysis products during fire exposure.

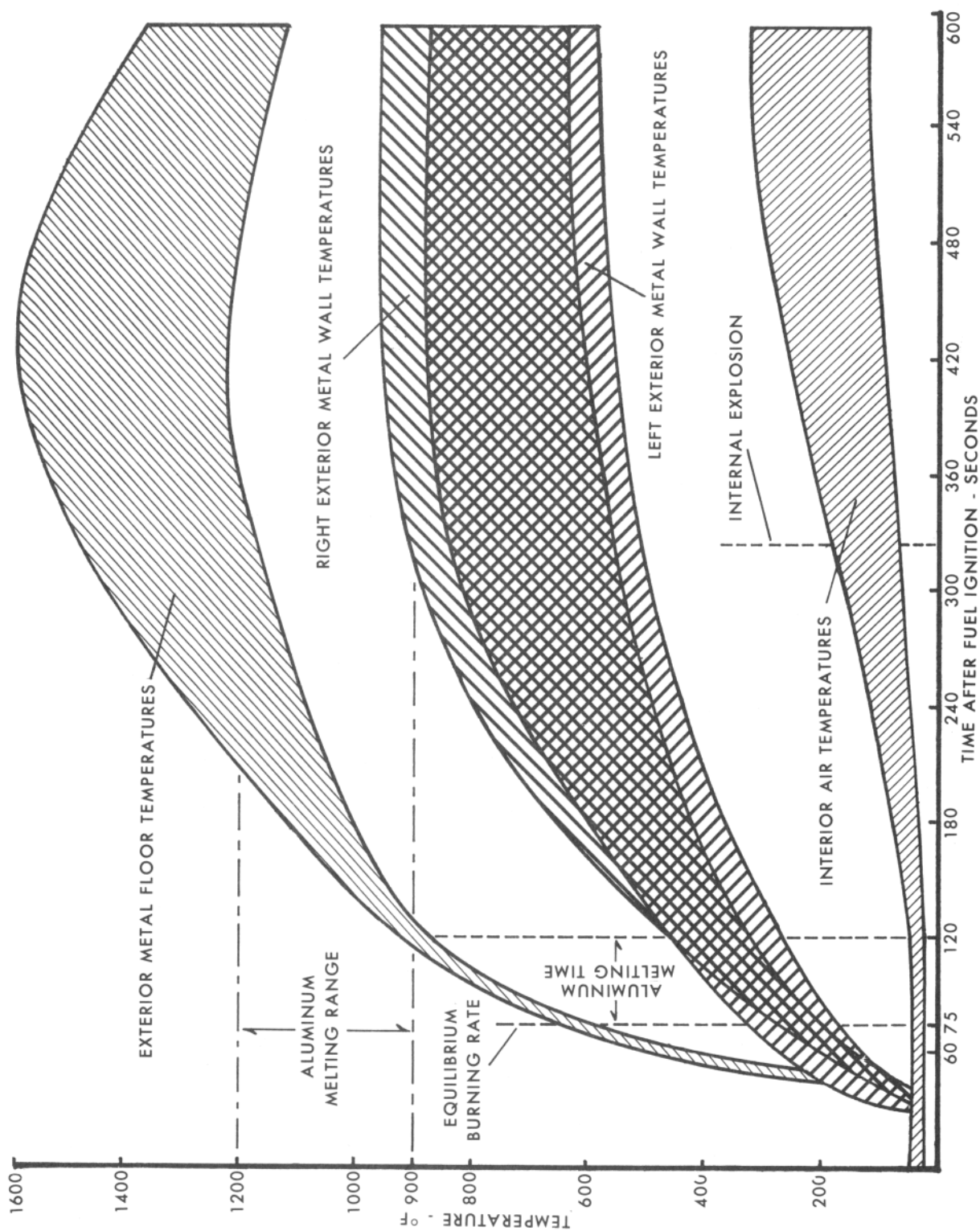


FIGURE 20. SUMMARY OF THE TIME-TEMPERATURE DATA OBTAINED FOR THE AIRCRAFT LOADING WALKWAY DURING FIRE EXPOSURE



The first evidence of smoke within the walkway interior was obtained from an analysis of the interior instrumentation camera films which showed visible wisps of smoke at floor level in the vicinity of the bumper within 18 seconds after fuel ignition followed by small flames starting at approximately 30 seconds.

The profiles developed from the smoke meter data are presented in Figure 21 where visibility is expressed as percent and plotted as a function of time after fuel ignition.

For comparative purposes, the visual obscuration times obtained from an analysis of the instrumentation camera films are presented in Table 1 and superimposed on the profiles in Figure 21. These data show the progressive visual obscuration of the "EXIT" signs, when photographed from a distance of 21 feet 4 inches, within the walkway as a result of smoke formation. The hot gases and smoke were observed to accumulate at ceiling level and rapidly fill the interior of the walkway proceeding from ceiling to floor in a progressive manner. Obscuration of the lower "EXIT" sign occurred within approximately 96 seconds, and total obscuration of the walkway interior within 120 seconds after fuel ignition.

TABLE 1. VISUAL OBSCURATION OF THE "EXIT" SIGN ARRAY BY SMOKE

Array Component	Visual Obscuration Times (Seconds)	
	Upper Motion-Picture Camera	Lower Motion-Picture Camera
Top "EXIT" Sign	(Not in view)	78.6
Clock	87.0	86.9
Middle "EXIT" Sign	94.4	90.4
Bottom "EXIT" Sign	97.1	94.1
Total Obscuration	120.0	119.5

Significant practical smoke density information was provided by observing the obscuration time of each of the three manikins, since they were located at various distances from the fuselage section. The position of the manikins were 7 feet, 15 feet 6 inches, and 22 feet 6 inches from the camera lenses, and the time for obscuration of each, after fuel ignition, was 120 seconds, 96 seconds, and 87 seconds, respectively (Table 2).

These data tend to indicate that under the test conditions, exiting passengers would be unable to see the end of the walkway and, consequently, have lost their positive sense of visual orientation in approximately 120 seconds after fuel ignition. The lachrymatory effects of the smoke and pyrolysis products would also impose an additional hazard toward achieving a prompt and safe evacuation.

FIGURE 21. OBSCURATION OF THE WALKWAY INTERIOR BY PYROLYSIS PRODUCTS AND SMOKE



TABLE 2. VISUAL OBSCURATION OF THE MANIKINS BY SMOKE

Manikin Distance From Camera Lens (Feet)	Visual Obscuration Times (Seconds)	
	Upper Motion-Picture Camera	Lower Motion-Picture Camera
22.5	88	86
15.5	97	95
7.0	121	119

INTERIOR RADIOMETER DATA. The thermal radiation within the walkway is indicated by the profile presented in Figure 22 in which the heat flux is plotted as a function of time after fuel ignition. The profile shows two periods of measurable radiation, the first between 165 and 225 seconds after fuel ignition and the second starting 330 seconds after ignition.

The vertical dashed line drawn at approximately 326 seconds after fuel ignition indicates the instant at which a rather severe internal explosion blew open the steel entrance door in Tunnel A which had been secured by a steel latch. It is speculated that the explosion was caused by ignition of the gaseous pyrolysis products from the plywood floor paneling which completely filled the walkway at that time.

A practical estimation of the intensity of the heat flux developed within the walkway may be made by considering the fact that approximately 0.10 BTU per square foot per second is delivered by the sun, at sea level, during the summer in temperate zones, and that exposure to 0.20 BTU per square foot per second for periods in excess of 30 seconds will cause severe pain in humans.

FLOOR RAMP FIRE. After the external fuel fire had been extinguished, it was observed that the overlapping floor section between Tunnels B and C was on fire. To obtain access to this area, it was necessary to remove some of the Waylite blocks and chop out a section of the flooring. Upon investigation it was evident that the seat of the fire was in the sloping wooden ramp between the walkway sections. The cut-away floor ramp section is shown in Figure 23. There was strong evidence indicating that the cause of this fire was by flame penetration beneath the ramp resulting from the complete thermal disintegration of the weather stripping between the two floor sections. The extent of damage to the weather stripping between Tunnels B and C is indicated in Figure 24.

FIRE DAMAGE TO THE WALLS AND CEILING. As a consequence of the thermal disintegration of the weather stripping and the pyrolysis of the plywood flooring, smoke and hot gases penetrated the space between the corrugations in the sidewalls and above the ceiling tiles of the walkway causing the damage indicated in Figure 25. This photograph shows a buckled asbestos-cement wall panel and the condition of the mineral acoustical ceiling tiles in the section of the walkway (Tunnel C) adjacent to the fuselage section after the test. The condition of these ceiling tiles is representative of only a relatively small portion of the ceiling adjacent to the fuselage. Furthermore, this

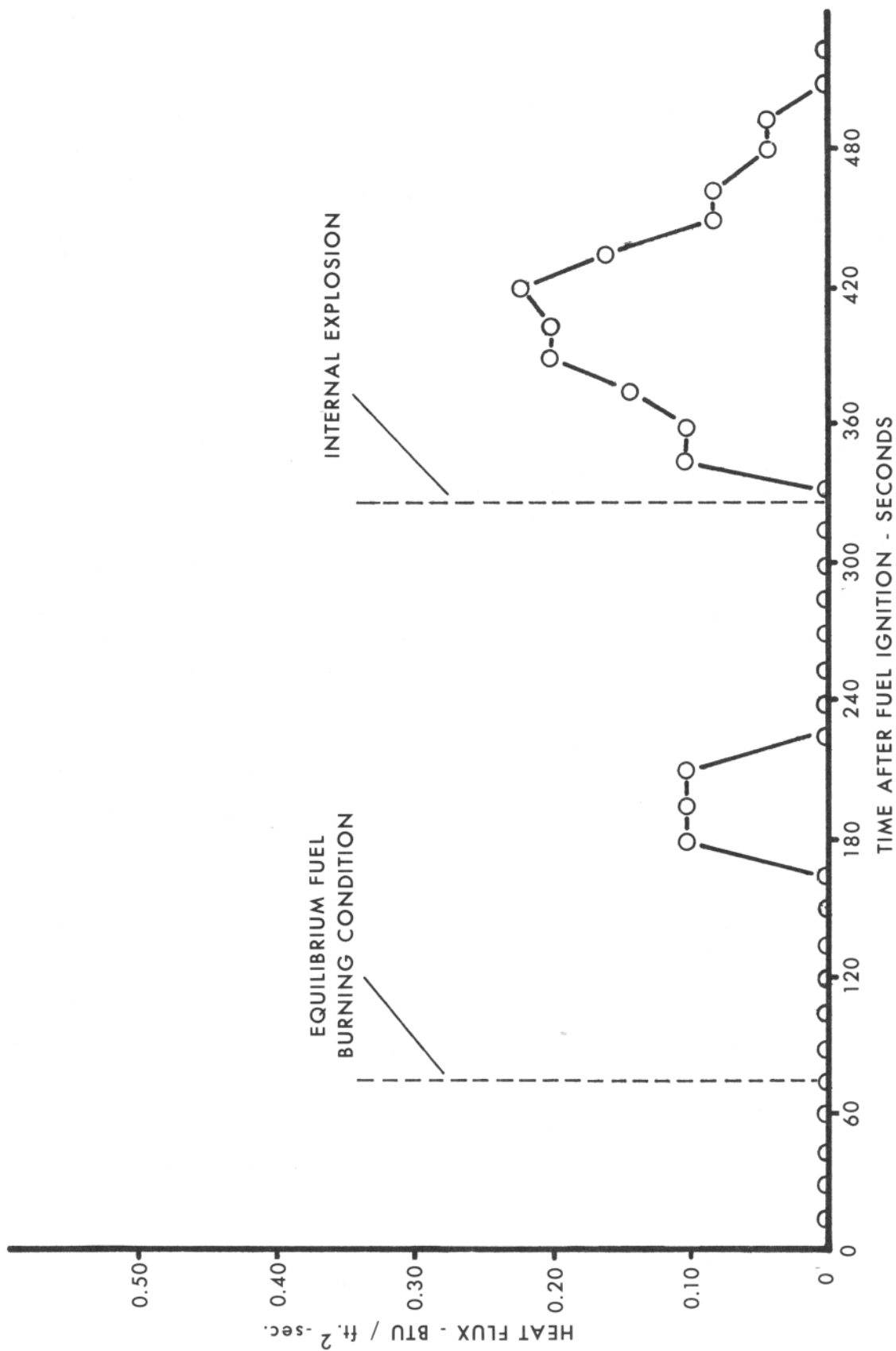
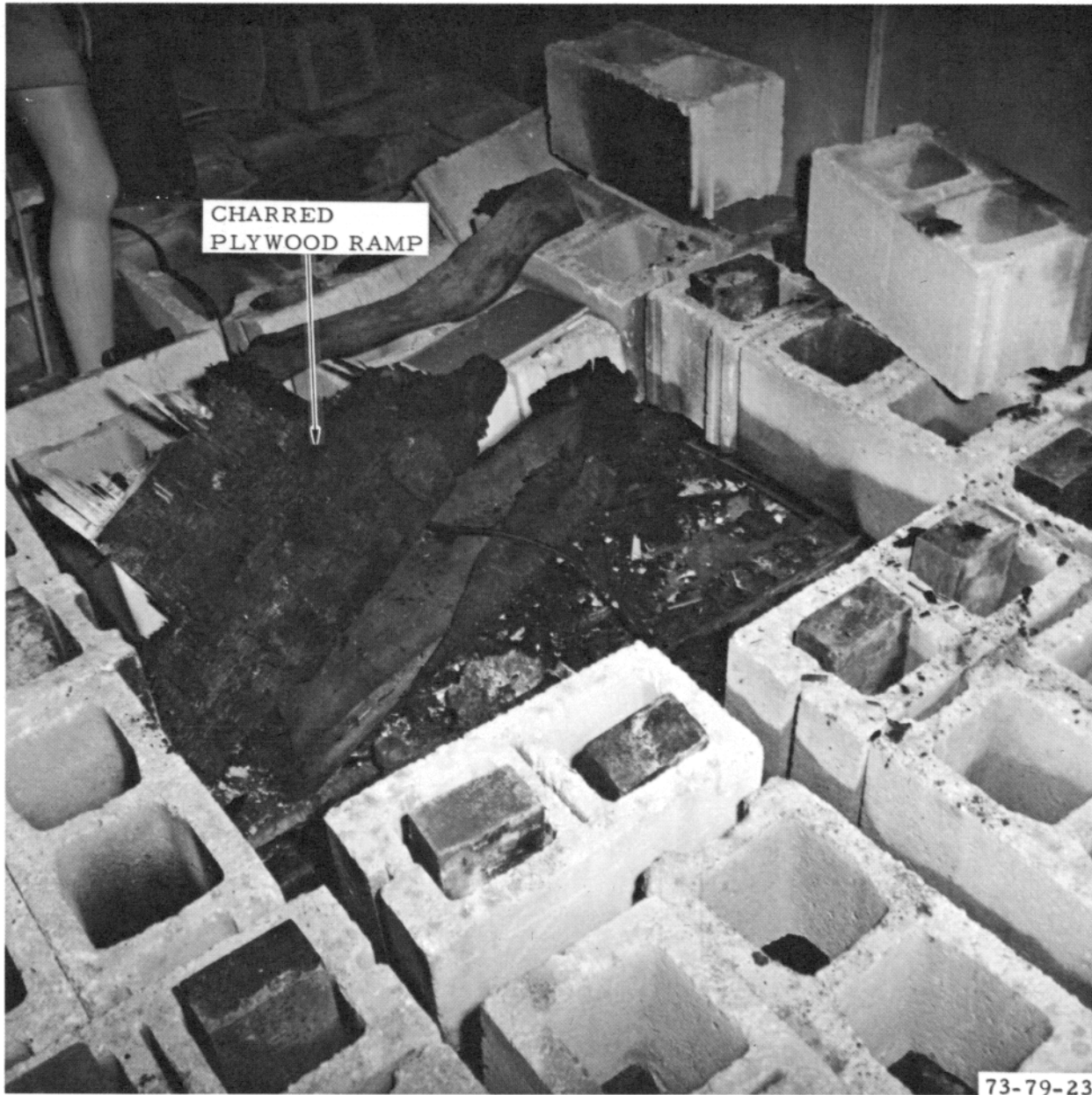


FIGURE 22. WALKWAY INTERIOR HEAT FLUX AS A FUNCTION OF TIME AFTER FUEL IGNITION



73-79-23

FIGURE 23. EFFECTS OF FIRE IN THE FLOOR RAMP SECTION BETWEEN TUNNELS B AND C

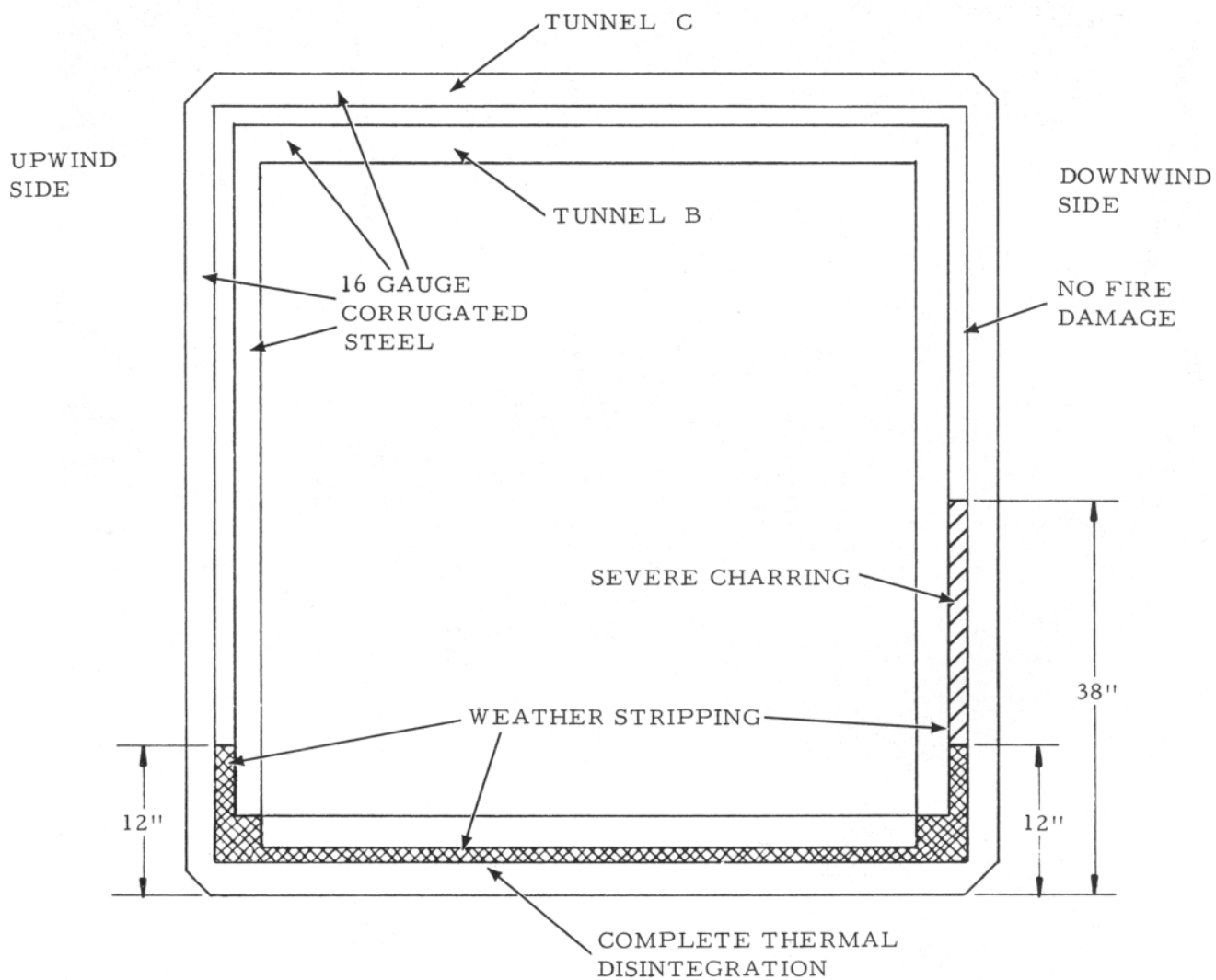


FIGURE 24. CROSS SECTION THROUGH TUNNELS B AND C INDICATING THE EFFECTS OF FIRE EXPOSURE ON THE WEATHER STRIPPING



73-79-25

FIGURE 25. CEILING AND WALL FIRE DAMAGE IN TUNNEL C

section of the walkway had been damaged in transit to NAFEC and the tiles were reset on the existing structure. In Figure 26 the wall and ceiling tiles, and the uppermost "EXIT" sign and clock show evidence of smoke penetration and discoloration. However, in this regard it is also of interest to note that the dress on the manikin in Figure 27, which was approximately 15 feet from the fuselage section, shows no appreciable deposit of smoke or soot.

DAMAGE TO THE SERVICE ENTRANCE DOOR. The service entrance door on the downwind side of the aircraft walkway at Station Y warped as a consequence of flame impingement which caused an opening of several inches in one corner between the door and the top of the doorjamb.

METALLURGICAL EXAMINATION OF THE EXTERIOR STEEL SHELL OF THE WALKWAY AFTER FIRE EXPOSURE. After fire exposure, a total of 16 samples of the exterior metal components of the walkway were removed from areas monitored by thermocouples and subjected to structural testing and metallurgical examination.

The sheet metal components of the walkway were fabricated from 16-gauge cold-rolled steel sheet. This material is not generally sold to specified physical properties. However, the anticipated tensile strength range is usually from 45,000 to 55,000 pounds per square inch. All of the sheet metal samples exhibited properties within this anticipated range and no significant loss of strength appears to have resulted as a consequence of fire exposure.

The results of the examination of the steel samples are presented in detail in Appendix D and indicate that the most severe conditions were experienced on the underside of the walkway where steel temperatures ranged from 1,380° to 1,570°F and the average tensile strength of the sheet metal coupons varied from 47,300 to 49,800 pounds per square inch.

The metal specimens taken from the sides of the walkway showed variations in the average tensile strength on the right or downwind side from 47,000 to 51,900 pounds per square inch over a temperature range from 640° to 1,000°F while samples taken from the left or upwind side varied from 48,500 to 56,000 pounds per square inch for temperatures between 600° and 900°F.

The welded sheet metal seams were found to have tensile strengths within the anticipated range, although some reduction in strength was noted in samples exposed to the higher temperatures, probably due to annealing effects.

Photomicrographs of the sheet metal samples and weld functions indicated that the structure of all samples examined consisted of ferrite and pearlite which is typical of low-carbon steel in the annealed or lightly rolled condition. No significant structural degradation due to heat effects was observed on any of the samples, although some grain coarsening, possibly due to heating, was noted on one sample which had been exposed to 1,570°F. However, this condition would not be expected to detract from the structural integrity of the metal.



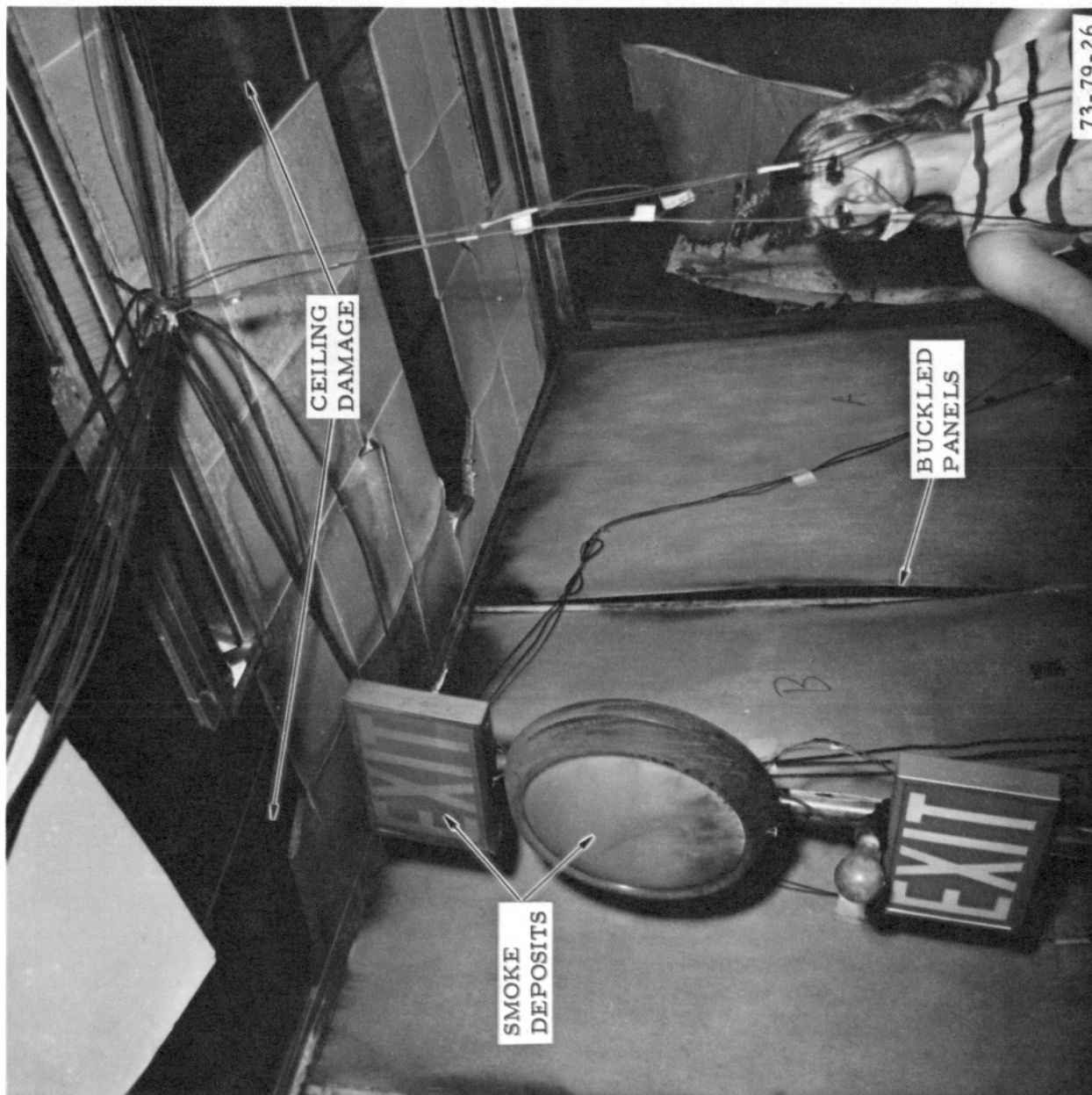


FIGURE 26. "EXIT" SIGN ARRAY SHOWING EVIDENCE OF SMOKE PENETRATION AND DISCOLORATION

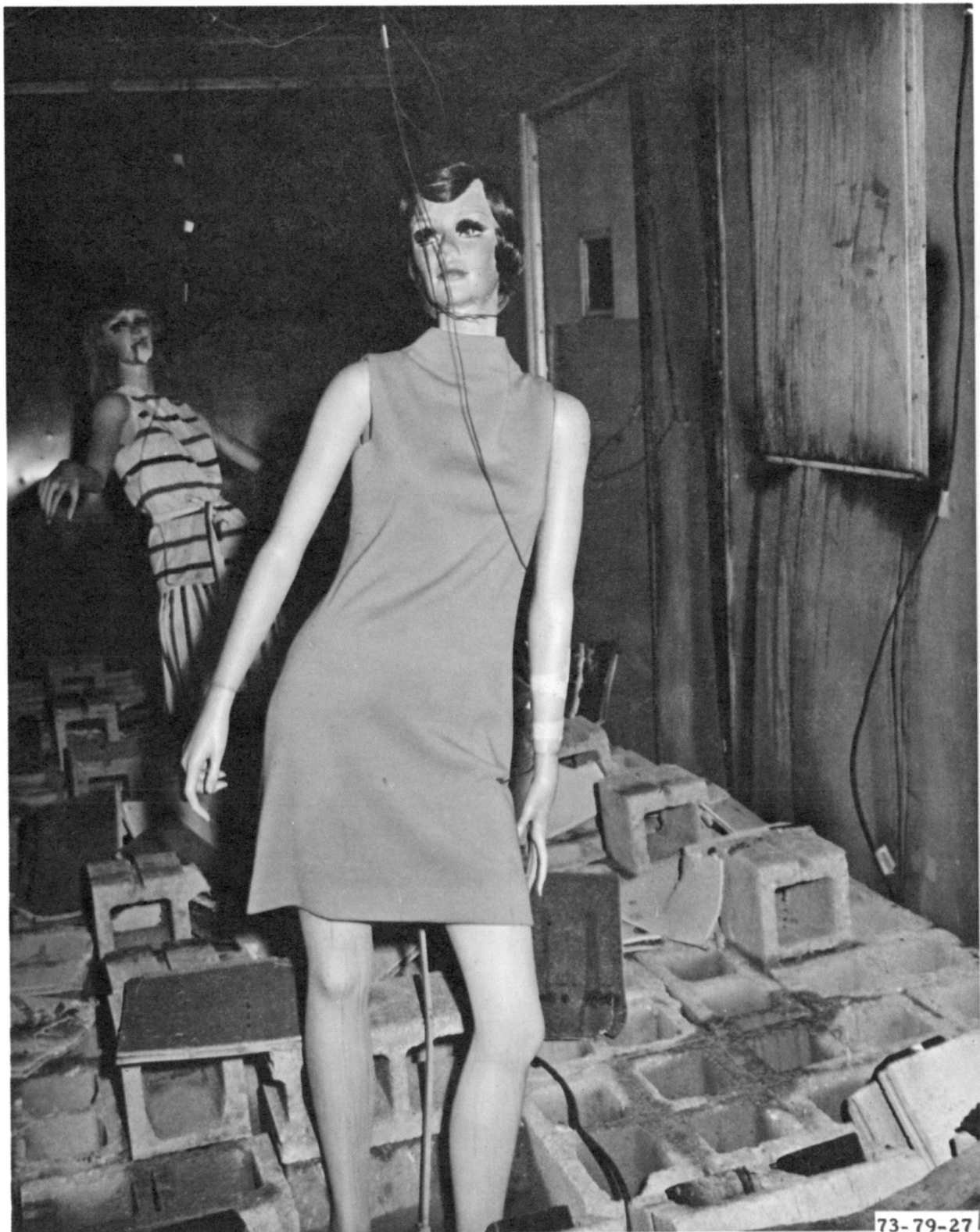


FIGURE 27. VISUAL CONDITION OF THE MANIKINS AFTER FIRE EXPOSURE OF THE WALKWAY



No deterioration of the welded seams or longitudinal structural members was observed on any of the specimens examined.

THERMAL EFFECTS ON THE ALUMINUM PANELS. The maximum temperature to which the aluminum panels on the fuselage section was exposed was not recorded because of the destruction of the thermocouple cable by the fire on the downwind side of the walkway. However, examination of the two sheets did show evidence of warping but no actual melting of the aluminum. Therefore, it may be assumed that the maximum temperature of the panels was below the incipient melting temperature for aluminum (900°F) which is in general accord with the temperatures recorded on the steel sides of the walkway.

The photographs in Figure 28 show the relatively "sheltered" positions of the two aluminum panels with regard to flame impingement. Figure 28A shows the soot-covered panel on the left side of the walkway which is generally indicative of a relatively "cool" metal surface, while Figure 28B shows the aluminum panel on the right side of the walkway and a definitive line of demarcation where flame impingement on the fuselage section was most severe.

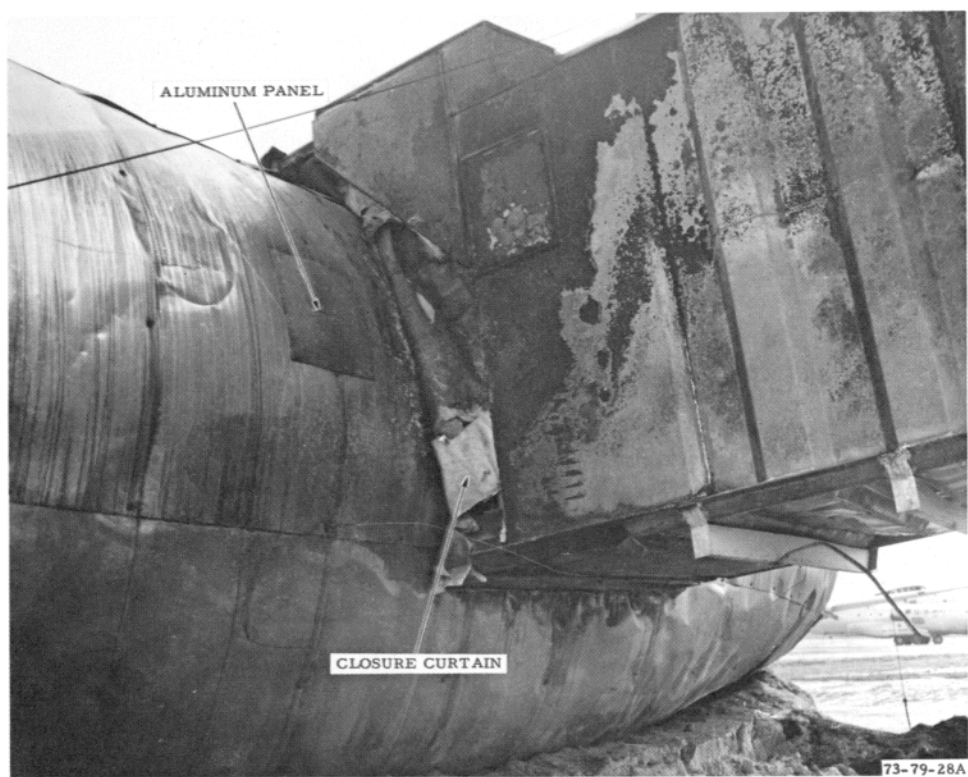
SMALL-SCALE PANEL TESTS. Prior to conducting the full-scale fire test with the aircraft loading walkway, a series of three small-scale experiments was performed on representative structural configurations of the walls, floor, and closure canopy of the unit. A description of the laboratory equipment and test procedure employed in these tests is presented in Appendix E.

Test No. 1 - Sidewall Panel. This 2-foot square unit was representative of the wall construction of the walkway. It was fabricated of a 16-gauge corrugated steel outer shell adjacent to a 3/16-inch thick sheet of asbestos-cement board. As a result of the steel corrugations a 3 3/16-inch deep airspace was formed alternately between the bearing surfaces as indicated in Figure 29. The asbestos-cement board was bonded to aluminum strips which were held to the corrugated steel by screws.

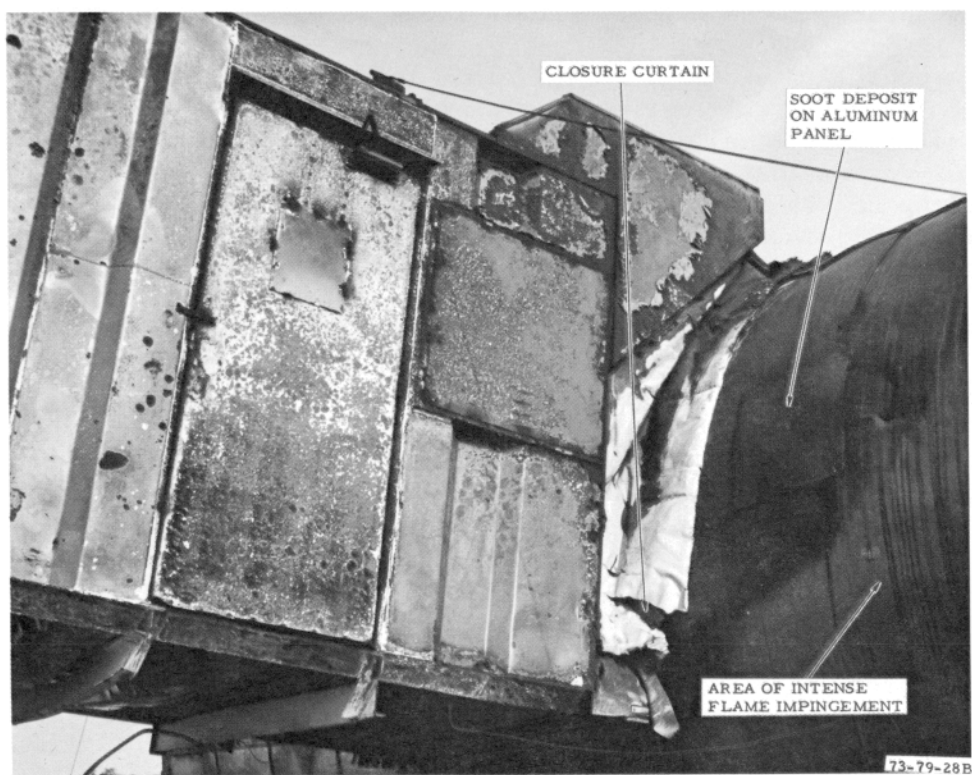
The thermal effects on the test panel during fire exposure are indicated by the profiles in Figure 29 in which temperature is plotted as a function of the flame exposure time.

The profiles show that the asbestos-cement board reached a temperature of approximately 440°F within 5 minutes after the start of flame impingement which caused severe warping but no cracking of the panel. However, during this same period the ambient air temperature within the smoke chamber did not exceed 120°F and reached a maximum temperature of 160°F after 10 minutes of fire exposure which is well within the limits of human tolerance.

The profile in Figure 30 shows the reduction in transmitted light caused by the smoke generated from the wall panel configuration in the smoke meter housing as a function of time after the start of flame exposure. This profile indicates that no smoke was generated during a period of 120 seconds after the start of flame impingement, after which smoke developed rapidly causing a 65 percent reduction in light transmittance within 210 seconds which decreased to 30 percent within 5 minutes and to 15 percent after 10 minutes.



A. ALUMINUM PANEL EXPOSED ON THE UPWIND SIDE OF THE WALKWAY



B. ALUMINUM PANEL EXPOSED ON THE DOWNWIND SIDE OF THE WALKWAY

FIGURE 28. THE EFFECTS OF FLAME IMPINGEMENT ON THE ALUMINUM PANELS

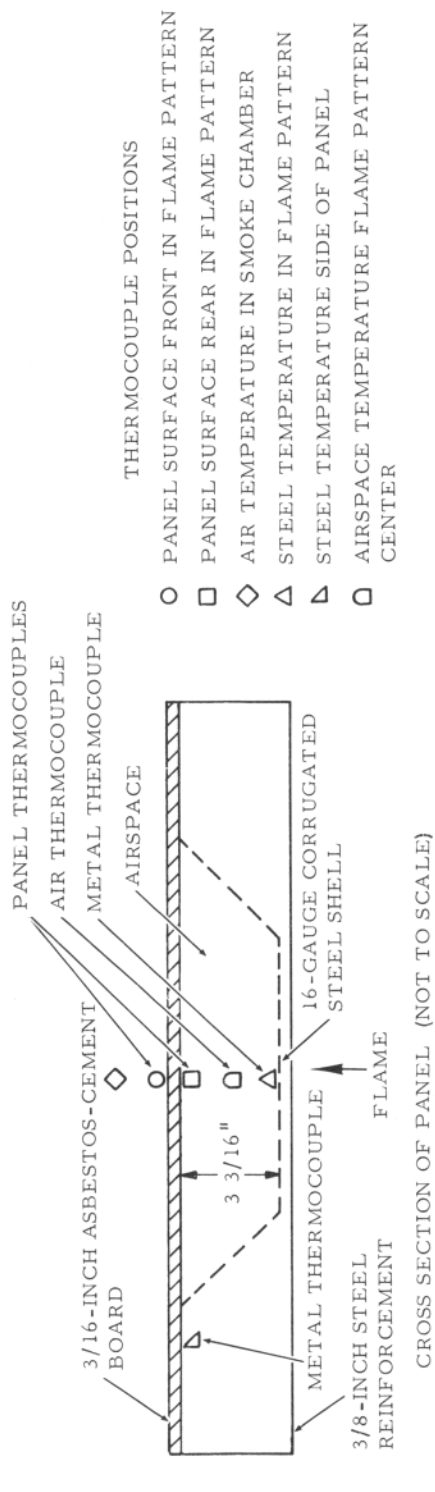


FIGURE 29. THERMAL EFFECTS ON A REPRESENTATIVE WALL PANEL SECTION WHERE THE CORRUGATED METAL AND ASBESTOS-CEMENT BOARD ARE SEPARATED BY AN AIRSPACE

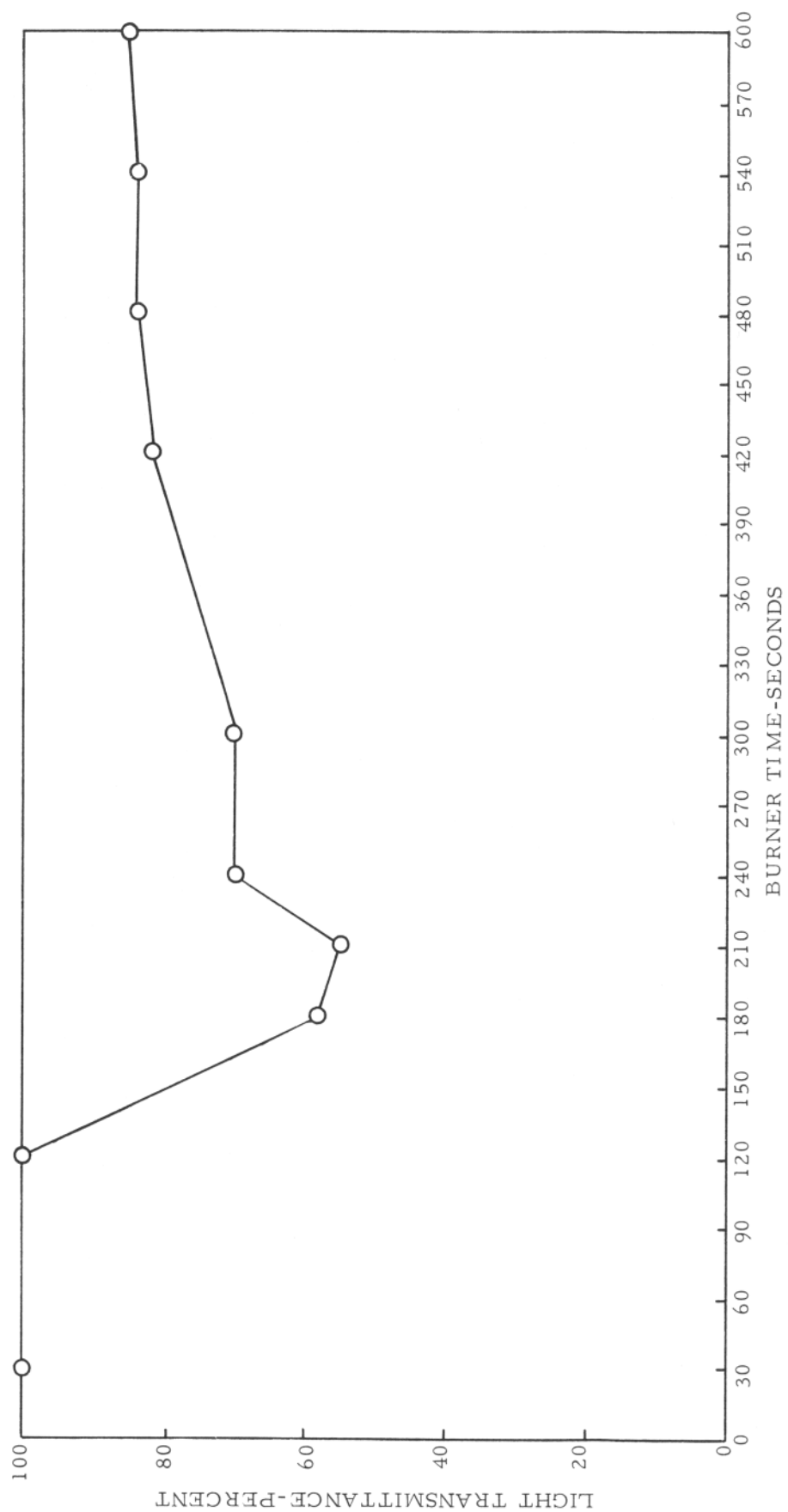


FIGURE 30. SMOKE GENERATED FROM A WALL PANEL SECTION AS A FUNCTION OF FIRE EXPOSURE TIME

Upon inspection of the wall sample at the conclusion of the experiment, it was apparent that the smoke recorded in the housing derived primarily from the pyrolysis of the adhesive bonding material between the asbestos-cement board and the aluminum retaining strips, which showed extensive charring.

Test No. 2 - Floor Panel Sections. The construction of the floor test panels was the same as that employed in the aircraft loading walkway. However, as a consequence of the corrugations in the steel, two different test configurations are possible. The most severe condition is shown schematically in Figure 31 in which the plywood flooring is bearing directly on the metal corrugation in the area of burner flame impingement, while the least severe condition is shown in Figure 32 where there is a 3 3/16-inch deep airspace between the metal and plywood flooring within the area of flame impingement.

Each floor sample configuration included a 16-gauge corrugated steel outer shell and 3/4-inch thick plywood subflooring covered with commercial rubber-backed nylon carpet. The carpet was installed in conventional manner with metal tack-strips nailed to the outer edges of the plywood flooring and the center section glued down. The entire assembly was then bolted to the outer steel housing of the smoke chamber.

The thermal profiles developed from the test data for each floor configuration are presented in Figures 31 and 32. These data tend to indicate that there were no significant differences in the overall environmental effects produced by the two different test configurations. However, when the metal and plywood flooring were in contact (Figure 31), the rug surface and the air temperature within the housing were slightly higher (approximately 10°F) than when they were separated by the airspace.

During fire exposure, copious quantities of smoke and gas were generated from both floor configurations caused by the pyrolysis of the plywood flooring, which ultimately escaped from the edges of the closure into the atmosphere. However, no smoke penetrated through the floor structure into the chamber containing the smoke meter when the steel and plywood were separated by an airspace (Figure 32) but, approximately 5 percent light obscuration was noted when the metal and plywood were in contact (Figure 31). No damage to the carpet was visible with either structural configuration after the test. Figure 33 shows the charred condition of the plywood flooring after flame exposure for the panel configuration shown in Figure 32.

Test No. 3 - Flexible Closure Canopy. The panel test material was similar in construction to the flexible closure on the aircraft loading walkway. The canopy material was of composite construction comprising a weather resistant ply of 10-ounce neoprene-coated nylon fabric, one ply of treated asbestos fabric, one ply of 1/2-inch thick refractory felt, and one ply of 4-ounce fire retardant muslin. There was no metallic reinforcement employed in the fabrication of the canopy material. The canopy fabric is shown installed in the sample housing in Figure 34 prior to flame exposure.

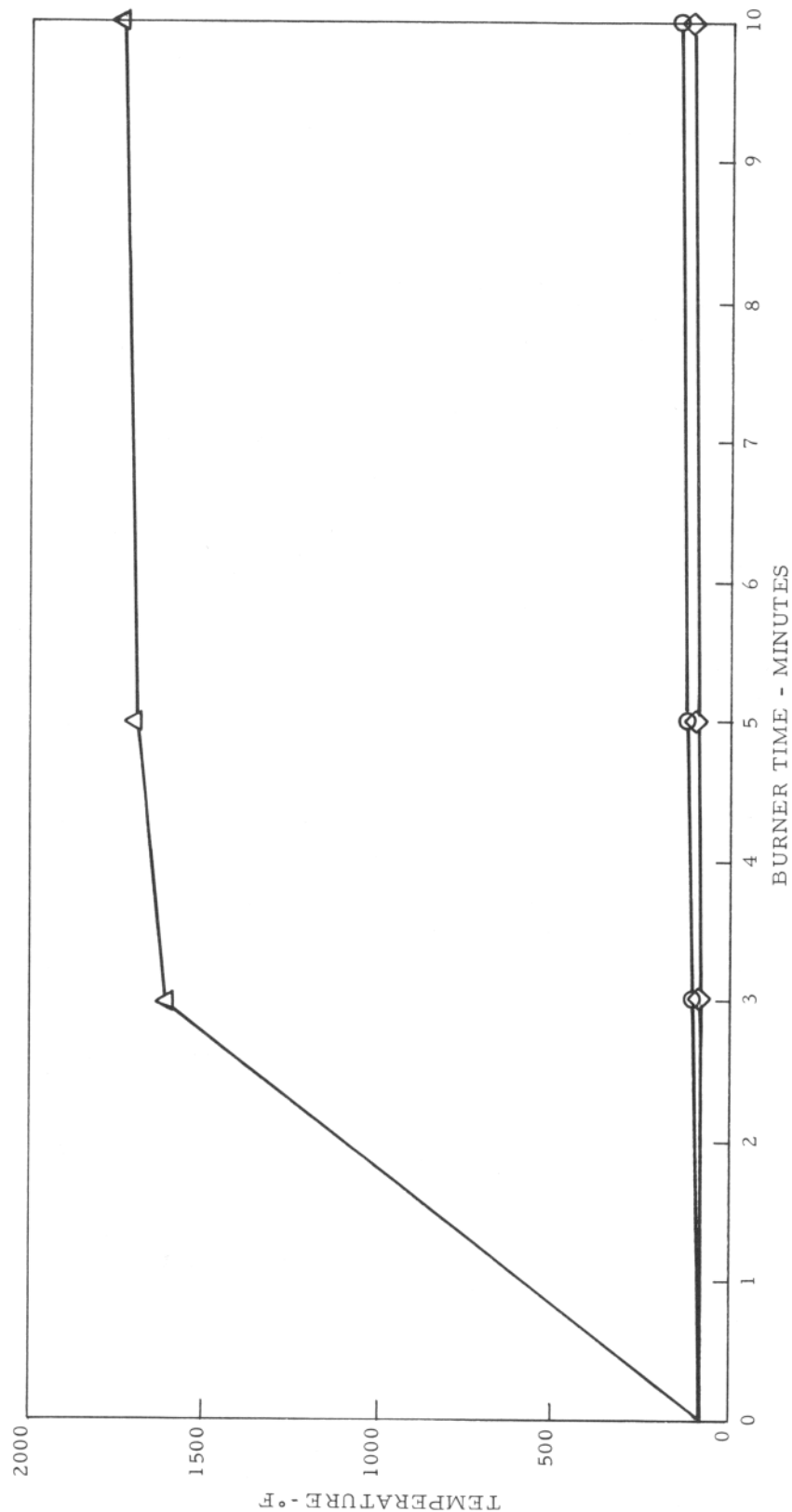
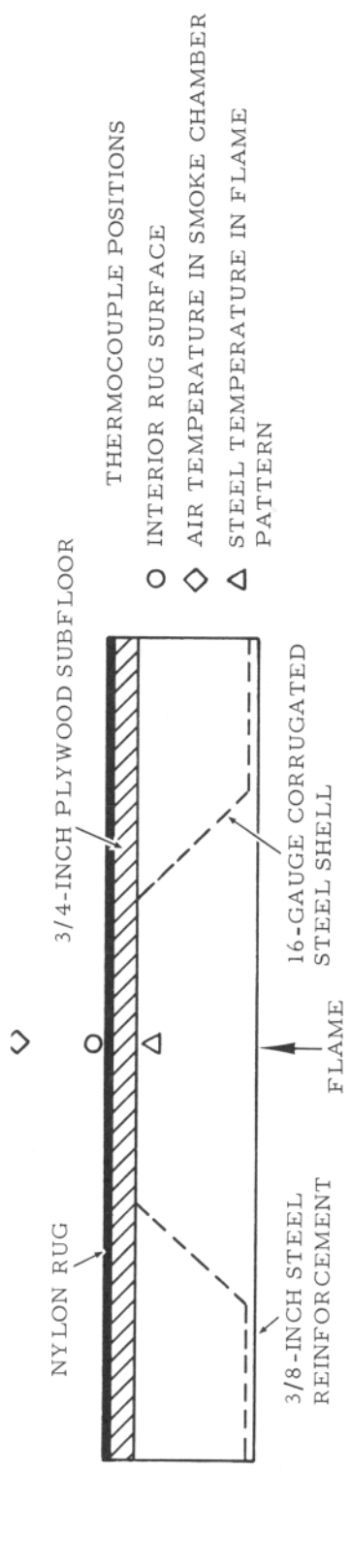


FIGURE 31. THERMAL EFFECTS ON A REPRESENTATIVE WALKWAY FLOOR PANEL WHERE THE CORRUGATED METAL AND PLYWOOD ARE ADJACENT TO ONE ANOTHER

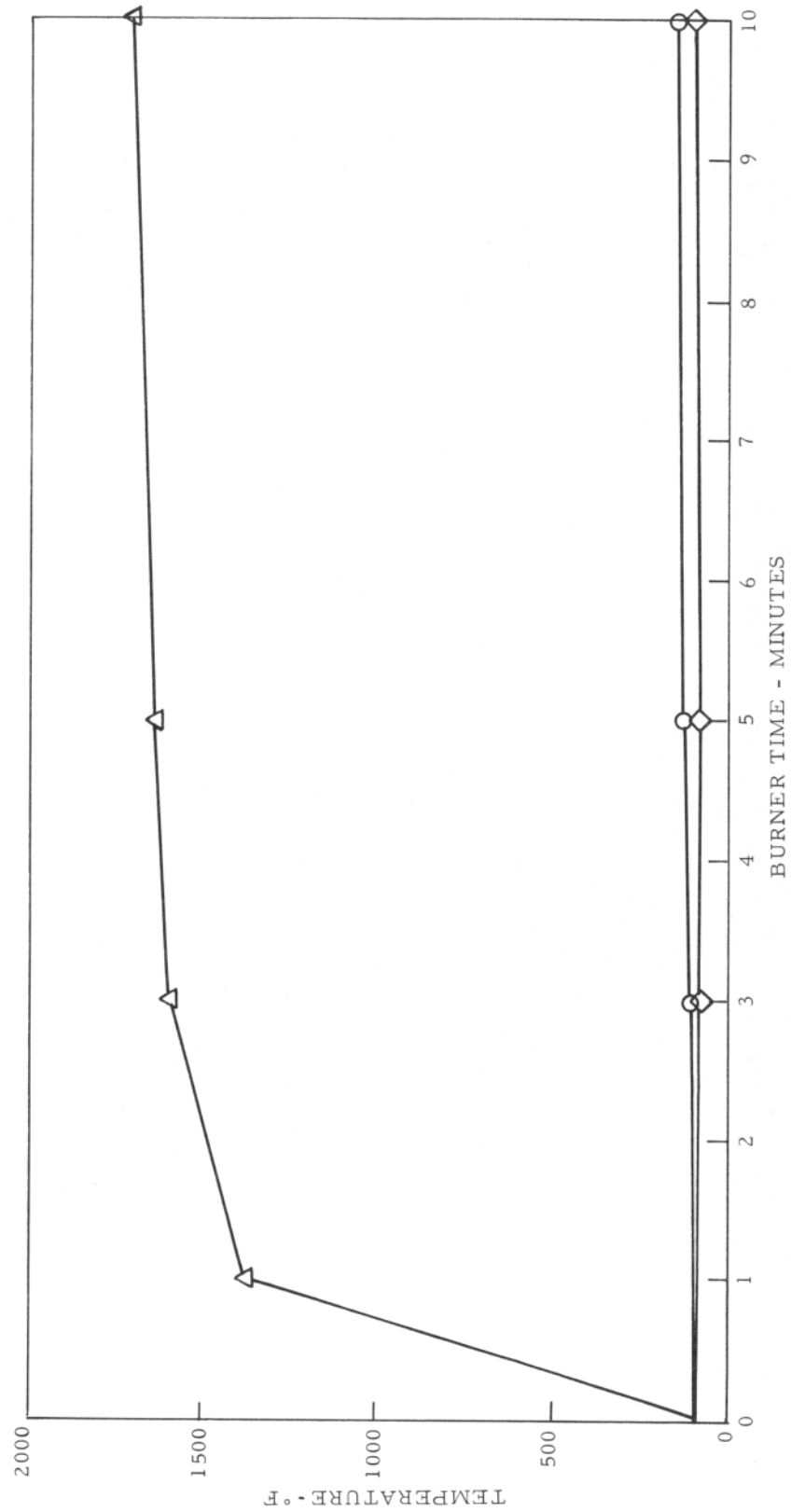
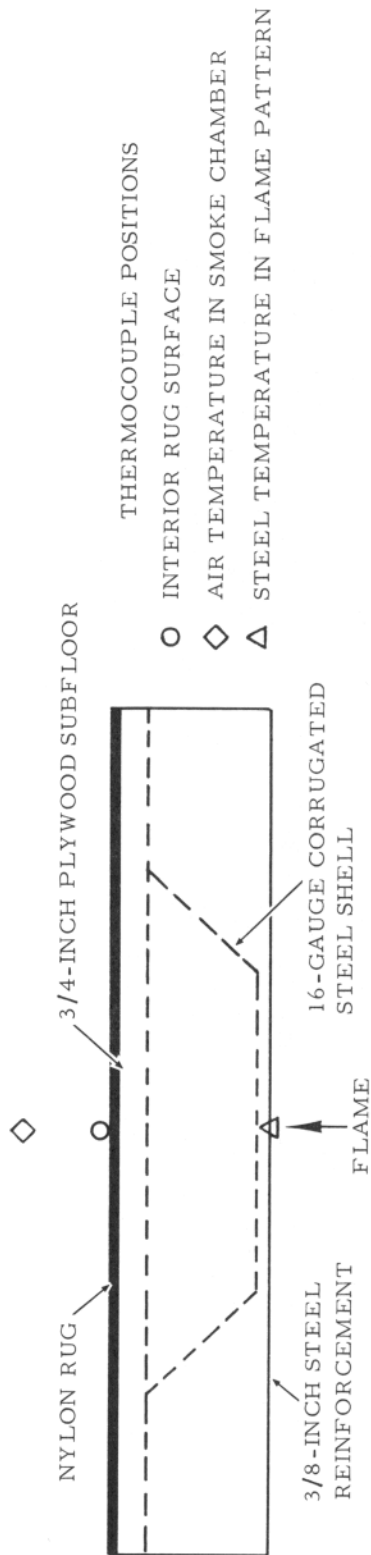


FIGURE 32. THERMAL EFFECTS ON A REPRESENTATIVE WALKWAY FLOOR PANEL WHERE THE CORRUGATED METAL AND PLYWOOD FLOORING ARE SEPARATED BY AN AIRSPACE



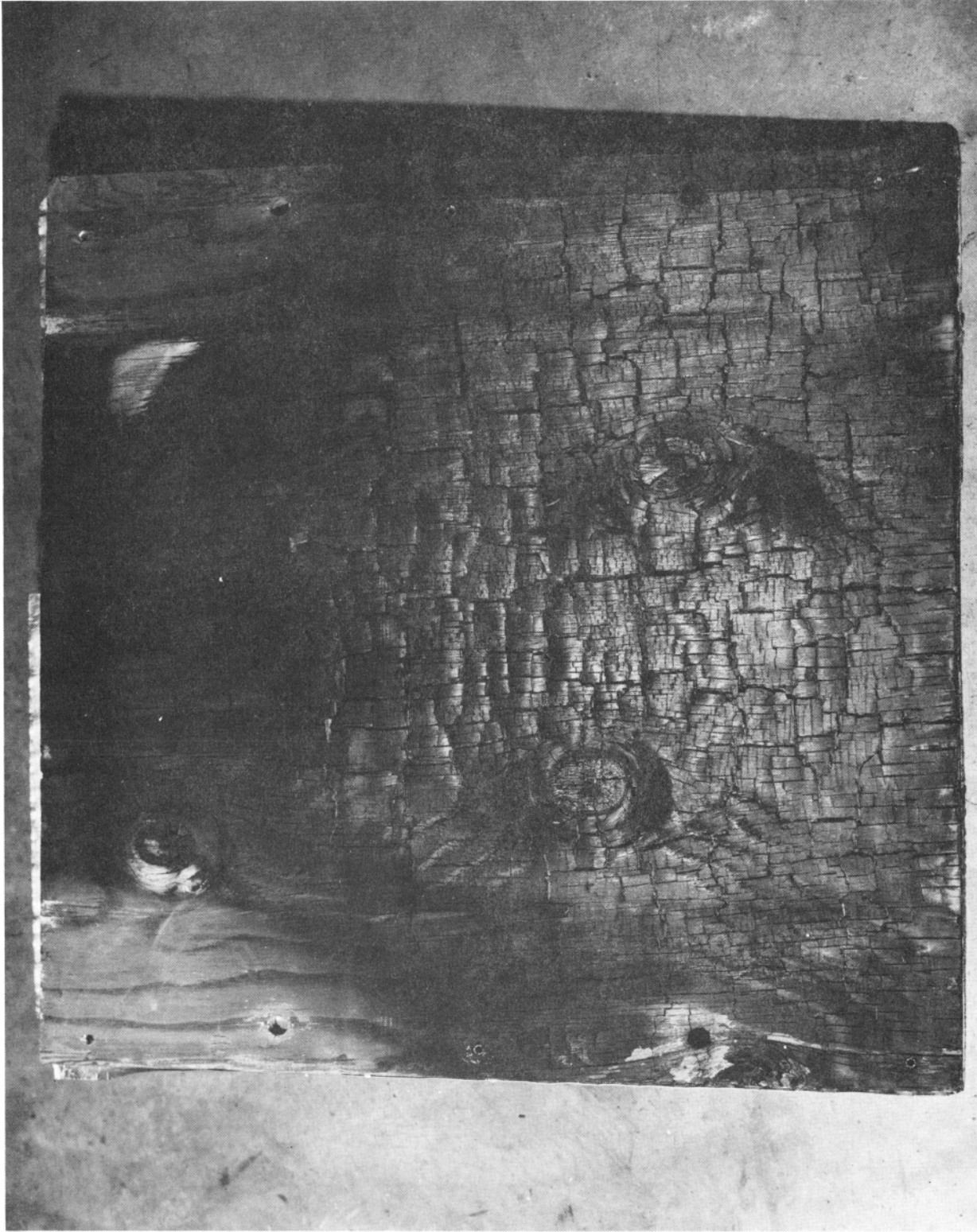


FIGURE 33. CHARRING OF THE PLYWOOD FLOORING SEPARATED FROM THE CORRUGATED METAL BY AN AIRSPACE

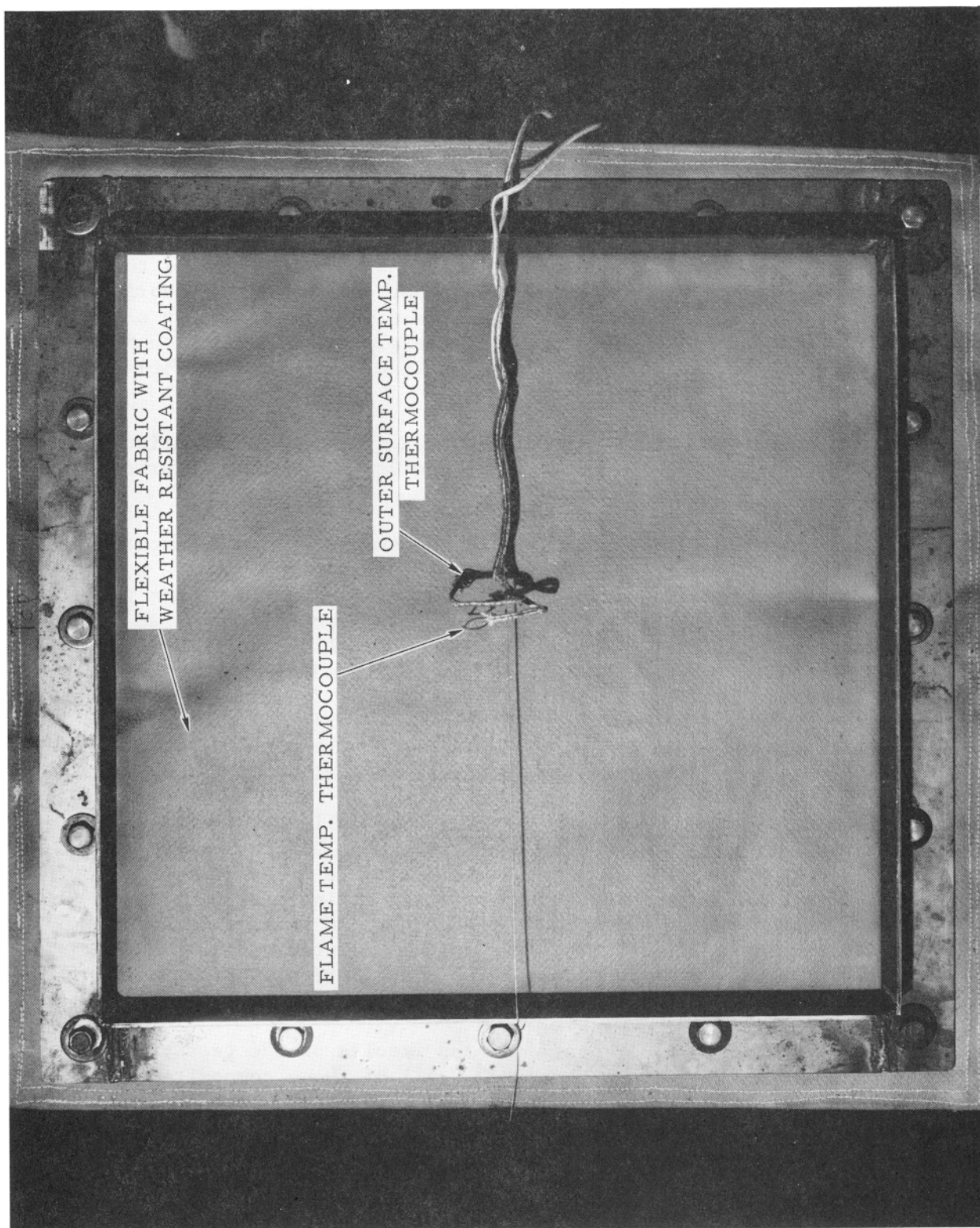


FIGURE 34. FLEXIBLE WALKWAY CLOSURE CANOPY BEFORE FLAME EXPOSURE

The effects of the burner flame impingement on the canopy material are indicated by the profiles in Figure 35 where temperature rise is plotted as a function of fire exposure time. From these data it is evident that the air temperature within the smoke chamber remained relatively low, reaching 110°F after 5 minutes and a maximum of only 130°F at the end of the 10-minute fire exposure period.

At the outset of the test, significant quantities of smoke were released from the exterior surface of the panel as a consequence of the pyrolysis and combustion of the weather resistant coating on the fabric. The interior of the smoke chamber also showed a significant buildup of pyrolysis products and smoke generated from the plastic binders used in the manufacture of the fabric, which resulted in 82 percent light obscuration after 5 minutes of fire exposure.

The damage caused by 10 minutes of flame exposure on the exterior surface of the canopy sample is shown in Figure 36A and on the interior surface in Figure 36B.

FLOOR STRUCTURE MODIFICATIONS. From all of these data it was apparent that the most serious problem confronting passengers passing through the walkway would be caused by smoke, and the primary source of smoke within the walkway was the pyrolysis of the underside of the plywood flooring adjacent to the corrugated steel shell. Therefore, the most effective means for controlling smoke within the walkway would be to provide adequate insulation between the exterior corrugated steel and the plywood flooring to reduce the rate of heat transfer or by employing a thermally stable structural floor material. Accordingly, four 2-foot-square modified floor panels were prepared for evaluation in the laboratory apparatus described in Appendix E.

Three of the modified test panels were a composite of 16-gauge corrugated steel sheets and several different thicknesses and configurations of asbestos-cement board, untreated plywood and synthetic fiber carpeting. The various components were assembled by riveting as indicated in Figure 37, and the panel bolted to the smoke chamber housing. In these experiments the test panels were modified by drilling 1-inch diameter holes through each corner of the structure to equalize the distribution of smoke and pyrolysis products within the smoke chamber.

The configuration of each floor panel and the results of the tests are presented in Appendix F, Tests 1 through 3. All of these composite panels were found to be unsatisfactory when subjected to fire exposure because of the structural failure of the asbestos-cement board due to differential thermal expansion and cracking, which exposed the plywood surface causing the generation of large quantities of smoke and gaseous pyrolysis products. A typical example of the thermal and structural damage to an asbestos-cement board in one test panel is shown in Figure 38A.

During the course of the first experiment employing a composite panel, it was evident that when the plywood flooring was riveted to the corrugated steel in the configuration shown in Figure 38A the rivet in the

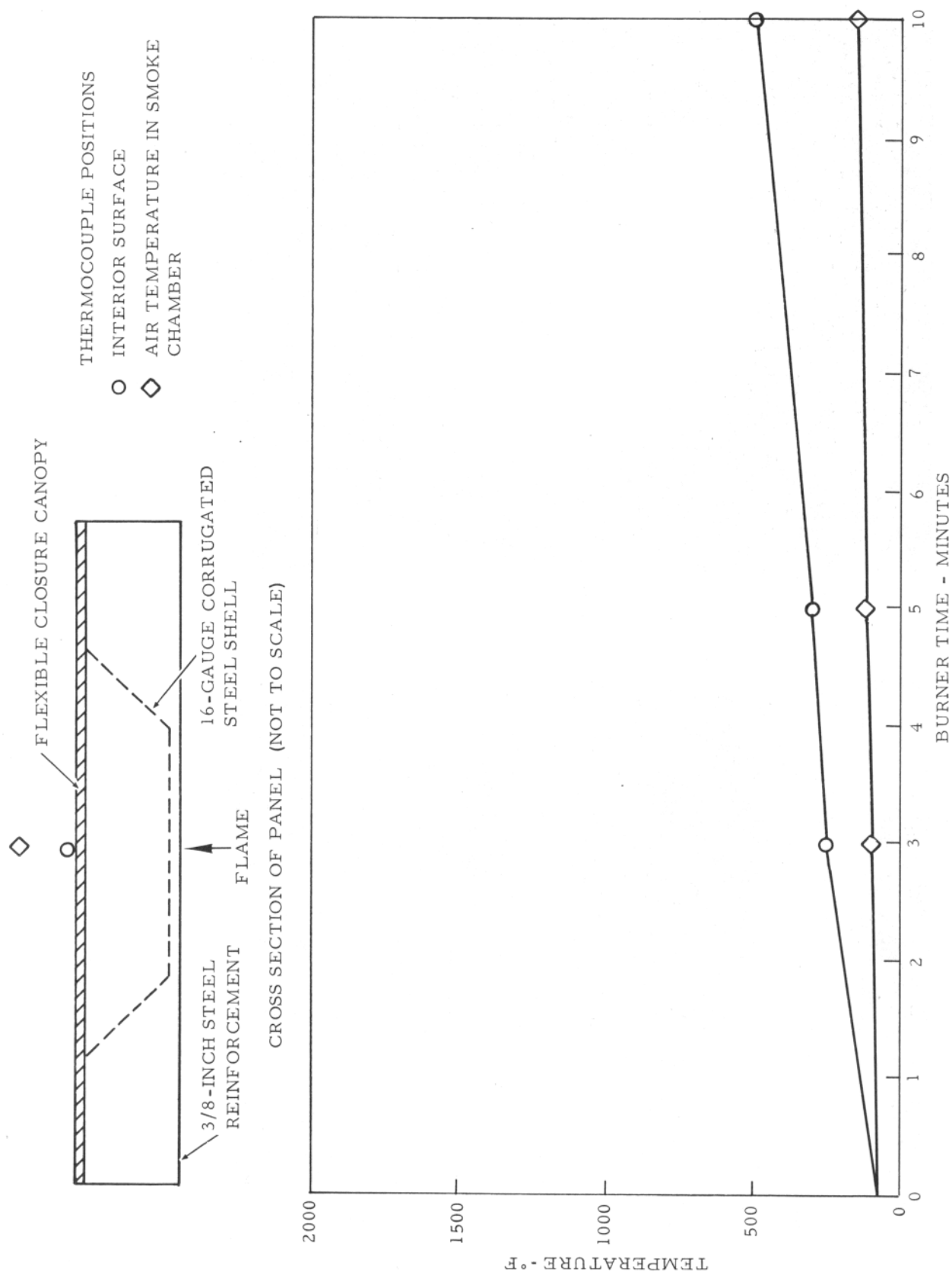
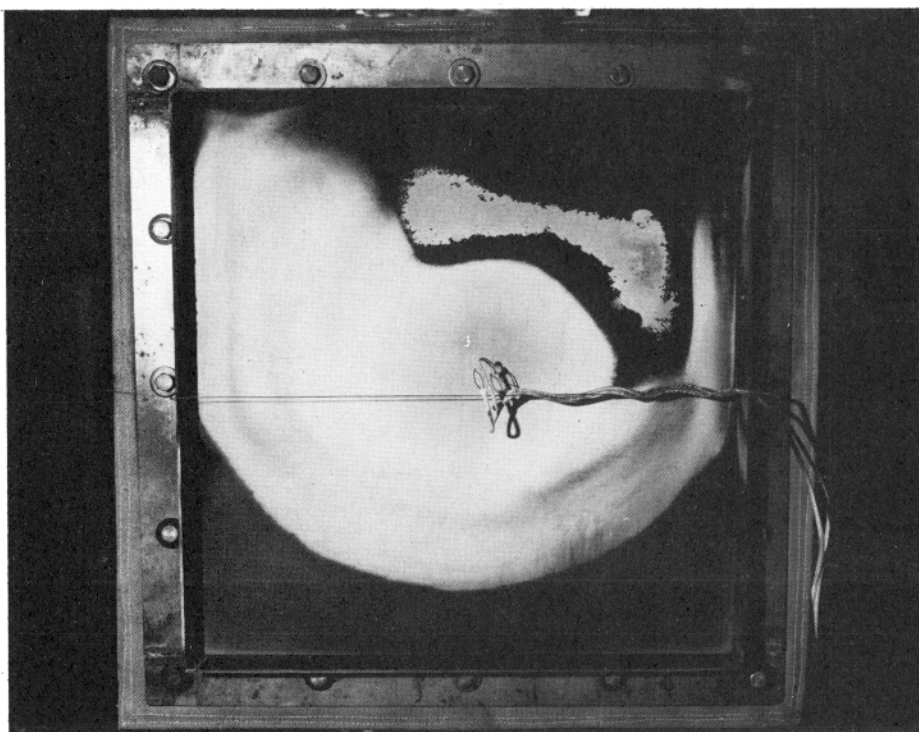
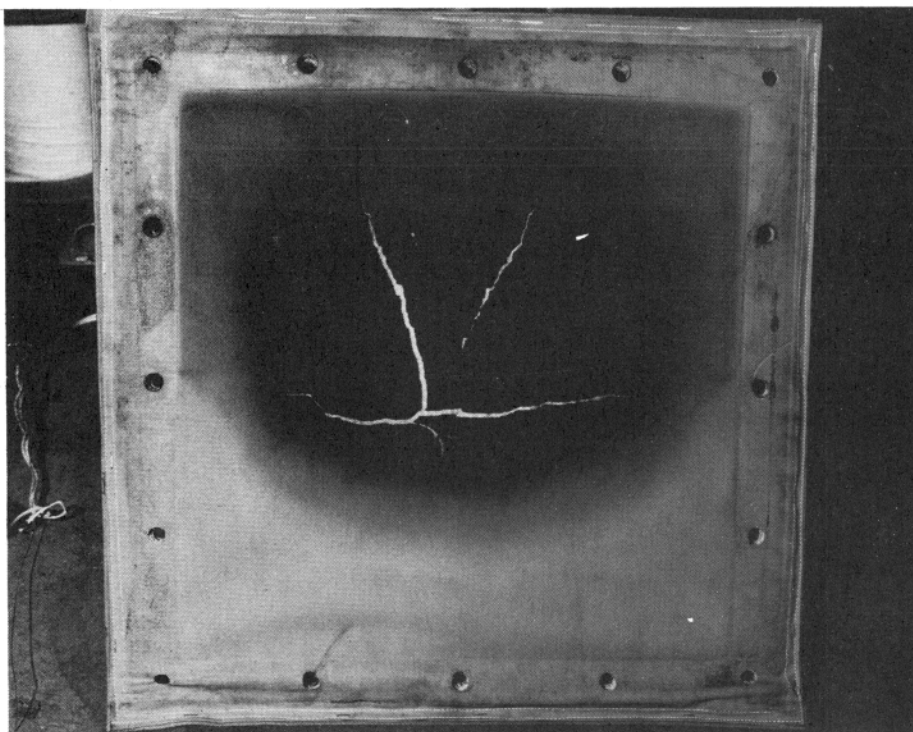


FIGURE 35. THERMAL EFFECTS ON THE WALKWAY CLOSURE CANOPY AS A FUNCTION OF FIRE EXPOSURE TIME





a. Exterior View After 10 Minutes Flame Exposure.



b. Interior View After 10 Minutes Flame Exposure.

FIGURE 36. DAMAGE TO THE WALKWAY CLOSURE CANOPY CAUSED BY FIRE EXPOSURE

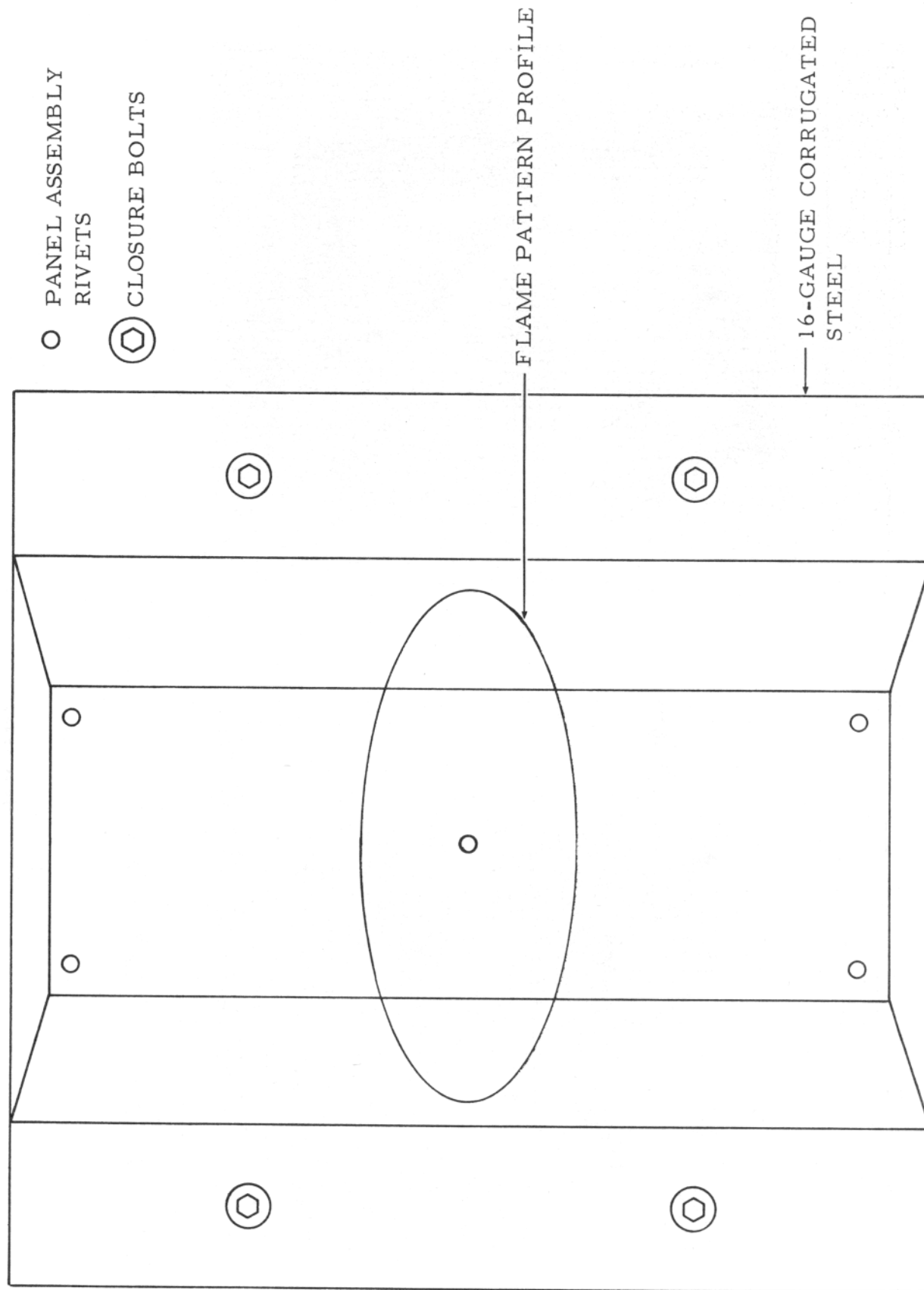
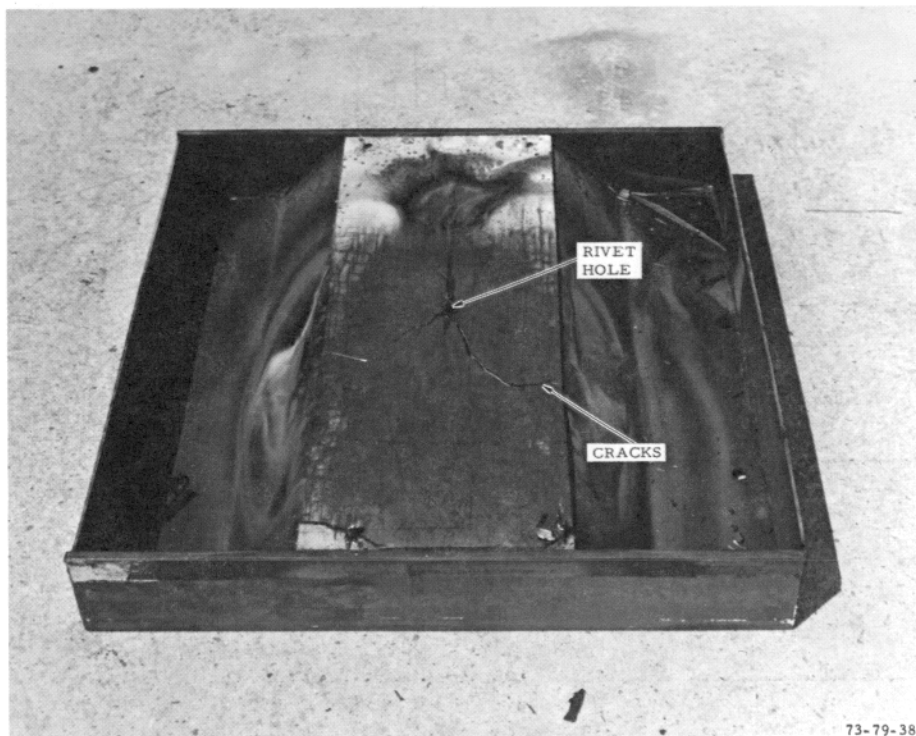
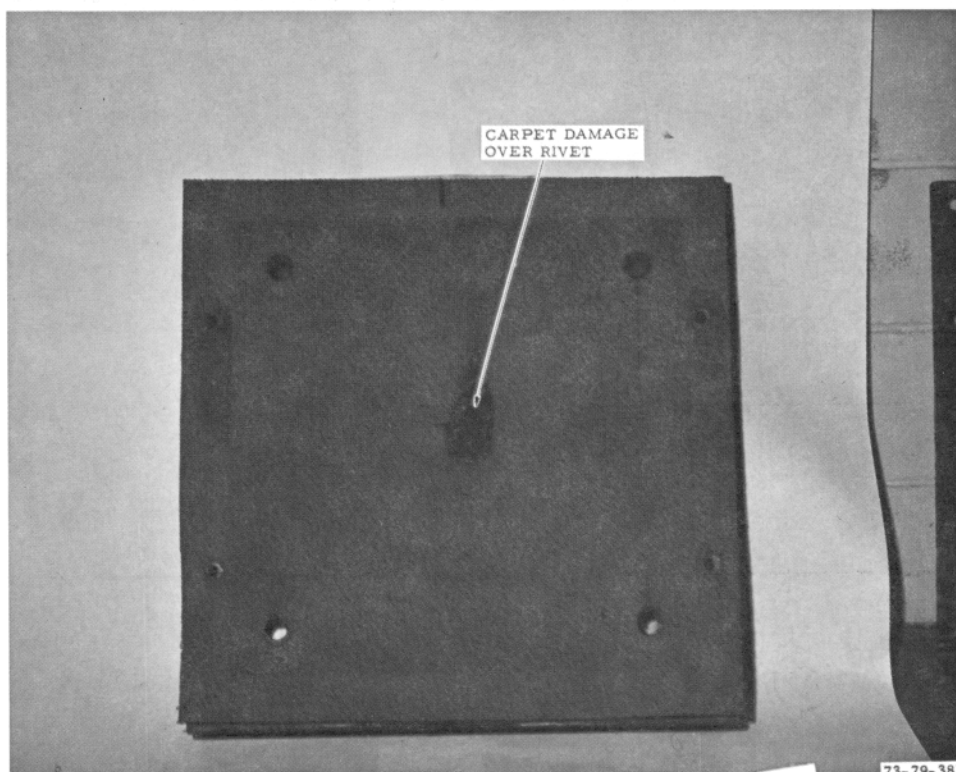


FIGURE 37. EXTERIOR CONFIGURATION OF THE MODIFIED FLOOR TEST PANELS



73-79-38A

A. THERMAL CRACK IN THE ASBESTOS-CEMENT BOARD



73-79-38B

B. RUG DAMAGE AT POINT OF RIVET CONTACT

FIGURE 38. TYPICAL THERMAL AND STRUCTURAL DAMAGE TO THE ASBESTOS-CEMENT BOARD MODIFIED FLOOR PANELS



center of flame impingement acted as a thermal conductor causing damage to the carpet shown in Figure 38B. To overcome this condition it was found necessary to countersink the rivet heads approximately 1/2 inch below the plywood surface and to fill the void with an inert insulating compound to retard the rate of heat transfer from the external metal shell to the underside of the rug.

The configuration of the fourth floor panel is indicated in Appendix F, Test 4. It was of similar composite construction to the three previous panels but employed a 3/4-inch thick structural insulating board in place of the asbestos-cement board and plywood. This structural panel material was found to combine low-thermal conductivity with good dimensional stability and a low order of smoke generation. The low smoke development may be attributed in part to the inorganic materials employed in its manufacture, which include asbestos fibers, diatomaceous silica and hydrothermally produced inorganic binders. Some significant physical and thermal properties of this insulating structural panel material are included in Appendix A.

A summary of the smoke data developed for each of the four modified floor panels is presented in Figure 39 where light transmission, expressed in percent, is plotted as a function of time after the start of flame impingement on the test specimen.

The overall results of the small-scale modified floor panel tests tend to indicate that, by employing a thermally stable structural floor panel or by providing adequate thermal and structurally stable insulation between the corrugated steel and plywood flooring, the quantity of pyrolysis products and smoke can be controlled to assure adequate visibility and maintain satisfactory walkway environmental conditions to provide for safe passenger egress over a period of 5 minutes or longer.

- TEST 1 3/4-INCH PLYWOOD, 1/8-INCH ASBESTOS-CEMENT BEARING PLATE
- TEST 2 3/4-INCH PLYWOOD, 1/8-INCH ASBESTOS-CEMENT BOARD COMPLETE COVERAGE
- △ TEST 3 1/2-INCH PLYWOOD, 3/16-INCH ASBESTOS-CEMENT BEARING PLATE
- ◇ TEST 4 3/4-INCH ASBESTOS-SILICA STRUCTURAL PANEL

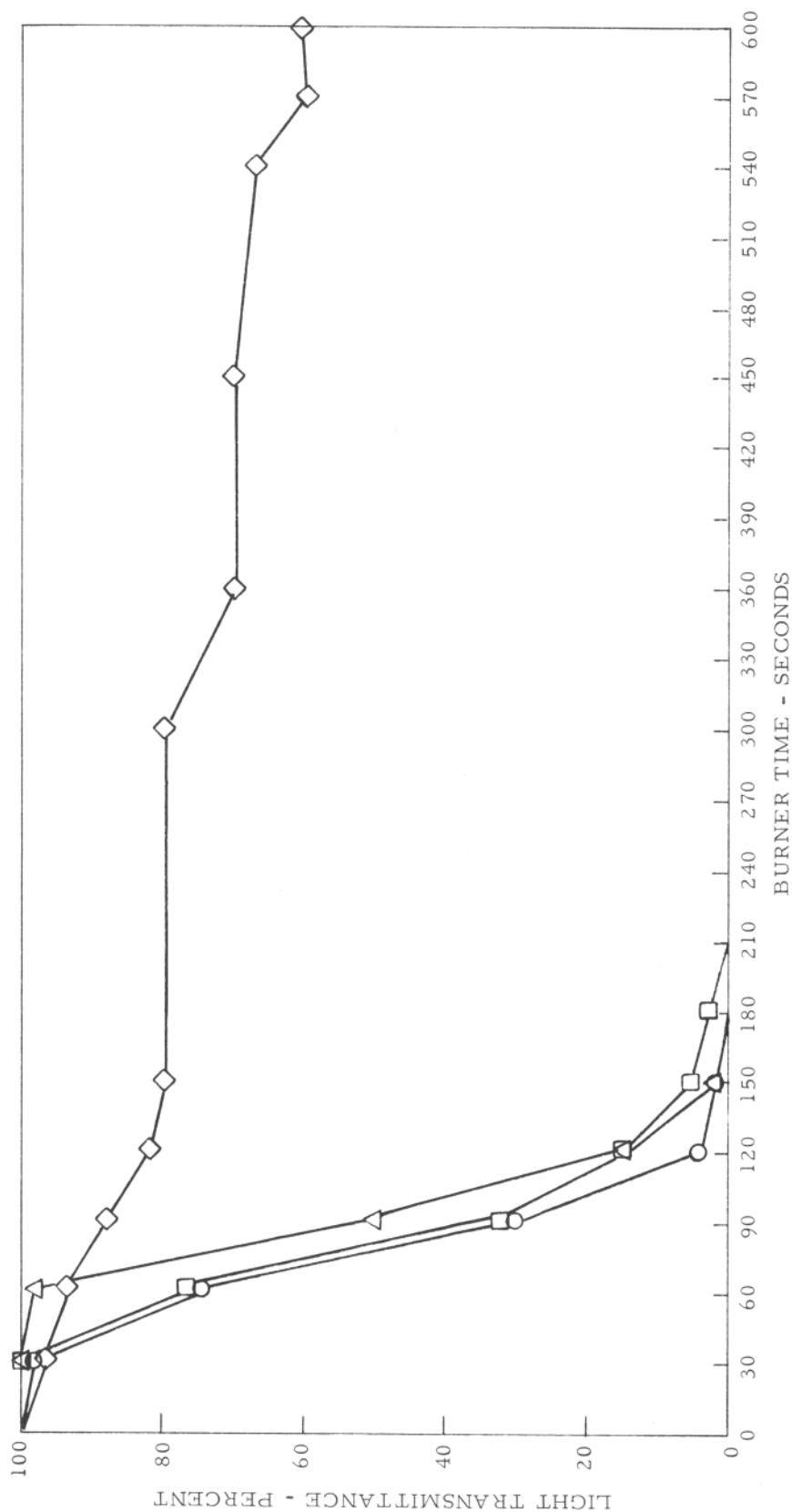


FIGURE 39. SUMMARY OF THE SMOKE DATA FOR THE MODIFIED FLOOR SAMPLE CONFIGURATIONS

## SUMMARY OF RESULTS

The results obtained from the full-scale fire test simulating conditions of an aircraft fuel-spill fire beneath an aircraft loading walkway are:

1. The walkway remained in its original position on the steel supports and no warping or buckling of the exterior corrugated metal skin or structural members was observed after fire exposure.
2. The tensile strength of coupons made from samples of corrugated steel cut from the floor and sidewalls of the walkway after fire exposure was within the anticipated range of 45,000 to 55,000 pounds per square inch for the unexposed metal.
3. Photomicrographs of the sheet metal samples and structural members showed no significant physical modifications caused by thermal exposure but some minor grain coarsening was apparent.
4. The welded seams and longitudinal structural steel members of the aircraft loading walkway showed no significant deterioration after fire exposure.
5. The environmental air temperature and heat flux within the walkway were within the limits of human tolerance over the time required by passengers passing through the walkway at a normal walking stride.
6. Total obscuration of the walkway interior by smoke and pyrolysis products from the plywood flooring occurred within 120 seconds after fuel ignition.
7. The thermal failure of the aircraft bumper (spacer) produced smoke and flame within the interior of the walkway within 30 seconds after fuel ignition.
8. The weather stripping between Tunnels B and C at floor level was completely destroyed during fire exposure which resulted in flame penetration and the ignition of the plywood ramp between the tunnels.
9. The aircraft closure curtain retained its thermal integrity during fire exposure although the exterior neoprene-coated nylon fabric showed evidence of fire damage.
10. The 1,500 cubic feet per minute of fresh air flowing into the walkway contributed to preventing or retarding the penetration of heat and smoke from the exterior free-burning pool fire.
11. The ignition of the plywood pyrolysis products resulted in a flash fire which blew the steel entrance door open 326 seconds after fuel ignition.

12. The interior asbestos-cement wall panels warped during fire exposure which facilitated the penetration of heat and smoke into the interior of the walkway.

13. The 960-square-foot pool fire beneath the walkway was extinguished by two 60-gallon-per-minute handline nozzles dispensing AFFF at a solution application rate of 0.125 gallons per minute per square foot in 65 seconds.

14. One modified 2-foot-square floor sample constructed of thermally stable structural floor paneling demonstrated low thermal conductivity and smoke production when evaluated in small-scale laboratory equipment.

## CONCLUSIONS

Based upon the experiments conducted with the aircraft loading walkway under free-burning pool fire conditions beneath the structure, it is concluded that:

1. The structural integrity of the aircraft loading walkway was maintained throughout the 10-minute fire-exposure period.
2. No significant structural damage to the steel components of the aircraft loading walkway was sustained as a consequence of fire exposure.
3. The environmental air temperature and heat flux were not in themselves limiting factors in providing a safe passenger egress route through the walkway.
4. The parameters limiting the safe egress of passengers through the walkway were the early release of excessive amounts of smoke after fuel ignition and the potential lachrymatory effects produced by pyrolysis products from the plywood flooring.
5. Adequate means should be provided to minimize flame and heat penetration between the telescoping tunnel sections of the walkway.
6. External flame penetration into an aircraft walkway should be minimized by providing a positive flow of fresh air from an external source into the interior during the time it is in use.
7. Interior wall paneling of the walkway should be provided which is thermally and dimensionally stable under fire-exposure conditions.
8. By providing adequate thermally stable insulation between the corrugated steel and floor carpeting, the quantity of pyrolysis products and smoke can be controlled to assure adequate visibility and to maintain satisfactory walkway environmental conditions and provide for safe passenger egress for a period of 5 minutes or longer.

## RECOMMENDATIONS

Based upon the full-scale fire test simulating conditions of a severe fuel-spill fire beneath an aircraft loading walkway it is recommended that:

1. The weather stripping between the telescoping tunnel sections be capable of resisting flame penetration into the interior of the walkway for a period of 5 minutes or longer.
2. The aircraft bumper and closure curtain system be able to resist flame penetration into the walkway for a period of 5 minutes or longer.
3. The construction of aircraft loading walkways preclude the use of wood in direct contact with the external metal skin.
4. The walkway walls and ceiling paneling be thermally and dimensionally stable to prevent heat and smoke from penetrating into the interior of the walkway.
5. Thermally stable materials be employed in the floor construction to provide adequate visibility and to maintain satisfactory walkway environmental conditions for safe passenger egress over a period of 5 minutes or longer.
6. A positive flow of fresh air from an external source be provided to flow into the interior of the walkway to minimize flame penetration from an external fuel-spill fire.



#### REFERENCES

1. National Fire Protection Association, "Standard on Construction and Protection of Aircraft Loading Walkways," NFPA No. 417, 1973.
2. Geyer, George B., "Effect of Ground Crash Fire on Aircraft Fuselage Integrity," Federal Aviation Administration, National Aviation Facilities Experimental Center, Atlantic City, New Jersey, Interim Report No. NA-69-37 (RD-69-46), December 1969.
3. Department of the Air Force, "Air Force Pamphlet AFP 161-18," December 1968.



## APPENDIX A

### ANCILLARY CONSTRUCTION COMPONENTS OF THE AIRCRAFT LOADING WALKWAY

The following information concerning the major ancillary construction components of the aircraft loading walkway was supplied by the manufacturer and comprised the following items:

#### STEEL FLANGE PLATES.

The structural support plates employed with the tunnel roller system were fabricated of heat treated alloy steel T-1.

#### AIRCRAFT SPACER.

The aircraft spacer or bumper on the walkway was of the older type and not fireproof.

#### CLOSURE CURTAIN MATERIALS.

The materials employed in fabricating the closure curtain listed in order from outside (fire side) to inside (backside) are:

one ply of 10-ounce neoprene-coated nylon fabric,

one thin (barely opaque) spray coat of Albi Clad No. 89X applied to one ply of No. 439R-coated asbestos fabric,

one ply of 1/2-inch layer 6 PCF refractory felt, and

one ply of 4-ounce muslin, fire retardant Anchor Packing No. 476 (treated).

#### FLOOR CONSTRUCTION.

The floor consisted of 3/4-inch-thick standard plywood (non-fire-retarding) and covered by a commercial grade of carpet.

#### CARPET SPECIFICATIONS.

Manufacturer:	Commercial Carpet Corporation
Brand:	Densylon
Quality:	Zenith
Pile Fiber:	100 percent continuous filament nylon
Backing:	Sponge rubber bonded 0.20-inch thick, overall thickness 0.35 inch.

STRUCTURAL PANEL MATERIALS, PHYSICAL AND THERMAL PROPERTIES.

<u>Property</u>	<u>Asbestos-Cement Board</u>	<u>Asbestos-Silica Board</u>
Density (Dry), lb/cu ft, minimum		36
Up to 7/8" thickness	100	
Over 7/8" thickness	95	
Moisture Content (Normal), Percent of dry weight	5 to 13	5
Water Absorption, Percent of dry weight, maximum (after 48 hour immersion)	22	
Transverse Strength (Dry), psi. (Modulus of Rupture)		1200
1/4" thickness	4500	
3/8" to 7/8" thickness	4000	
Over 7/8" thickness	3500	
Compressive Strength (Normal), psi.		
1/4" thickness	16000	
3/8" to 7/8" thickness	14000	
Over 7/8" thickness	12000	14000
Tensile Strength (Normal), psi. Parallel to face of sheet	1400	420
Shear Strength (Normal), psi.		
1/4" thickness	4000	
3/8" to 7/8" thickness	3500	
Over 7/8" thickness	3000	
Normal to face of sheet		700
Thermal Expansion, in./in./°F (Avg. over range of temp. up to 400°F)	5.0 x 10 <sup>-6</sup>	
(Avg. up to 250°F shrinkage thereafter)		1.3 x 10 <sup>-6</sup>
Maximum Service Temperature, °F	600	1200
Thermal Conductivity, Btu. in./sq ft/°F/hr	4.5	0.76
Fire Hazard Classification (Listed under Underwriters' Laboratories, Inc. Label Service Guide, No. 40 U8. 13)		
Flame Spread	0	0
Fuel Contributed	0	Negligible
Smoke Developed	0	0

APPENDIX B

INSTRUMENTATION THERMOCOUPLE POSITIONS OF THE AIRCRAFT LOADING WALKWAY



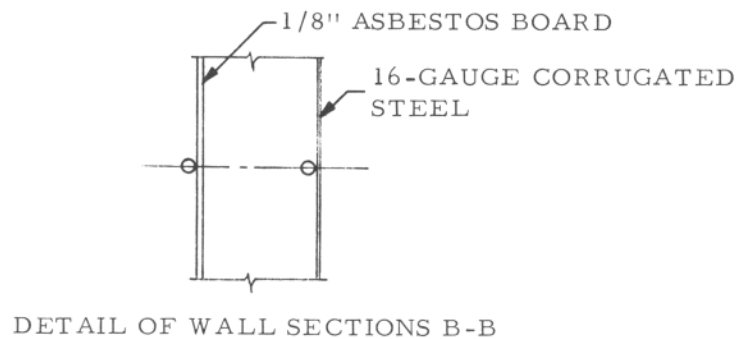
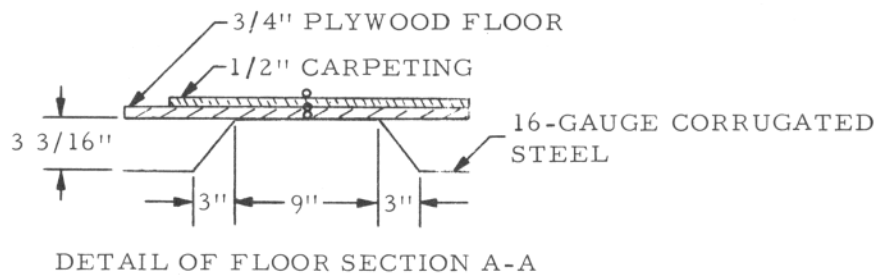
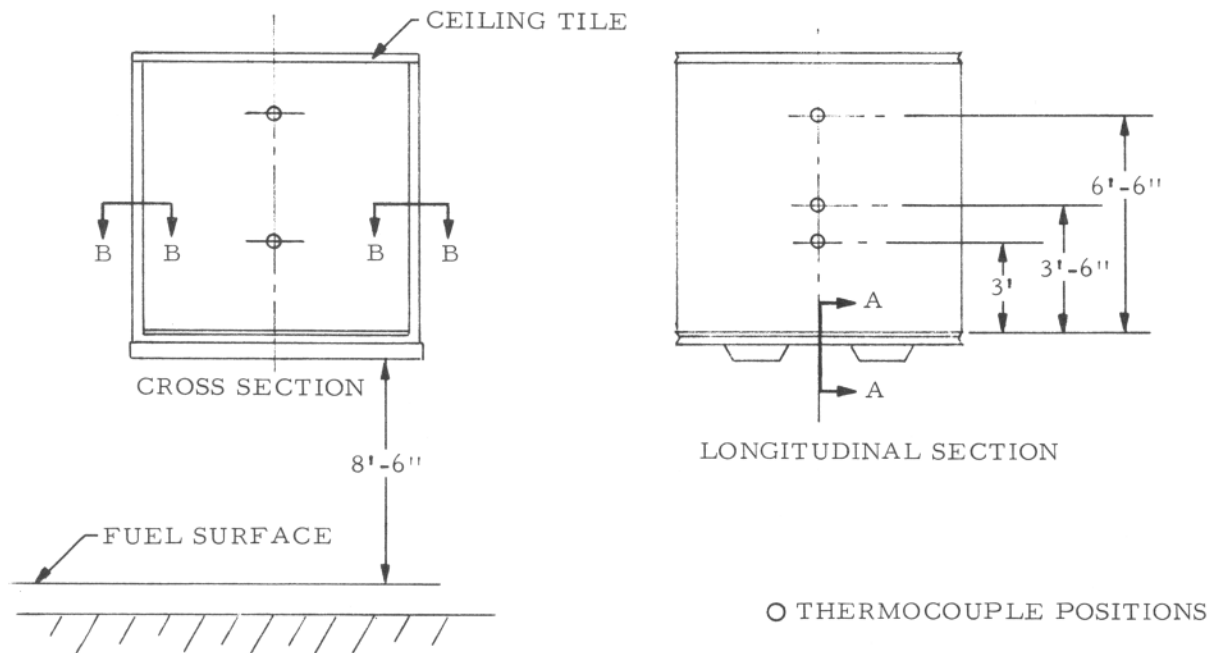


FIGURE B-1. AIRCRAFT LOADING WALKWAY THERMOCOUPLE POSITIONS AT STATION W



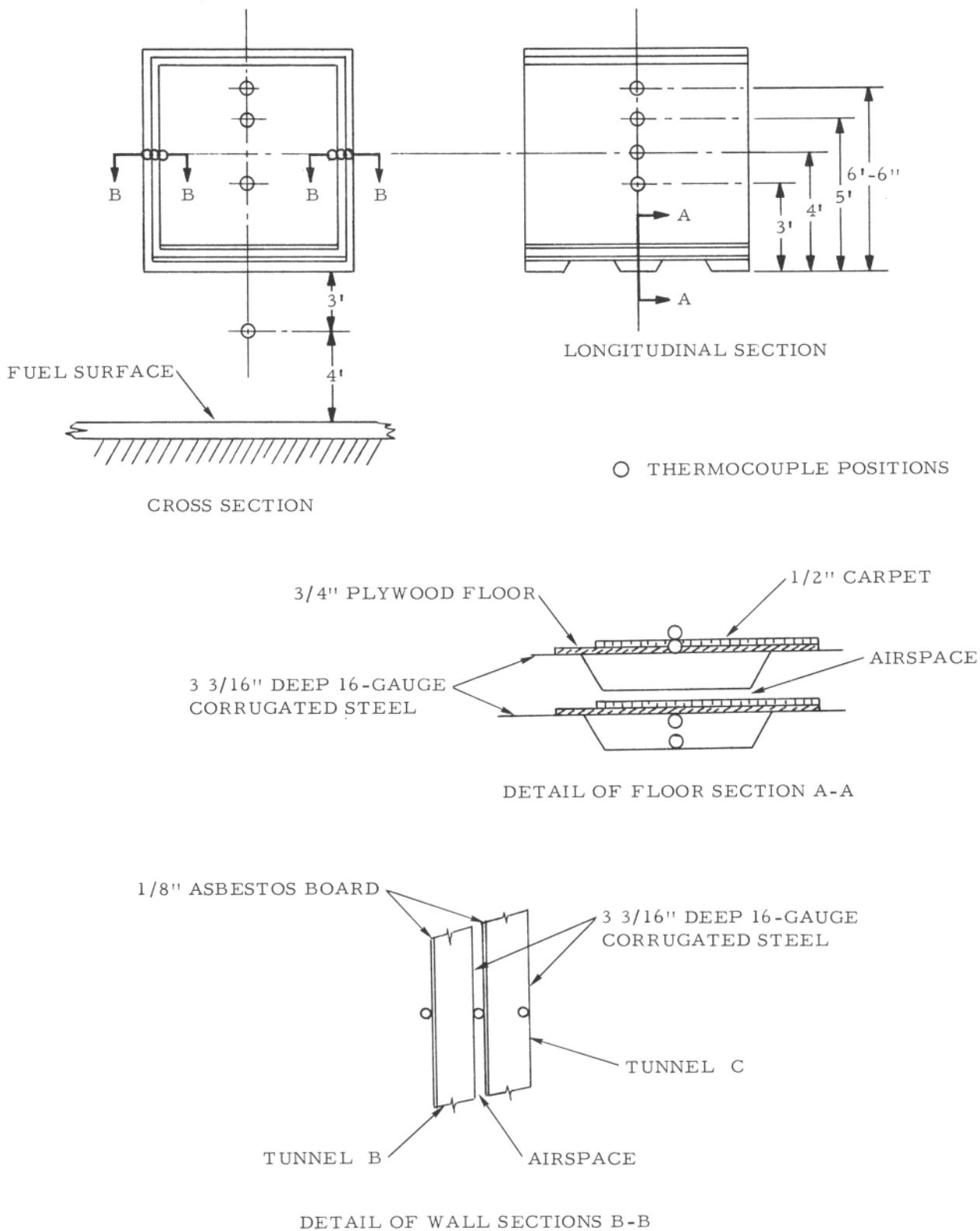


FIGURE B-2. AIRCRAFT LOADING WALKWAY THERMOCOUPLE POSITIONS AT STATION X

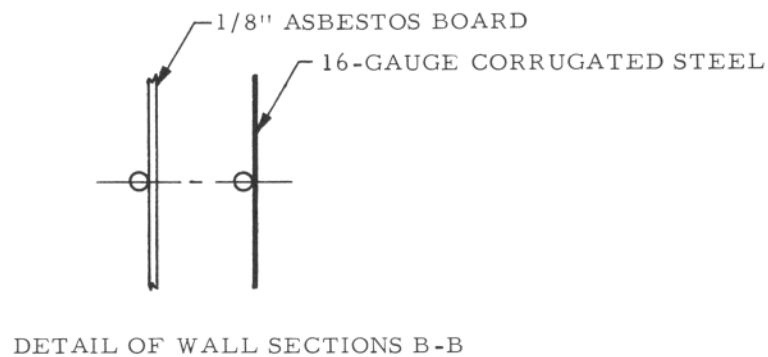
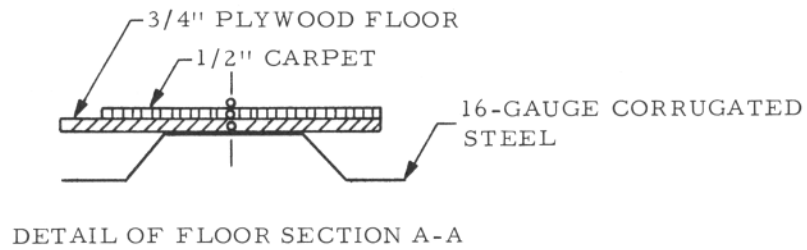
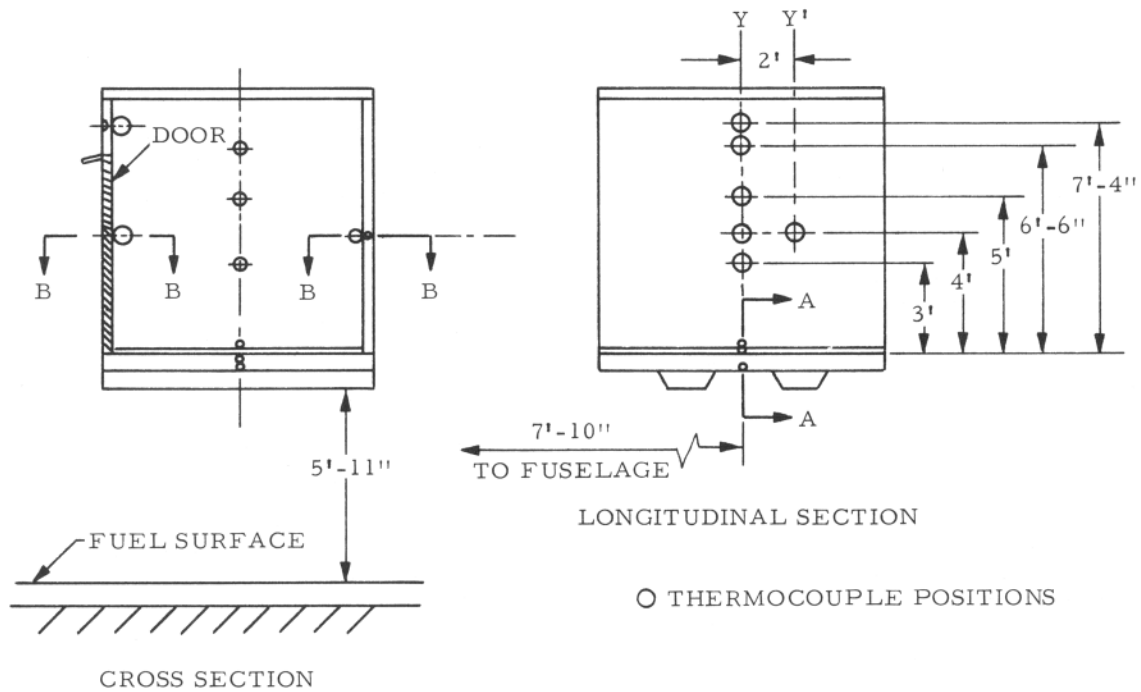


FIGURE B-3. AIRCRAFT LOADING WALKWAY THERMOCOUPLE POSITIONS AT STATION Y AND Y'

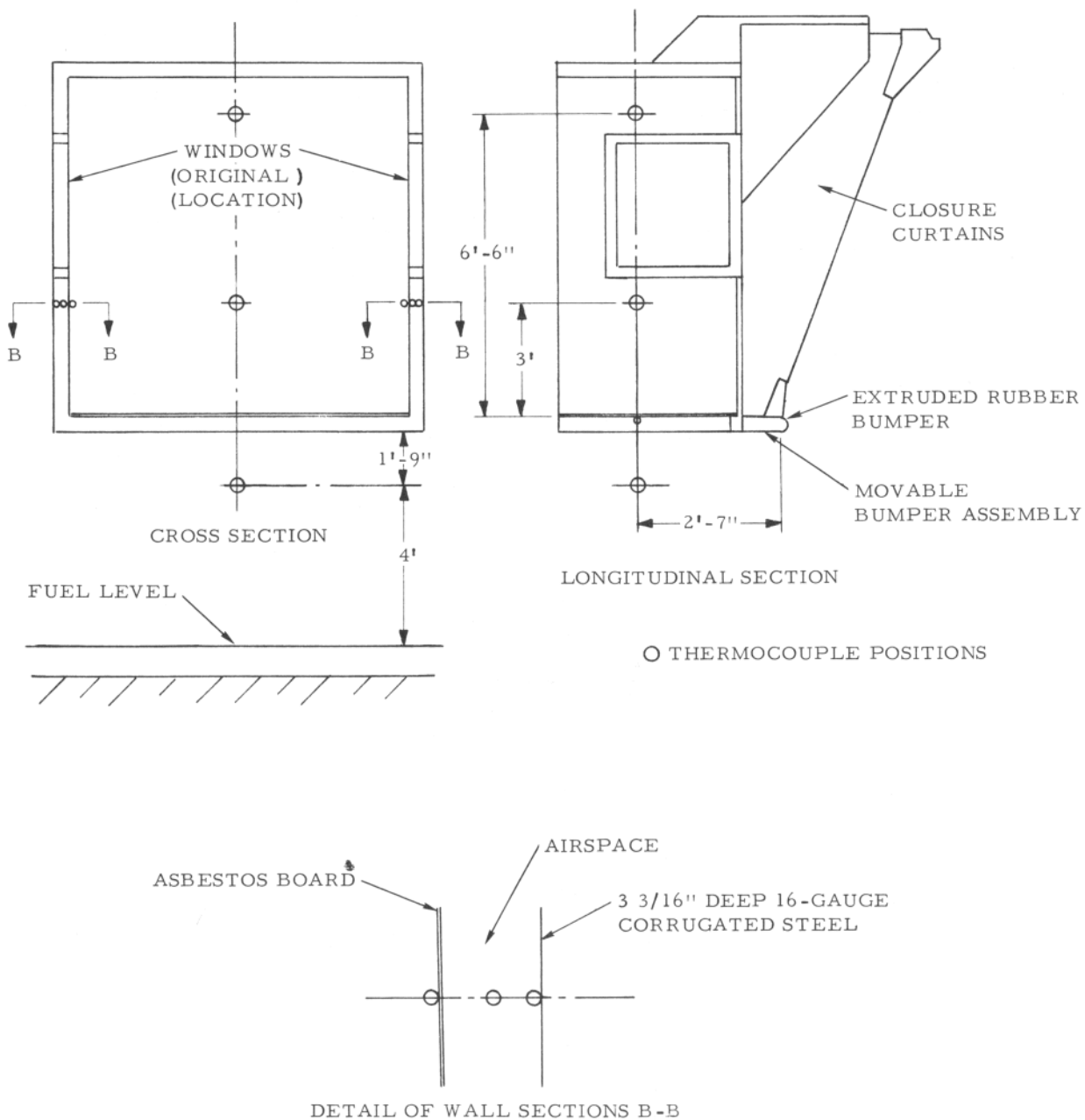


FIGURE B-4. AIRCRAFT LOADING WALKWAY THERMOCOUPLE POSITIONS AT STATION Z

APPENDIX C

TIME-TEMPERATURE THERMOCOUPLE PROFILES



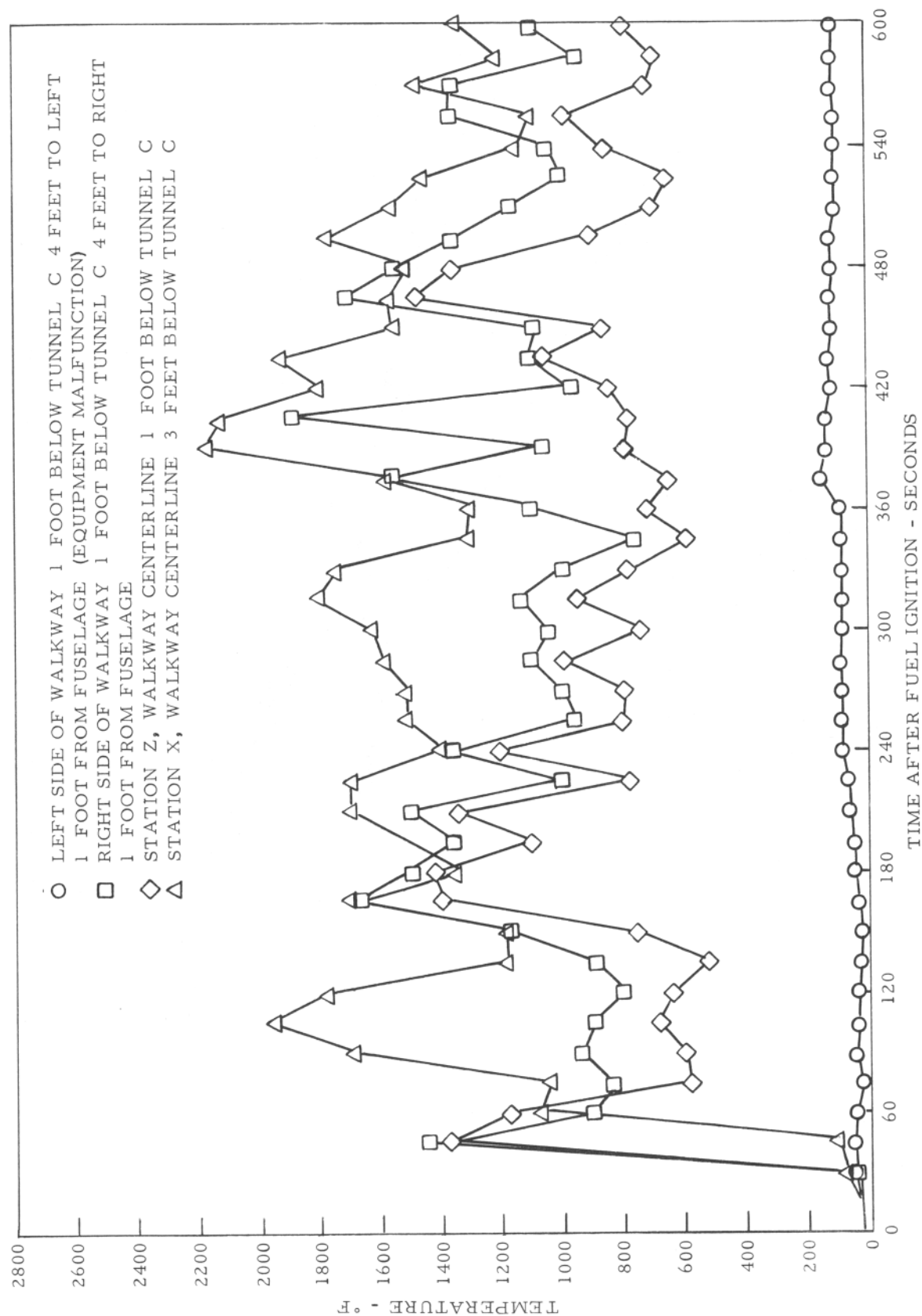


FIGURE C-1. FIRE PIT FLAME TEMPERATURES AS A FUNCTION OF TIME AFTER FUEL IGNITION

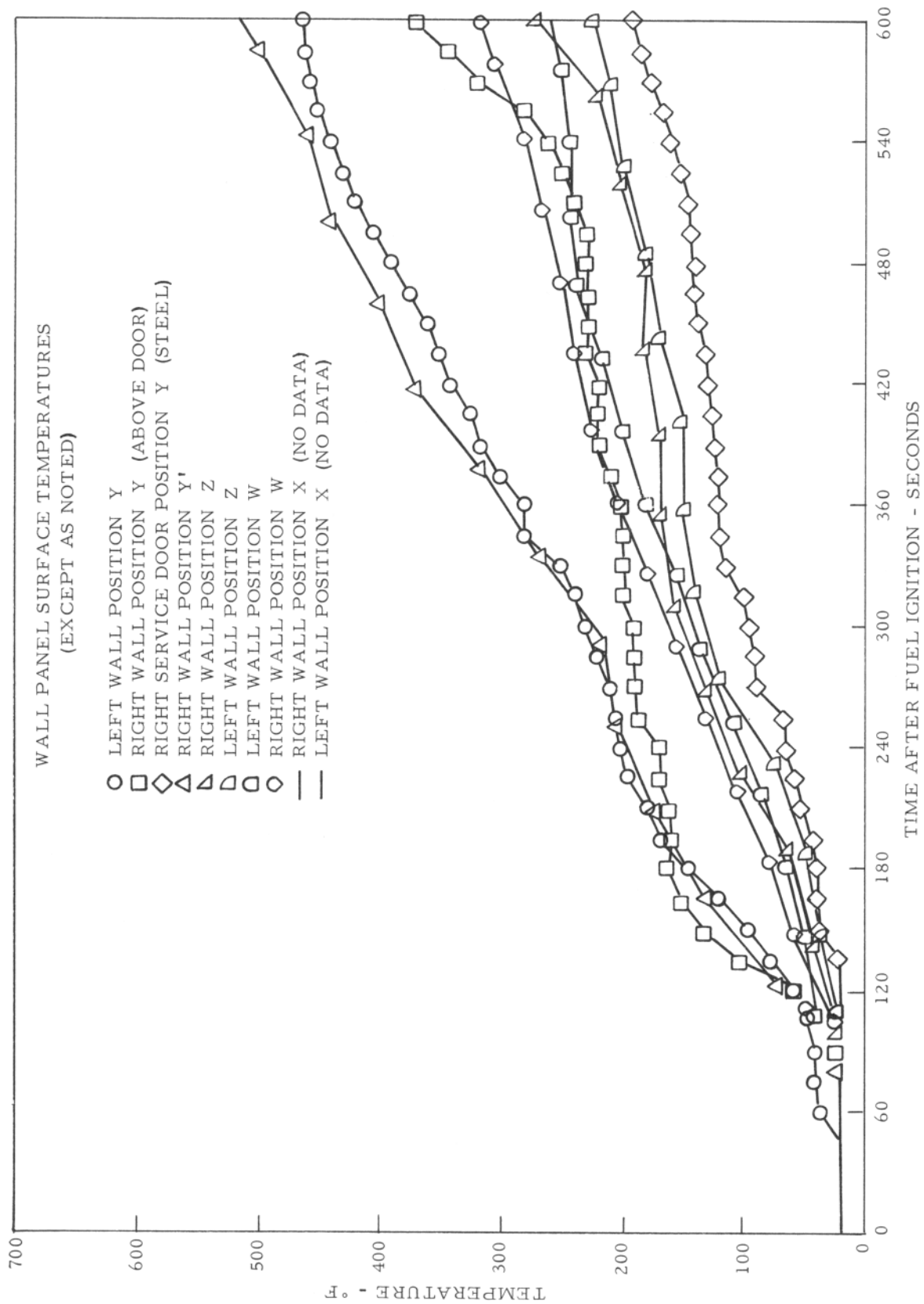


FIGURE C-2. INTERNAL WALL SURFACE TEMPERATURE AS A FUNCTION OF TIME AFTER FUEL IGNITION



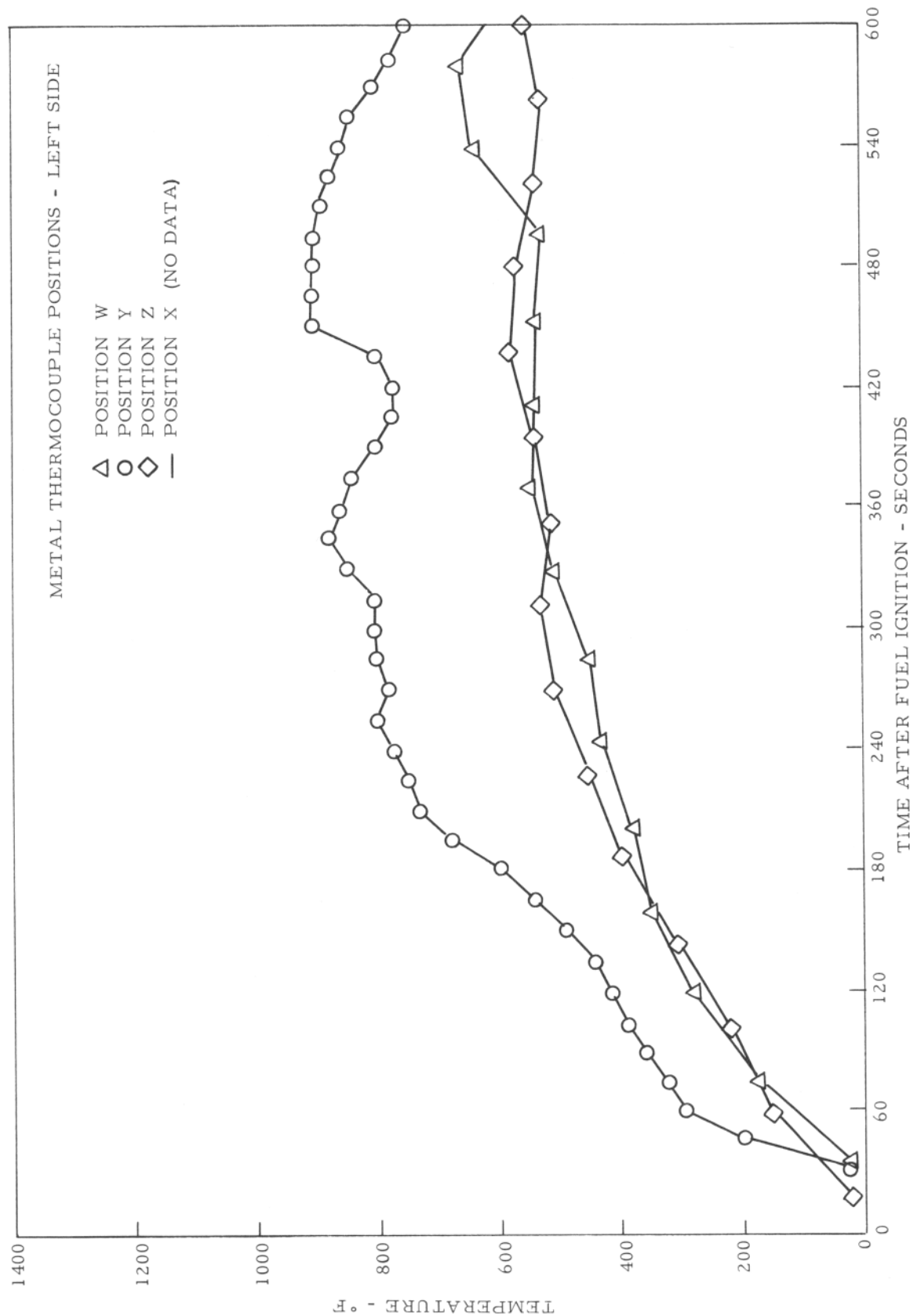


FIGURE C-3. TEMPERATURE ON THE LEFT SIDE EXTERIOR METAL SURFACE OF THE AIRCRAFT LOADING WALKWAY

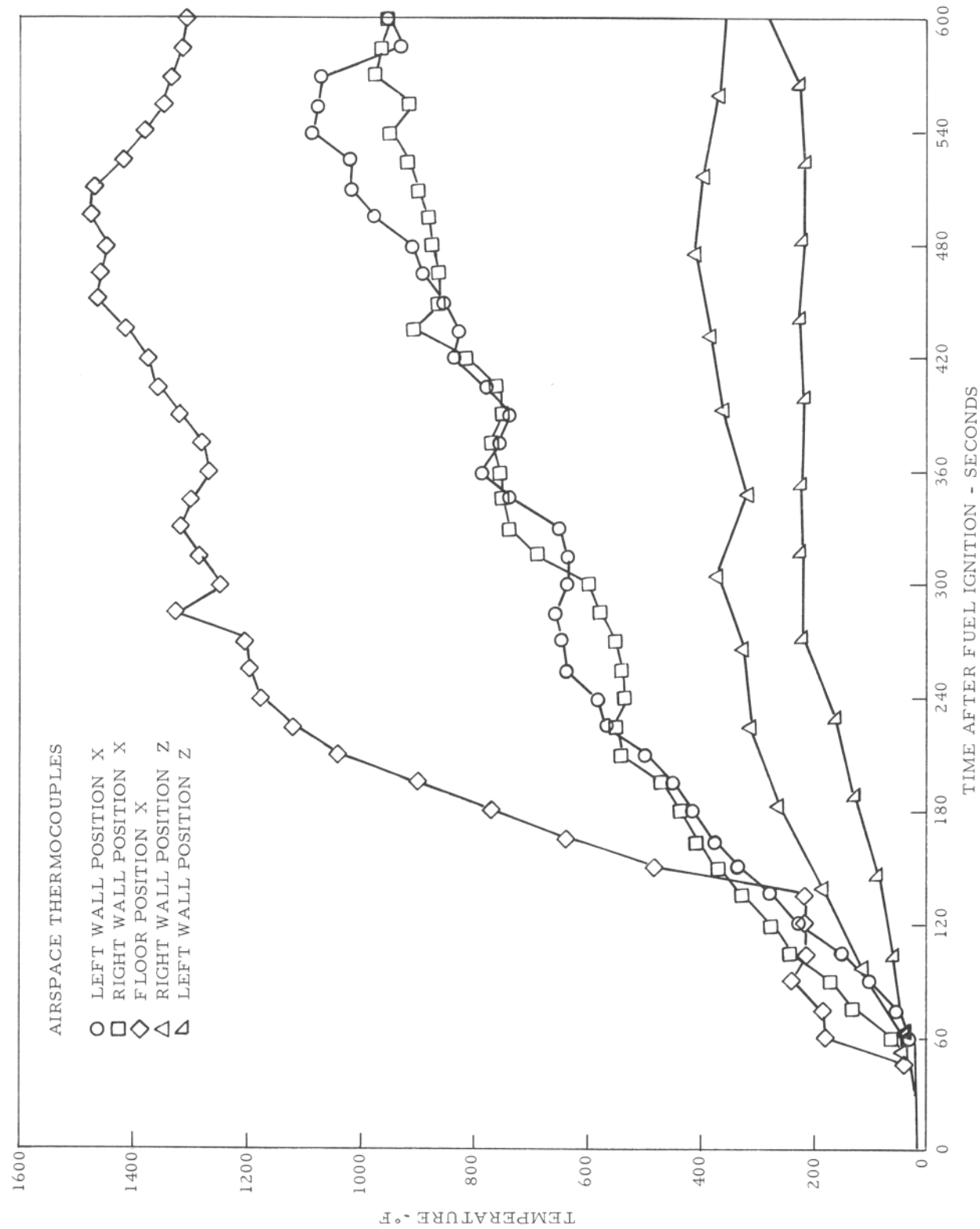


FIGURE C-4. ENCLOSED FLOOR AND WALL AIRSPACE TEMPERATURES OF THE AIRCRAFT LOADING WALKWAY

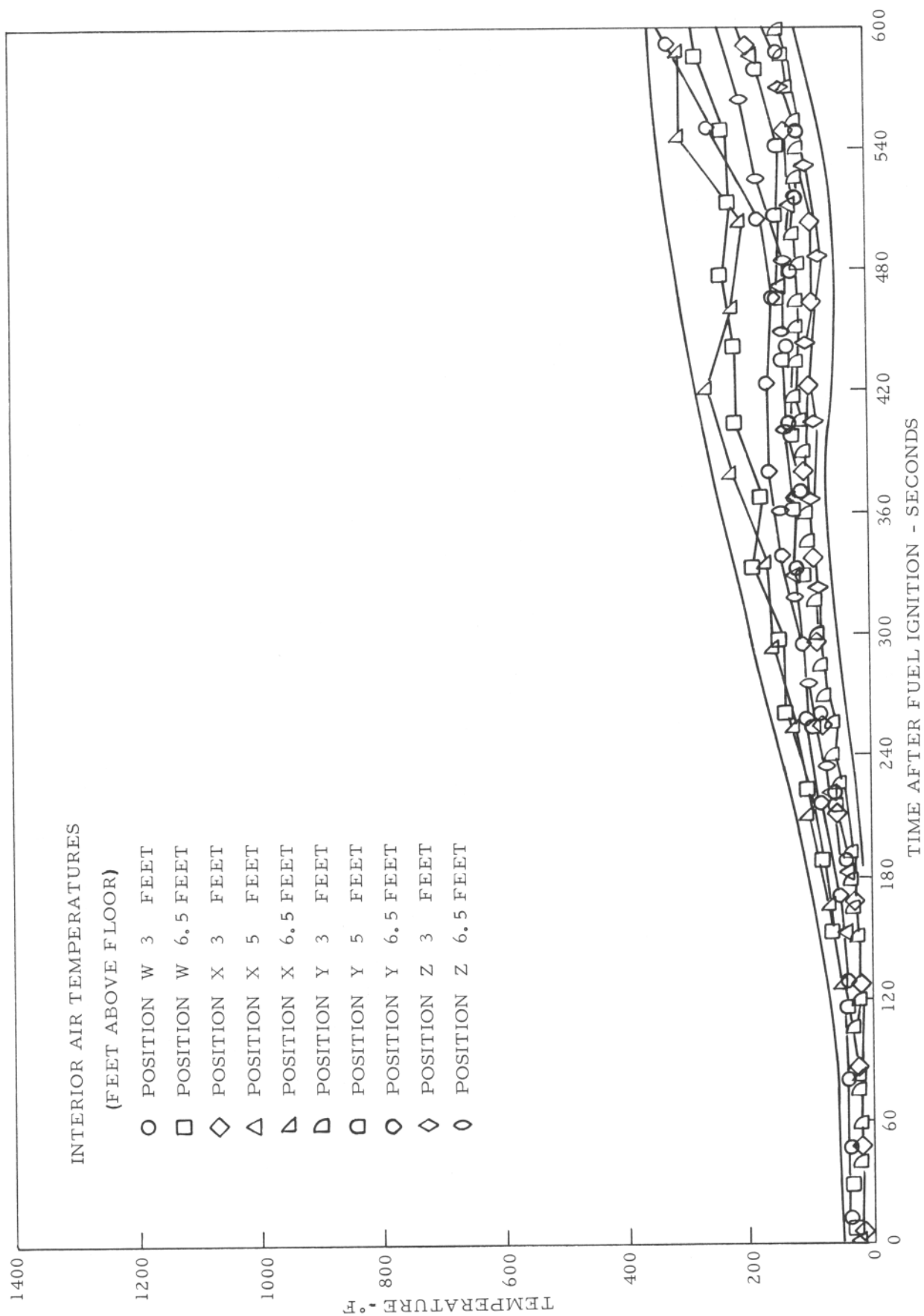


FIGURE C-5. INTERIOR AIR TEMPERATURE AS A FUNCTION OF TIME AFTER FUEL IGNITION

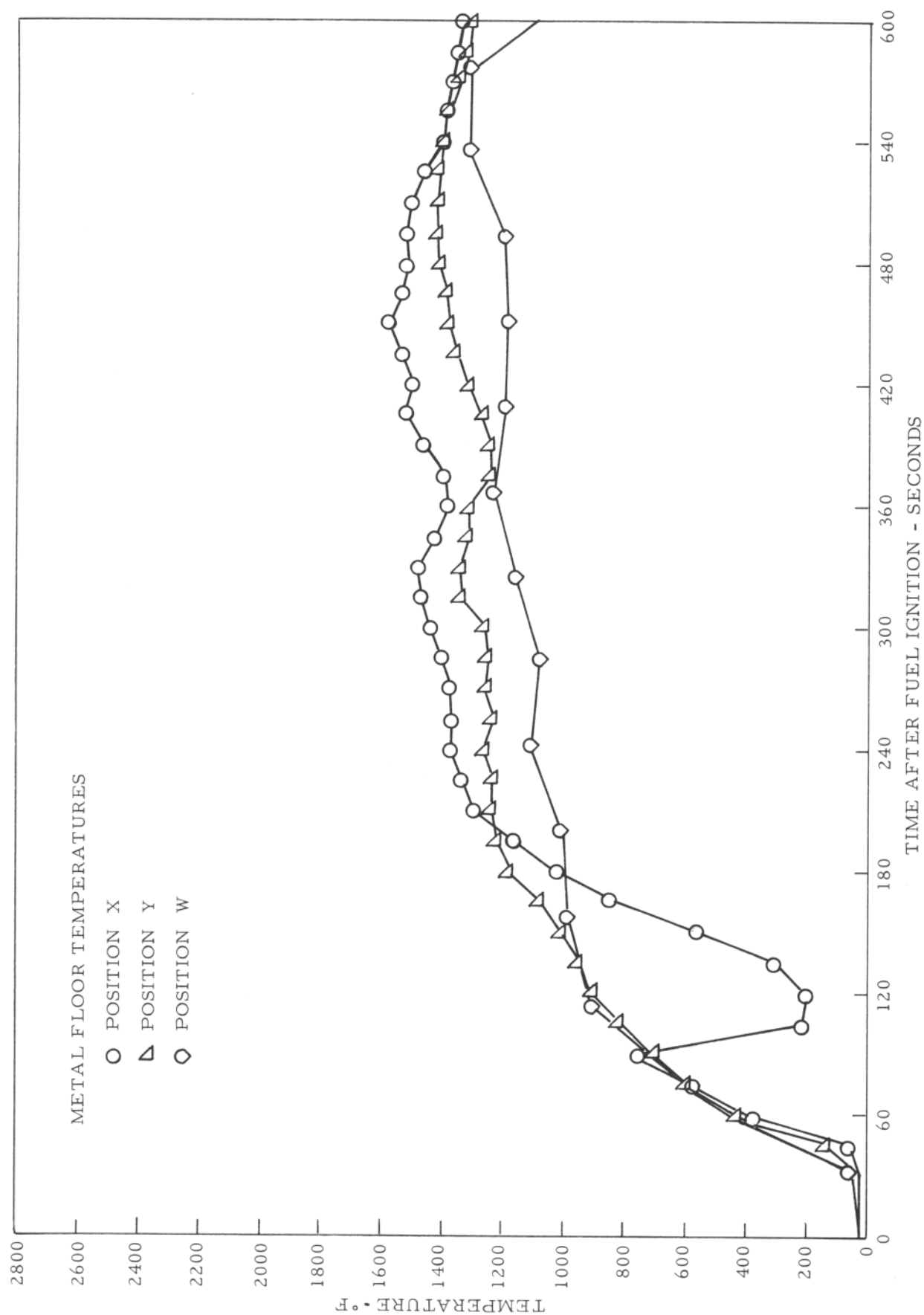


FIGURE C-6. EXTERIOR METAL FLOOR TEMPERATURE AS A FUNCTION OF TIME AFTER FUEL IGNITION

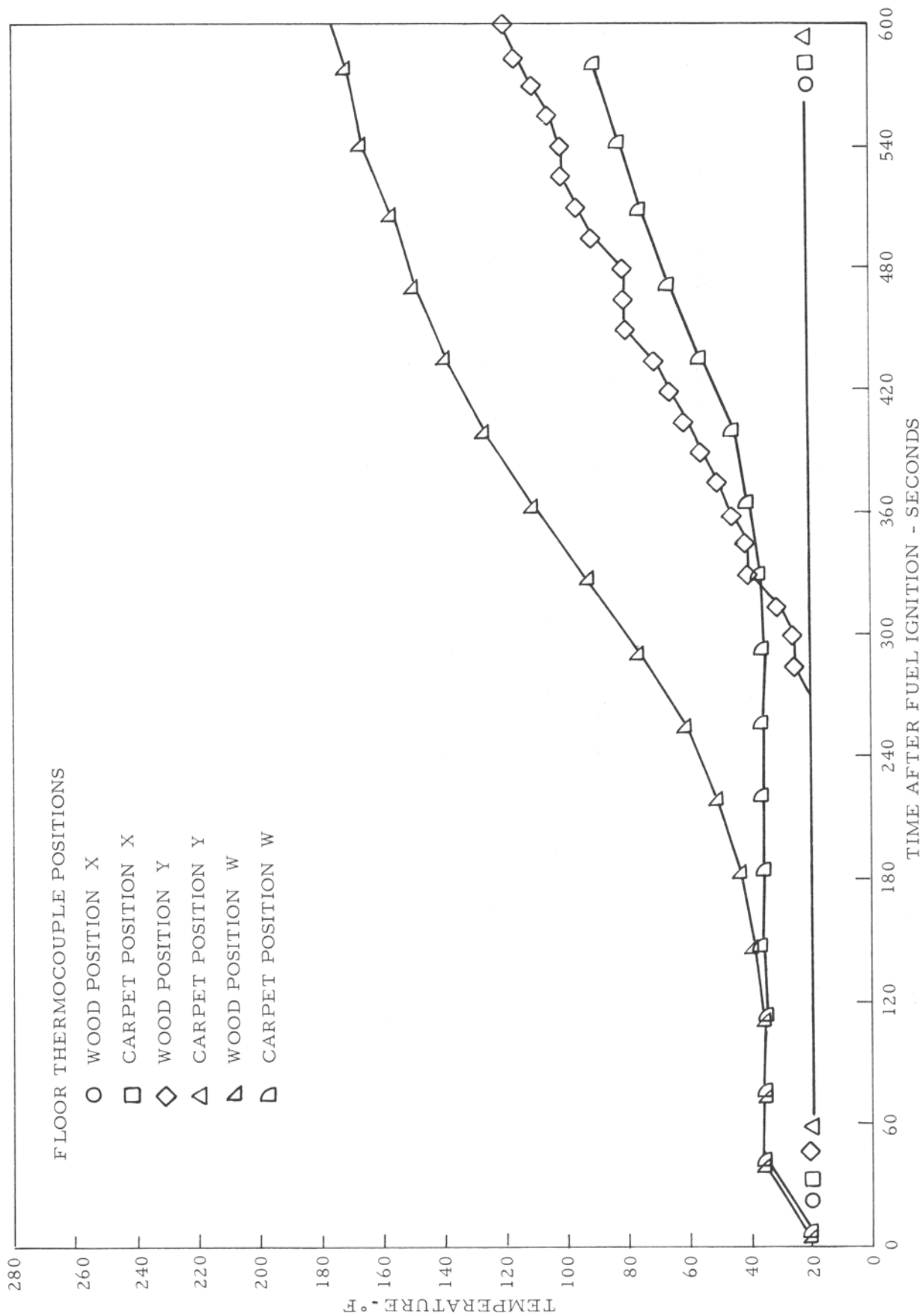


FIGURE C-7. INTERNAL WOOD AND CARPET FLOOR TEMPERATURES

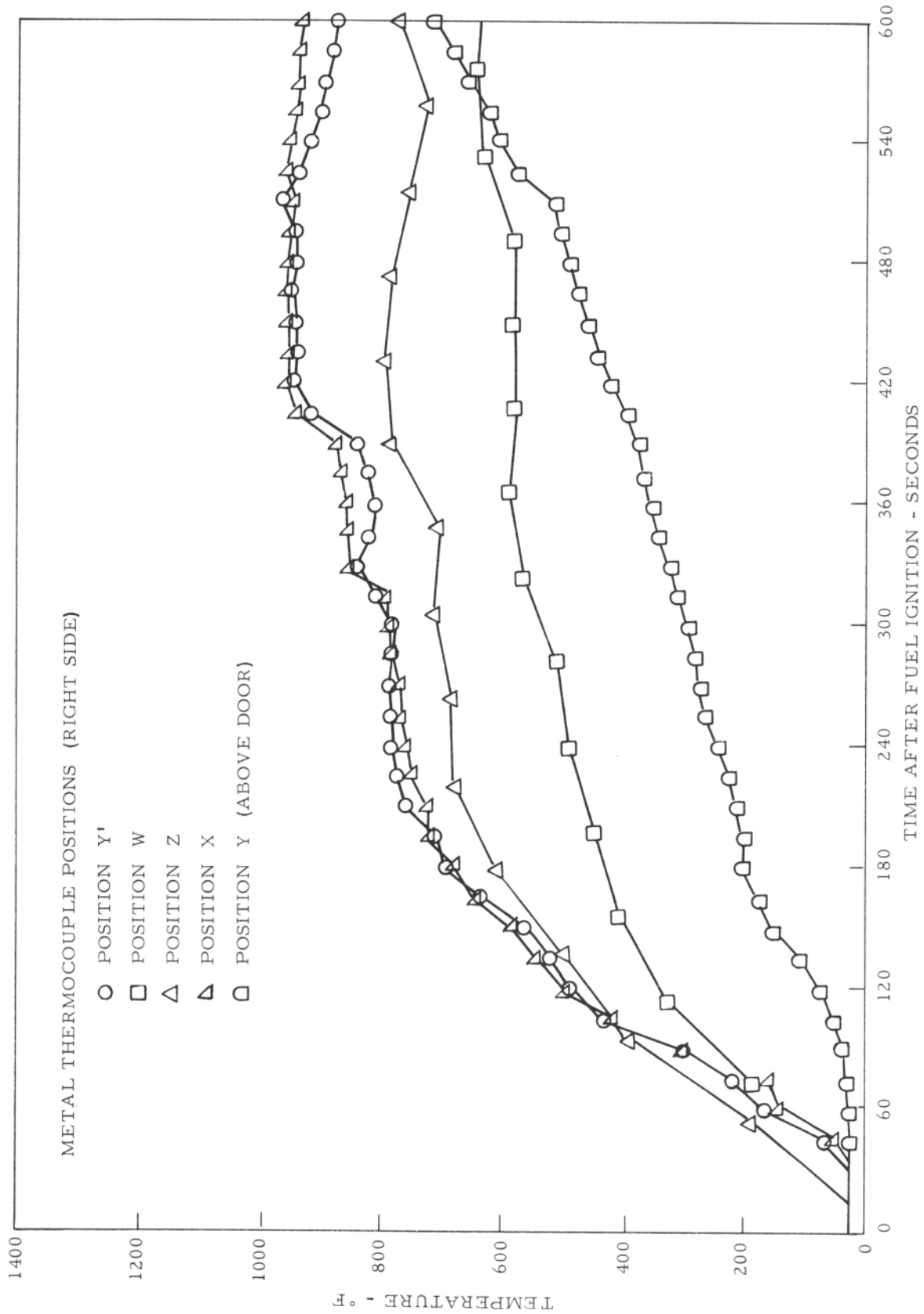


FIGURE C-8. TEMPERATURE ON THE RIGHT SIDE EXTERIOR METAL SURFACE OF THE AIRCRAFT LOADING WALKWAY

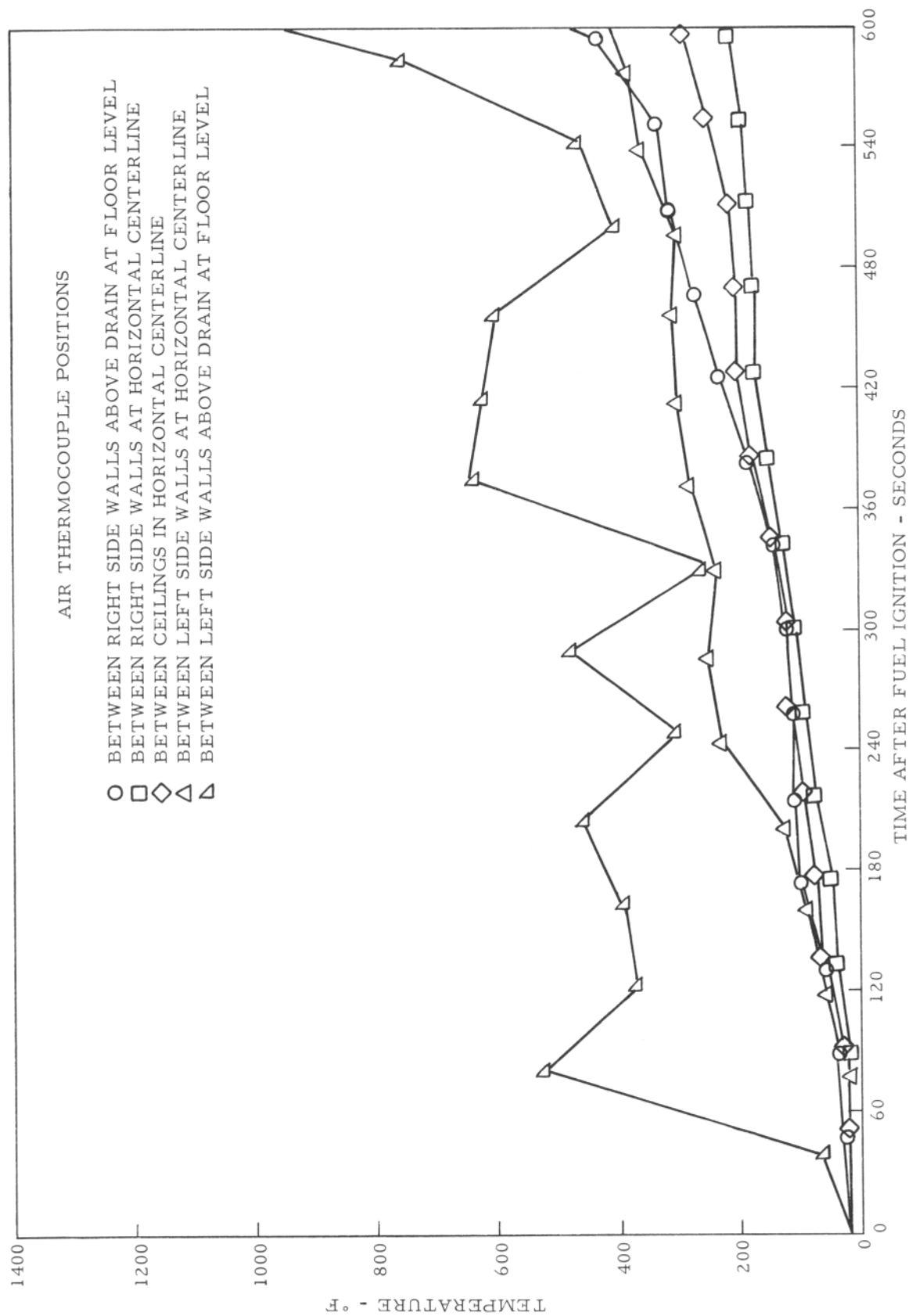


FIGURE C-9. AIR TEMPERATURE AS A FUNCTION OF TIME AFTER FUEL IGNITION IN THE OVERLAP SECTION BETWEEN TUNNELS B AND C





## APPENDIX D

### METALLURGICAL EXAMINATION OF THE AIRCRAFT LOADING WALKWAY MATERIAL

#### GENERAL.

The technical information presented in Appendix D was made available through the Air Transport Association of America (ATA) for inclusion in this document.

A Total of 16 metal samples were removed from the exterior components of the walkway at sites subjected to temperature monitoring during the fire test. The temperatures experienced by these samples ranged from 600° to 1,570°F.

#### SAMPLING PLAN.

Wherever possible samples were removed from the exterior structure at points of thermocouple attachment during the fire test. Specific sampling sites were as follows:

<u>Sample Designation</u>	<u>Material Description</u>	<u>Sample Location</u>	<u>Max. Temperature During Test, °F.</u>
W-1	Sheet Metal	Right side, 23 1/2' from fuselage	640
W-2	Sheet Metal	Left side, 23 1/2' from fuselage	660
W-3	Sheet Metal	Bottom floor pan, 23 1/2' from fuselage	1,380
X-1	Sheet Metal	Right side, 15' from fuselage	1,000
X-2	Sheet Metal	Left side, 15' from fuselage Tunnel C	Not monitored, estimated 780
X-3	Sheet Metal	Bottom floor pan, 15' from fuselage Tunnel C	1,570 (max. temperature developed during test)
Y-1	Sheet Metal	Right side, 10' from fuselage	970
Y-2	Sheet Metal	Left side, 10' from fuselage	900

<u>Sample Designation</u>	<u>Material Description</u>	<u>Sample Location</u>	<u>Max. Temperature During Test, °F.</u>
Y-3	Sheet Metal	Bottom floor pan, 10' from fuselage	1,420
Z-1	Sheet Metal	Right side, 3' from fuselage	780
Z-2	Sheet Metal	Left side, 3' from fuselage	600 (min. temperature developed during test)
Z-3	Sheet Metal	Bottom floor pan, 3' from fuselage	Not monitored. Closest site, Y-3, 1,420.
Z-3	Sheet Metal	Bottom floor pan, 3' from fuselage	Not monitored. Closest site, Y-3, 1,420.
S-1	Structural Member	Longitudinal frame support of floor pan, right side, 15' from fuselage	Estimated 1,250.
S-2	Structural Member	Longitudinal frame support of floor pan, left side, 15' from fuselage	Not monitored.
W-4	Structural Member	Longitudinal angle iron support of floor pan, right side, 25' from fuselage, Tunnel B.	Estimated 600.
W-5	Structural Member	Longitudinal angle iron support of floor pan, left side, 25' from fuselage, Tunnel B.	Estimated 600.

#### SPECIMEN PREPARATION.

MECHANICAL TESTS. Test coupons were taken from sheet metal samples in accordance with ASTM A370, "Mechanical Testing of Steel Products," Sheet Type (2' gauge length, 1/2" wide reduced section) as follows:

1. Longitudinal direction (suffix "a" in attached data sheets).
2. Transverse direction (suffix "b" in attached data sheets).
3. Perpendicular to weld with weld seam at center of reduced section.
4. At base of corrugations (suffix "c" in attached data sheets).
5. At crest of corrugations (suffix "d" in attached data sheets).

NOTE: "c" and "d" specimens could not be obtained on all samples. Test coupons were also taken from the structural specimens, S and W, in the longitudinal direction only.

METALLURGICAL EXAMINATION. Sections were removed from all samples, incorporating both base metal and welds (where present). These were mounted, polished, and suitably etched for microscopic examination. Photomicrographs of typical structural conditions were prepared at 200X magnification.

The mechanical properties of the steel components of the walkway after fire exposure were determined in accordance with American Society for Testing and Materials ASTM A370 and are summarized in Tables D-1 through D-3. The results of the tests in Table D-1 are plotted on Figure D-1. The results of the tests summarized in Table D-2 are plotted in Figure D-2.

Detailed test data are presented in Tables D-4 through D-16.

TABLE D-1. CORRUGATED SHEET METAL MECHANICAL TESTS

<u>Specimen Group</u>	<u>Tensile Strength, psi. average</u>	<u>Yield Strength, psi. average</u>	<u>Elongation, Avg. pct.</u>	<u>Max. Temperature During Tests °F</u>
W-1	47,000	38,400	33.3	640
W-2	47,100	40,400	27.7	660
W-3	49,800	36,900	34.5	1,380
X-1	50,700	42,600	26.0	1,000
X-2	51,300	41,700	20.3	780 Est.
X-3	47,300	35,500	26.0	1,570
Y-1	51,900	42,300	19.8	970
Y-2	48,500	41,300	24.6	900
Y-3	49,700	36,100	30.5	1,420
Z-1	51,700	43,500	28.0	780
Z-2	56,000	44,300	26.5	600
Z-3	48,900	38,400	30.0	1,420 Est.

Note: The above results are plotted on Figure D-1.

TABLE D-2. CORRUGATED SHEET METAL WELDS

<u>Specimen Group</u>	<u>Tensile Strength, psi. Avg.</u>	<u>Max. Temperature During Tests °F</u>
W-1	48,700	640
W-2	48,900	660
W-3	51,000	1,380
X-1	51,750	1,000
X-2	49,800	780 Est.
X-3	44,400	1,570
Y-1	50,600	970
Y-2	51,800	900
Y-3	47,500	1,420

Z group: No welds present.

Note: These results are plotted in Figure D-2

TABLE D-3. STEEL STRUCTURAL MEMBERS

	<u>Tensile Strength, psi.</u>	<u>Yield Strength, psi.</u>	<u>Elongation in 2" pct.</u>
S-1	57,500	40,800	28.0
S-2	52,000	36,100	25.0
W-4	154,000	148,000	16.0
W-5	160,000	152,000	14.0

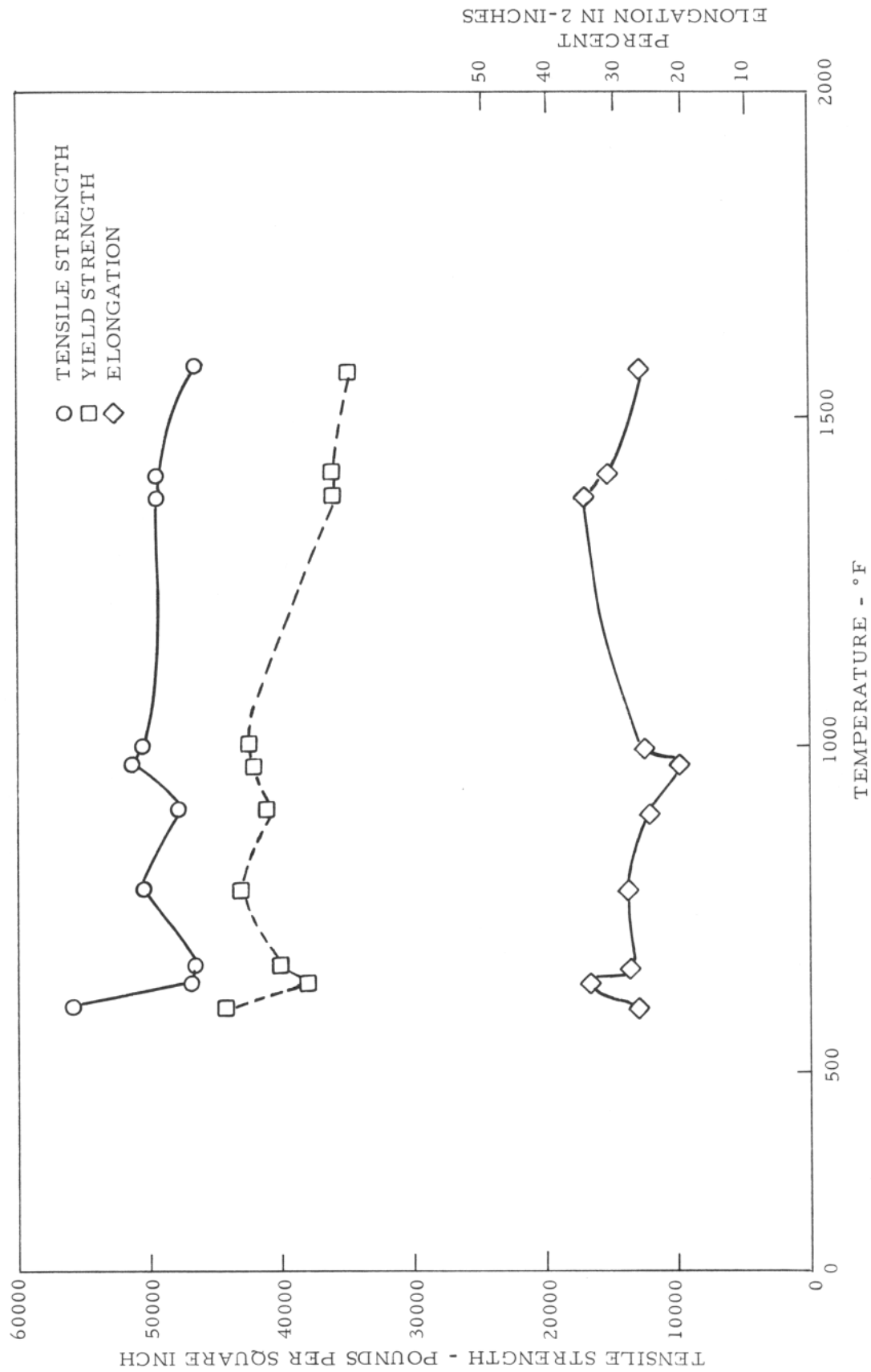


FIGURE D-1. AVERAGE MECHANICAL PROPERTIES OF THE CORRUGATED STEEL AS FUNCTIONS OF TEMPERATURE

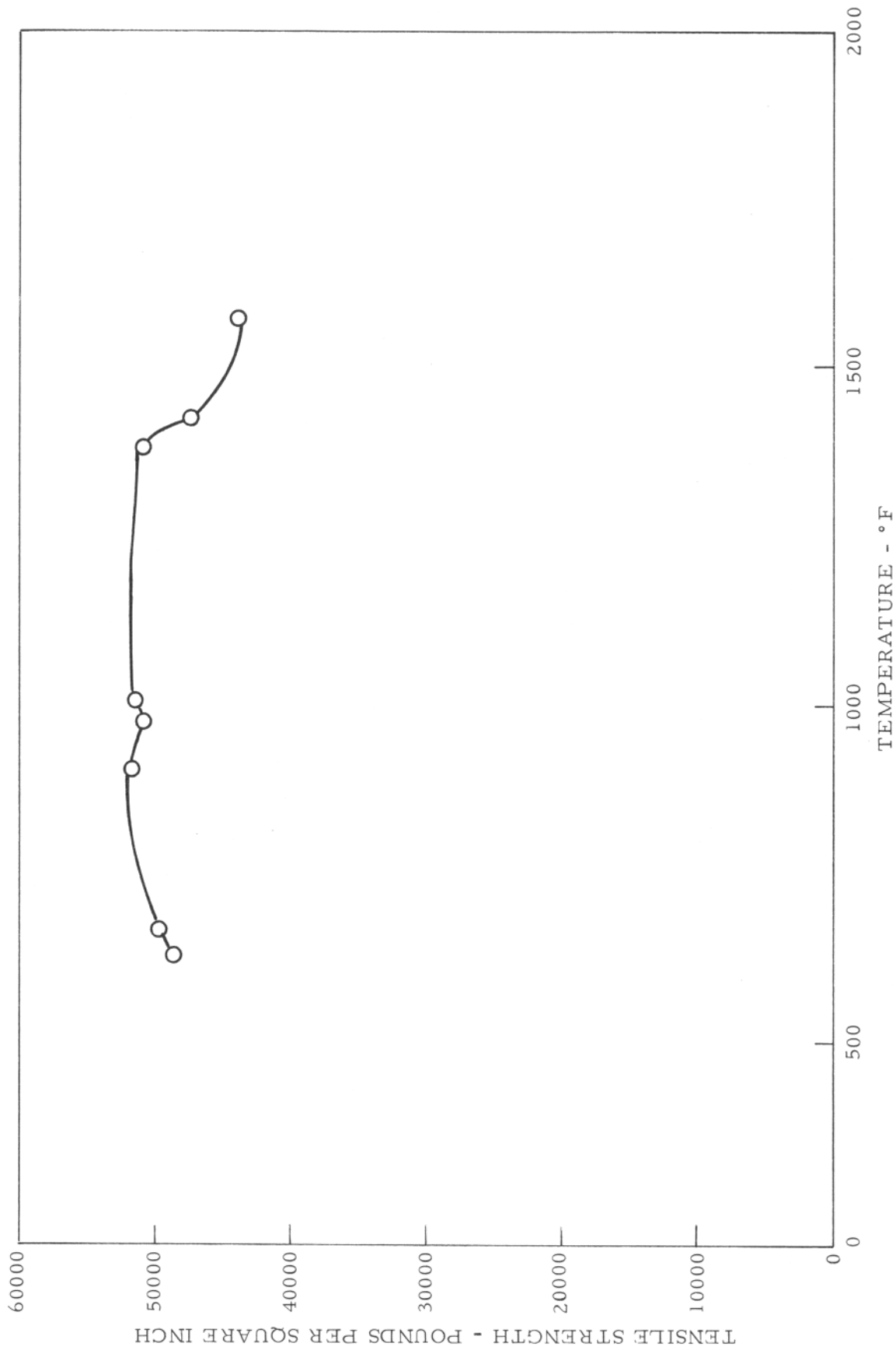


FIGURE D-2. TENSILE STRENGTH OF WELDED SEAMS AS A FUNCTION OF TEMPERATURE



TABLE D-4. TUNNEL B, MECHANICAL PROPERTIES OF THE CORRUGATED STEEL (Right Side)

Sample Identification: Tunnel B, Right Side, Location W-1  
Centerline, 23'6" From Fuselage  
Maximum Temperature Experienced: 640°F

Specimen	W-1, a	W-1, b	W-1, c	W-1, (Weld)
Width, in.	.503	.495	.495	.504
Thickness, in.	.062	.062	.061	.062
Area, sq. in.	.0312	.0307	.0317	.031
Yield Load, lbs.	1,260	1,175	1,160	-
Yield Strength, psi.	40,400	38,300	36,600	-
Breaking Load, lbs.	1,523	1,450	1,433	1,510
Tensile Strength, psi.	48,800	47,200	45,200	48,700
Elongation in 2", pct.	35	27	38	-
Yield Strength				
Avg. psi.*	38,400			
Tensile Strength				
Avg. psi.*	47,000			
Elong. Avg. pct.*	33.3			

\*Not including weld specimens.

TABLE D-5. TUNNEL B, MECHANICAL PROPERTIES OF THE CORRUGATED STEEL (Left Side)

Sample Identification: Tunnel B, Left Side, Location W-2  
Centerline, 23' 6" From Fuselage  
Maximum Temperature Experienced: 660°F

Specimen	W-2, a	W-2, b	W-2, c	W-2, (Weld)	W-2, (Weld)
Width, in.	.503	.505	.502	.511	.519
Thickness in.	.062	.061	.061	.061	.061
Area, sq. in.	.0312	.0308	.0306	.031	.032
Yield Load, lbs.	1,190	1,320	1,230	-	-
Yield Strength, psi	38,100	42,900	40,200	-	-
Breaking Load, lbs.	1,458	1,462	1,440	1,510	1,570
Tensile Strength, psi.	46,700	47,500	47,100	48,700	49,100
Elongation In 2", pct.	30	27	26	-	-
Yield Strength					
Avg. psi.*	40,400				
Tensile Strength					
Avg. psi*	37,100				
Elong. Avg. pct.*	27.7				

\*Not including weld specimens.

TABLE D-6. TUNNEL B, MECHANICAL PROPERTIES OF THE CORRUGATED STEEL (Bottom)

Sample Identification: Tunnel B, Bottom, Location W-3, 23' 6" From Fuselage  
Maximum Temperature Experienced: 1,380°F

Specimen	W-3, a	W-3, b	W-3, (Weld)
Width, in.	.505	.509	.499
Thickness, in.	.061	.061	.059
Area, sq. in.	.0308	.0310	.029
Yield Load, lbs.	1,140	1,140	-
Yield Strength, psi.	37,000	36,800	-
Breaking Load, lbs.	1,528	1,548	1,480
Tensile Strength, psi.	49,600	49,900	51,030
Elongation in 2", pct.	37	32	-

Yield Strength	
Avg. psi.*	36,900
Tensile Strength	
Avg. psi.*	49,800
Elong. Avg. pct.*	34.5

\*Not including weld specimens.

TABLE D-7. TUNNEL C, MECHANICAL PROPERTIES OF THE CORRUGATED STEEL (Right Side)

Sample Identification: Tunnel C, Right Side, Location X-1,  
15 Feet From Fuselage  
Maximum Temperature Experienced: 1,000°F

Specimen	X-1, a	X-1, b	X-1, c	X-1, (Weld)	X-1, (Weld)
Width, in.	.503	.507	.501	.501	.487
Thickness, in.	.065	.065	.065	.063	.063
Area, sq. in.	.0327	.0330	.0326	.032	.031
Yield Load, lbs.	1,350	1,400	1,440	-	-
Yield Strength, psi.	41,300	42,400	44,200	-	-
Breaking Load, lbs.	1,676	1,642	1,662	1,640	1,620
Tensile Strength, psi.	51,300	49,800	51,000	51,250	52,250
Elongation in 2", pct.	28	25	25	-	-

Yield Strength	
Avg. psi.*	42,600
Tensile Strength	
Avg. psi.*	50,700
Elong. Avg. pct.*	26.0

\*Not including weld specimens.

TABLE D-8. TUNNEL C, MECHANICAL PROPERTIES OF THE CORRUGATED STEEL (Left Side)

Sample Identification: Tunnel C, Left Side, Location X-2  
15' From Fuselage,

Maximum Temperature Experienced : Not Recorded  
(Estimated 780°F)

Specimen	X-2, a	X-2, b	X-2, c	X-2, (Weld)	X-2, (Weld)
Width, in.	.500	.503	.501	.516	.516
Thickness, in.	.065	.064	.064	.063	.064
Area, sq. in.	.0325	.0322	.0321	.033	.033
Yield Load, lbs.	1,400	1,340	1,300	-	-
Yield Strength, psi.	43,100	41,600	40,500	-	-
Breaking Load, lbs.	1,710	1,612	1,630	1,660	1,620
Tensile Strength, psi.	52,600	50,100	50,800	50,300	49,100
Elongation in 2", pct.	14	26	21	-	-
Yield Strength					
Avg. psi.*	41,700				
Tensile Strength					
Avg. psi.*	51,300				
Elong. Avg. pct.*	20.3				

\*Not including weld specimens.

TABLE D-9. TUNNEL C, MECHANICAL PROPERTIES OF THE CORRUGATED STEEL (Bottom)

Sample Identification: Tunnel C, Bottom, Location X-3  
15' From Fuselage

Maximum Temperature Experienced: 1,570°F

Specimen	X-3, a	X-3, b	X-3, (Weld)
Width, in.	.504	.502	.496
Thickness, in.	.064	.064	.064
Area, sq. in.	.0323	.0321	.032
Yield Load, lbs.	1,140	1,150	-
Yield Strength, psi.	35,300	35,800	-
Breaking Load, lbs.	1,538	1,510	1,420
Tensile Strength, psi.	47,600	47,000	44,400
Elongation in 2", pct.	30	32	-

Yield Strength	
Avg. psi.*	35,550
Tensile Strength	
Avg. psi.*	47,300
Elong. Avg. pct.*	26

\*Not including weld specimens.

TABLE D-10. TUNNEL C, MECHANICAL PROPERTIES OF THE CORRUGATED STEEL (Right Side)

Sample Identification: Tunnel C, Right Side Location Y'-1

Centerline, 10' From Fuselage

Maximum Temperature Experienced: 970°F

Specimen:	Y'-1, a	Y'-1, b	Y'-1, c	Y'-1, d	Y'-1, (Weld)	Y'-1, (Weld)
Width, in.	.503	.505	.500	.497	.504	.510
Thickness, in.	.068	.066	.067	.067	.068	.067
Area, sq. in.	.0342	.0333	.0335	.0333	.034	.034
Yield Load lbs.	1,490	1,520	1,380	1,350	-	-
Yield Strength, psi.	43,600	45,600	39,400	40,500	-	-
Breaking Load, lbs.	1,740	1,817	1,694	1,714	1,720	1,720
Tensile Strength, psi.	50,900	50,600	50,600	51,500	50,600	50,600
Elongation in 2", pct.	16	17	28	18	-	-

Yield Strength Avg. psi.\* 42,300

Tensile Strength Avg. psi.\* 51,900

Elong. Avg. pct.\* 19.8

\*Not including weld specimens.

TABLE D-11. TUNNEL C, MECHANICAL PROPERTIES OF THE CORRUGATED STEEL (Left Side)

Sample Identification: Tunnel C, Left Side, Location Y'-2

10' From Fuselage

Maximum Temperature Experienced: 900°F

Specimen	Y-2, a	Y-2, b	Y-2, c	Y-2, (Weld)	Y-2, (Weld)
Width, in.	.500	.501	.500	.504	.507
Thickness, in.	.065	.066	.066	.064	.065
Area, sq. in.	.0325	.0331	.0330	.032	.033
Yield Load, lbs.	1,280	1,310	1,500	-	-
Yield Strength, psi.	39,400	39,600	45,000	-	-
Breaking Load, lbs.	1,562	1,602	1,620	1,680	1,690
Tensile Strength, psi.	48,100	48,400	49,100	52,500	51,200
Elongation in 2", pct.	25	25	24	-	-

Yield Strength

Avg. psi.\* 41,300

Tensile Strength

Avg. psi.\* 48,500

Elong. Avg. pct.\* 24.6

\*Not including weld specimens.

TABLE D-12. TUNNEL C, MECHANICAL PROPERTIES OF THE CORRUGATED STEEL (Bottom)

Sample Identification: Tunnel C, Bottom, Location Y-3  
 10' From Fuselage  
 Maximum Temperature Experienced: 1,420°F

Specimen	Y-3, a	Y-3, b	Y-3, (Weld)
Width, in.	.502	.504	.502
Thickness, in.	.067	.065	.064
Area, sq. in.	.0336	.0328	.032
Yield Load, lbs.	1,200	1,200	-
Yield Strength, psi.	35,700	36,600	-
Breaking Load, lbs.	1,662	1,640	1,520
Tensile Strength, psi.	49,500	50,000	47,500
Elongation in 2", pct.	25	36	-

Yield Strength	
Avg. psi.*	36,150
Tensile Strength	
Avg. psi.*	49,750
Elong. Avg. pct.*	30.5

\*Not including weld specimens.

TABLE D-13. TUNNEL C, MECHANICAL PROPERTIES OF THE CORRUGATED STEEL (Right Side)

Sample Identification: Tunnel C, Right Side, Location Z-1  
 3' From Fuselage  
 Maximum Temperature Experienced: 780°F

Specimen	Z-1, a	Z-1, b	Z-1, c	Z-1, d
Width, in.	.498	.500	.507	.499
Thickness, in.	.068	.068	.069	.069
Area, sq. in.	.0339	.0340	.0350	.0344
Yield Load, lbs.	1,520	1,440	1,520	1,480
Yield Strength, psi.	44,800	42,400	43,400	43,000
Breaking Load, lbs.	1,778	1,760	1,787	1,774
Tensile Strength, psi.	52,400	51,800	51,100	51,600
Elongation in 2", pct.	33	24	29	28

Yield Strength	
Avg. psi.	43,500
Tensile Strength	
Avg. psi.	51,700
Elong. Avg. pct.	28

No weld on this specimen.

TABLE D-14. TUNNEL C, MECHANICAL PROPERTIES OF THE CORRUGATED STEEL (Left Side)

Sample Identification: Tunnel C, Left Side, Location Z-2  
 3' From Fuselage  
 Maximum Temperature Experienced: 600°F

Specimen	Z-2, a	Z-2, b
Width, in.	.514	.493
Thickness, in.	.107	.108
Area, sq. in.	.0550	.0532
Yield Load, lbs.	2,440	2,350
Yield Strength, psi.	44,400	44,200
Breaking Load, lbs.	3,110	2,950
Tensile Strength, psi.	56,500	55,500
Elongation in 2", pct.	29	24
Yield Strength Avg. psi.	44,300	
Tensile Strength Avg. psi.	56,000	
Elong. Avg. pct.	26.5	

No weld on this specimen.  
 Heavier gauge than other skin specimens.

TABLE D-15. TUNNEL C, MECHANICAL PROPERTIES OF THE CORRUGATED STEEL (Bottom)

Sample Identification: Tunnel C, Bottom Location Z-3  
 3' From Fuselage  
 Maximum Temperature not recorded  
 Temperature at closest measuring point (Y) 1,420°F

Specimen	Z-3, a	Z-3, b
Width, in.	.511	.501
Thickness, in.	.062	.062
Area, sq. in.	.0317	.0311
Yield Load, lbs.	1,200	1,210
Yield Strength, psi.	37,900	38,900
Breaking Load, lbs.	1,513	1,558
Tensile Strength, psi.	47,700	50,100
Elongation in 2", pct.	24	36
Yield Strength, Avg. psi.	38,400	
Tensile Strength, Avg. psi.	48,900	
Elong. Avg. pct.	30	

No weld on this specimen.

TABLE D-16. TUNNEL C, MECHANICAL PROPERTIES OF THE CORRUGATED STEEL  
(Structural Members)

Sample Identification:

1. Samples S-1 and S-2 taken from longitudinal frame of floor pan, Tunnel C, 15' from fuselage, right and left side, respectively. Maximum temperature estimated to be 1,280°F for right side specimen.
2. Samples W-4 and W-5 taken from structural angle iron supports of floor of Tunnel B, right and left side, respectively, approximately 25' from fuselage. Maximum temperature estimated to be 1,000°F for right side specimen.

Specimen	S-1, (Right)	S-2, (Left)	W-4, (Right)	W-5, (Left)
Width, in.	.512	.501	.507	.509
Thickness, in.	.104	.104	.375	.375
Area, sq. in.	.0532	.0521	.190	.189
Yield Load, lbs.	2,170	1,880	28,100	28,800
Yield Strength, psi.	40,800	36,100	148,000	152,000
Breaking Load, lbs.	3,060	2,710	29,350	30,200
Tensile Strength, psi.	57,500	52,000	154,000	160,000
Elongation in 2", pct.	28	25	16	14





## APPENDIX E

### SMALL-SCALE FIRE TESTS ON AIRCRAFT LOADING WALKWAY PANEL SECTIONS

#### TEST EQUIPMENT.

The test equipment comprised a rectangular steel housing open at one end over which the test panel was bolted forming a seal over the opening prior to being subjected to flame impingement from the 2-gallon-per-hour kerosene burner (Figure E-1). The kerosene burner is described in FAA Power Plant Engineering Report No. 3 and produces a  $2,000^{\circ} \pm 100^{\circ}\text{F}$  flame temperature with a measured total heat flux of 16.3 Btu per square foot per second of which 11.7 Btu per second is radiative and 4.6 Btu per square foot per second is convective. The burner flame nozzle configuration is a 6- by 11-inch ellipse.

The thermal output provided by the burner approximates the conditions developed by aviation fuel-spill fires, although the steady state conditions inherent in the kerosene burner are seldom realized in large outdoor free-burning pool fires.

#### INSTRUMENTATION.

The instrumentation monitoring system included thermocouples for measuring the burner flame temperature, outer shell, and interior surface temperatures of the test panel and inside air temperature of the steel housing. Flame temperature measurements were made using 22 AWG chromel/alumel thermocouples. The corrugated steel shell, interior surface and the inside ambient air temperatures were measured using 30 AWG chromel/alumel thermocouples. Temperature measurements were continuously recorded on four Bristol Model 760 Strip Chart Dynamaster Recorders.

Smoke density measurements within the housing were made in accordance with "Method for Measuring Smoke from Burning Materials," Technical Report No. 422, 1967, Published by the American Society for Testing and Materials.

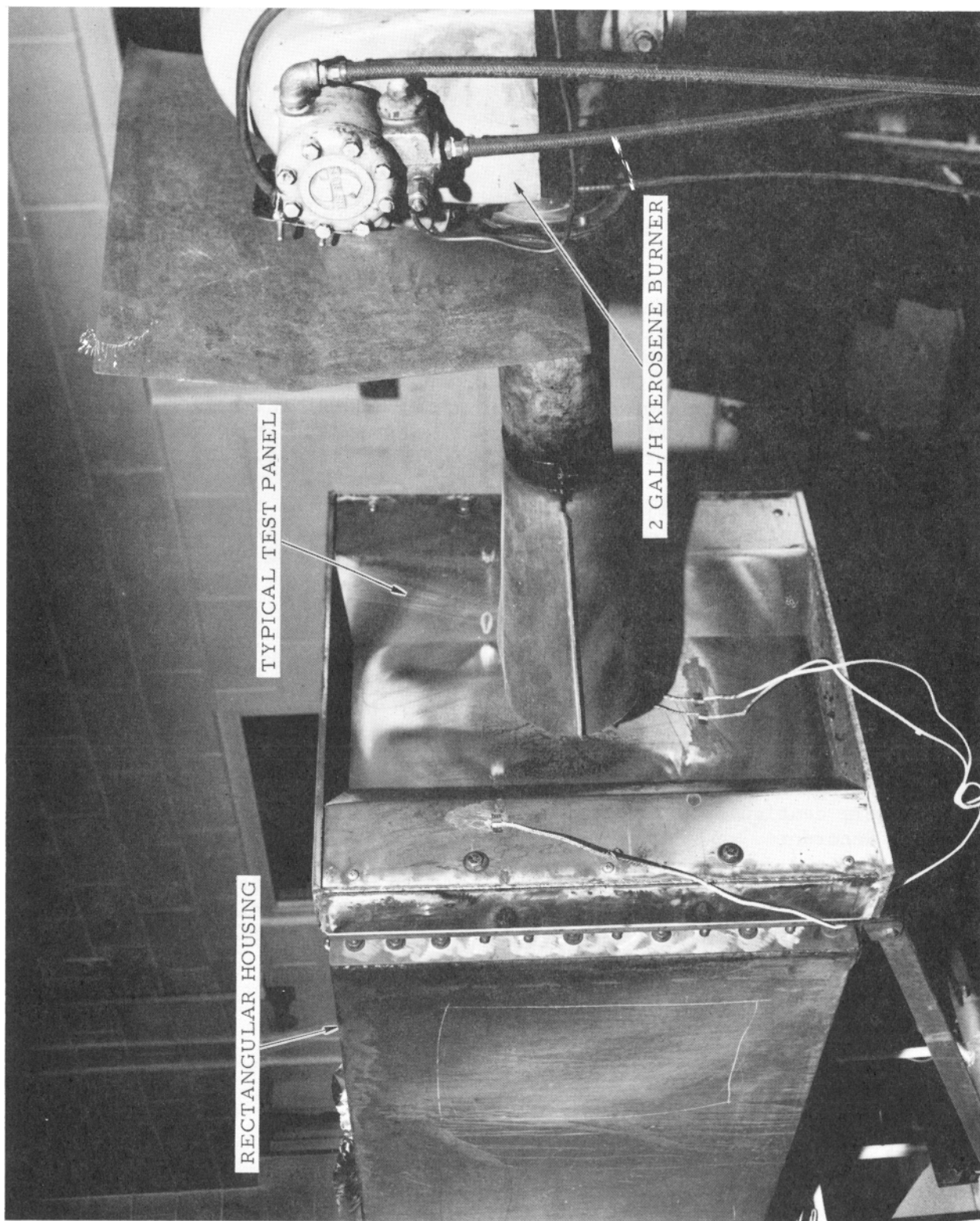


FIGURE E-1. FIRE TEST SETUP FOR EVALUATION OF AIRCRAFT LOADING WALKWAY PANELS

APPENDIX F

MODIFIED FLOOR PANEL CONFIGURATIONS AND

FIRE TEST RESULTS



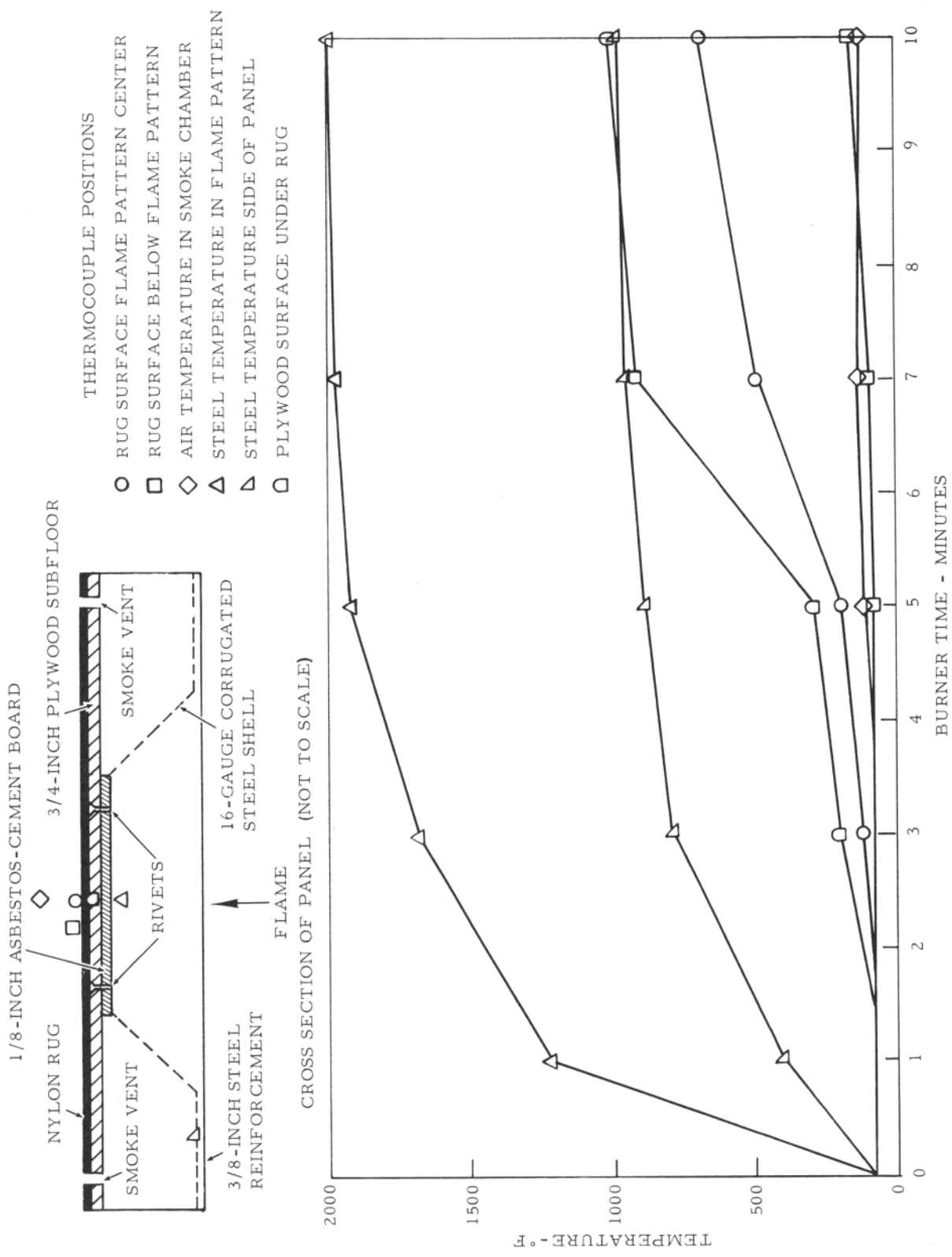


FIGURE F-1. TEST 1 - FLOOR PANEL CONFIGURATION AND THERMAL PROFILES

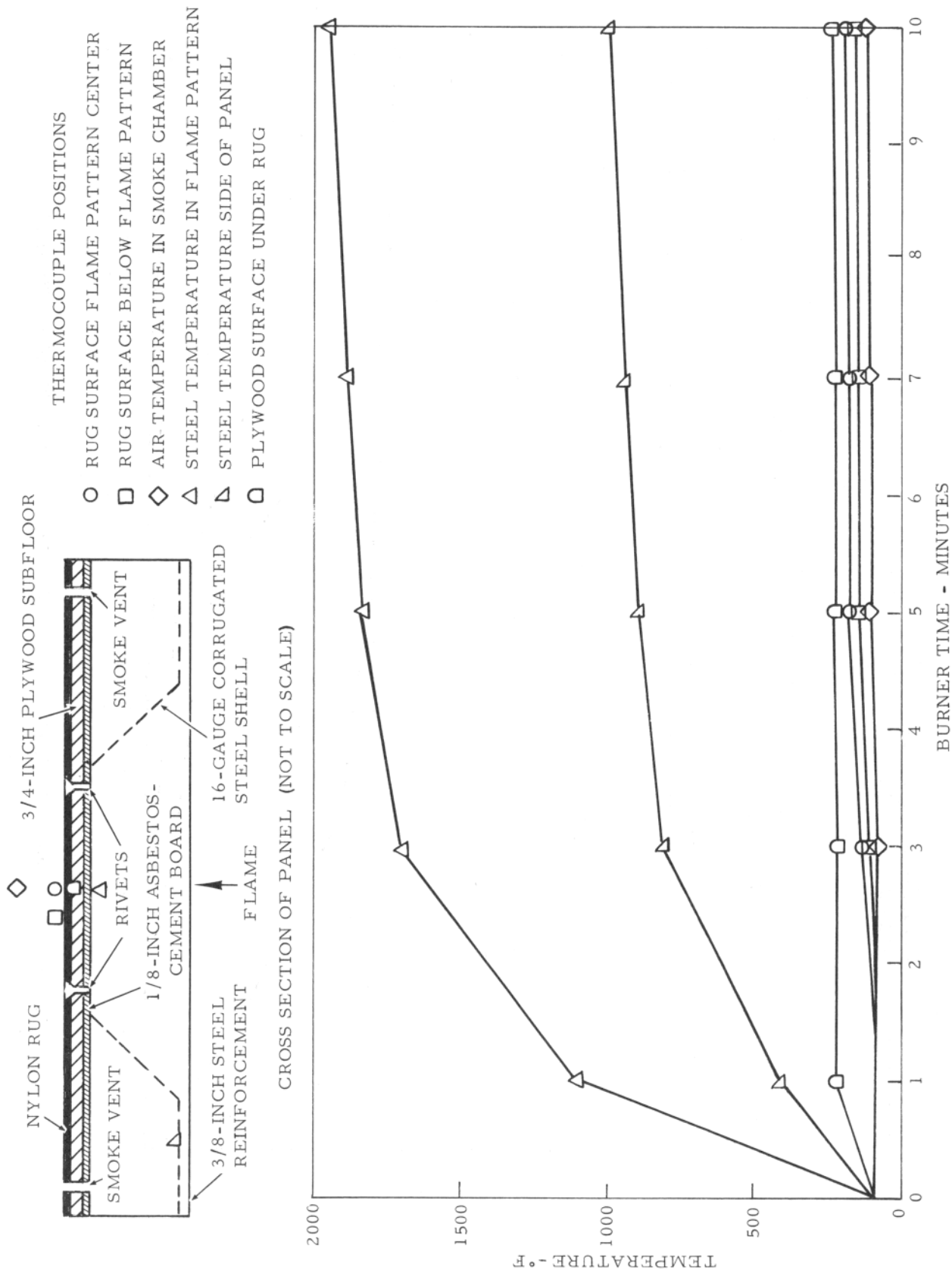


FIGURE F-2. TEST 2 - FLOOR PANEL CONFIGURATION AND THERMAL PROFILES

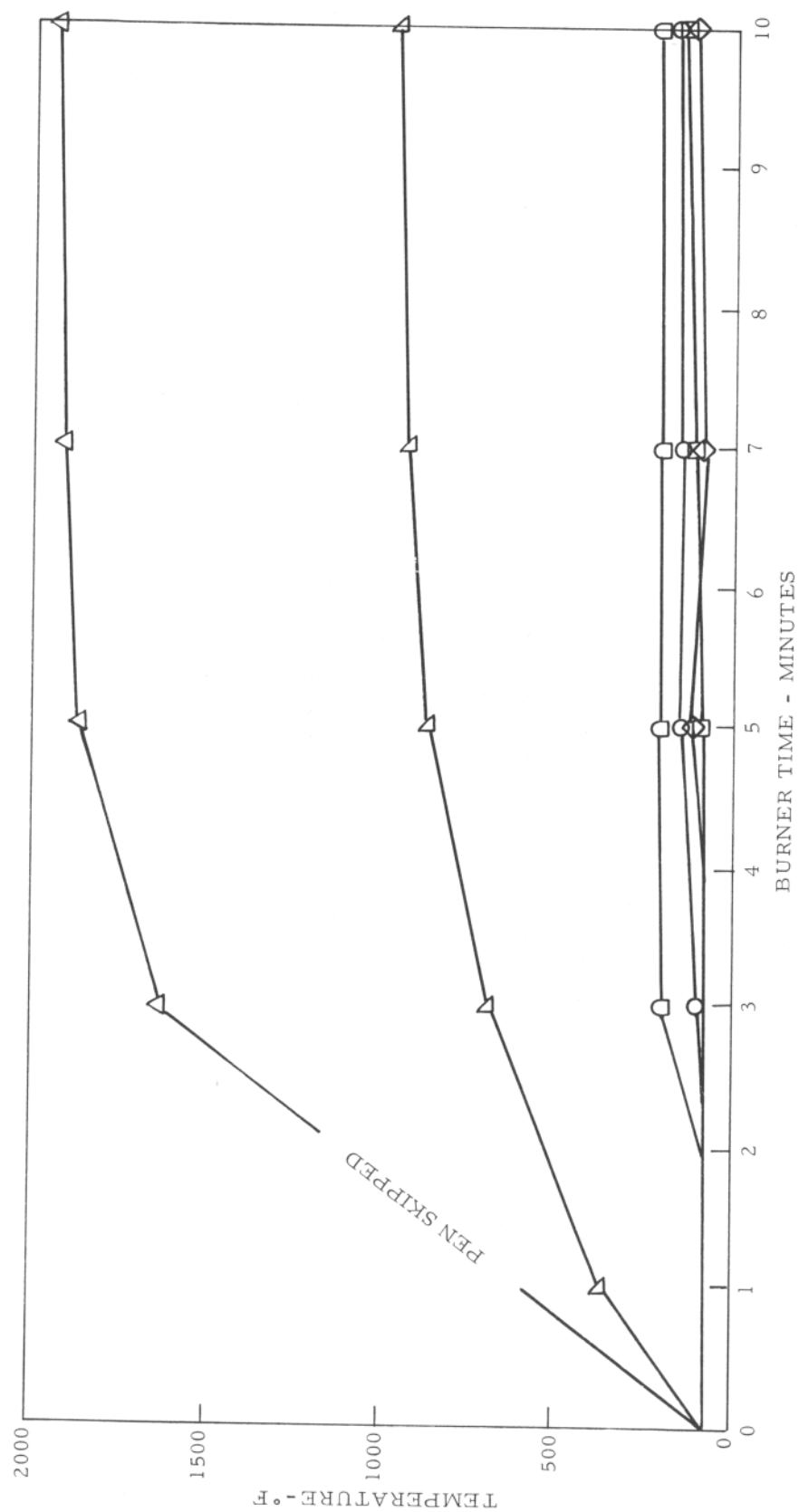
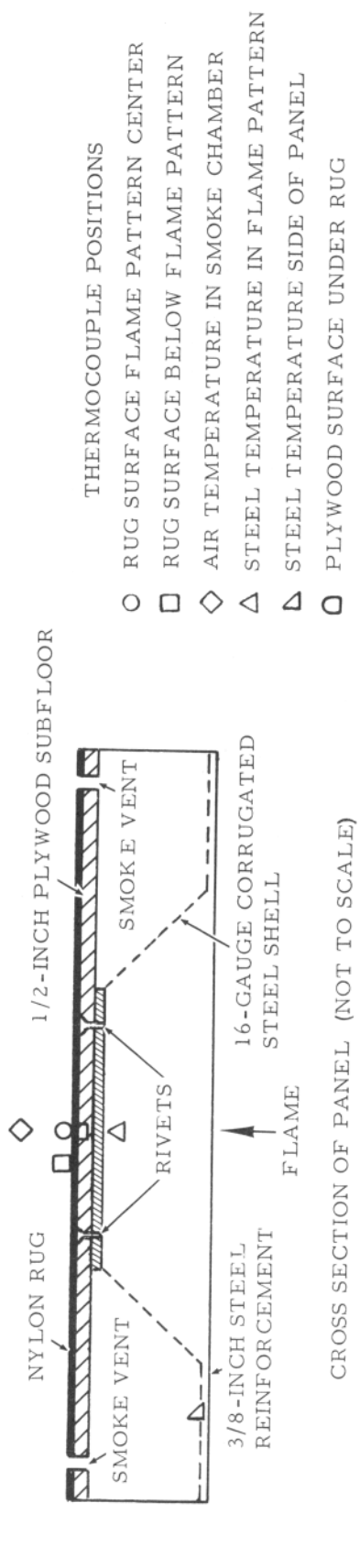
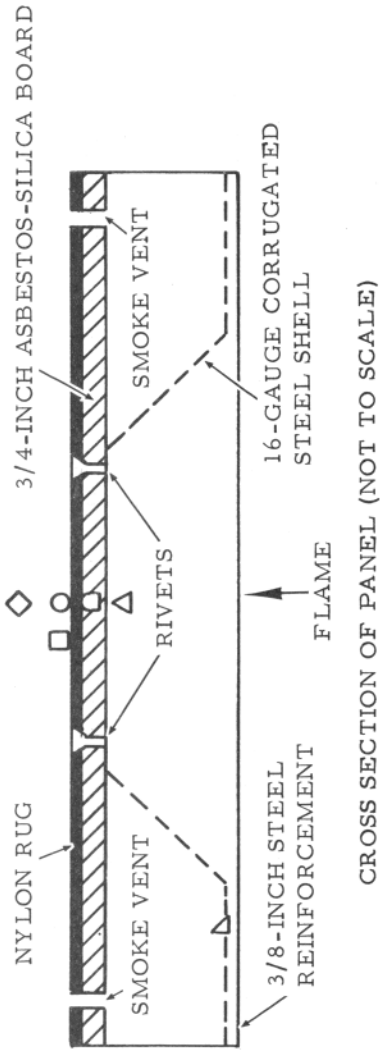


FIGURE F-3. TEST 3 - FLOOR PANEL CONFIGURATION AND THERMAL PROFILES



CROSS SECTION OF PANEL (NOT TO SCALE)

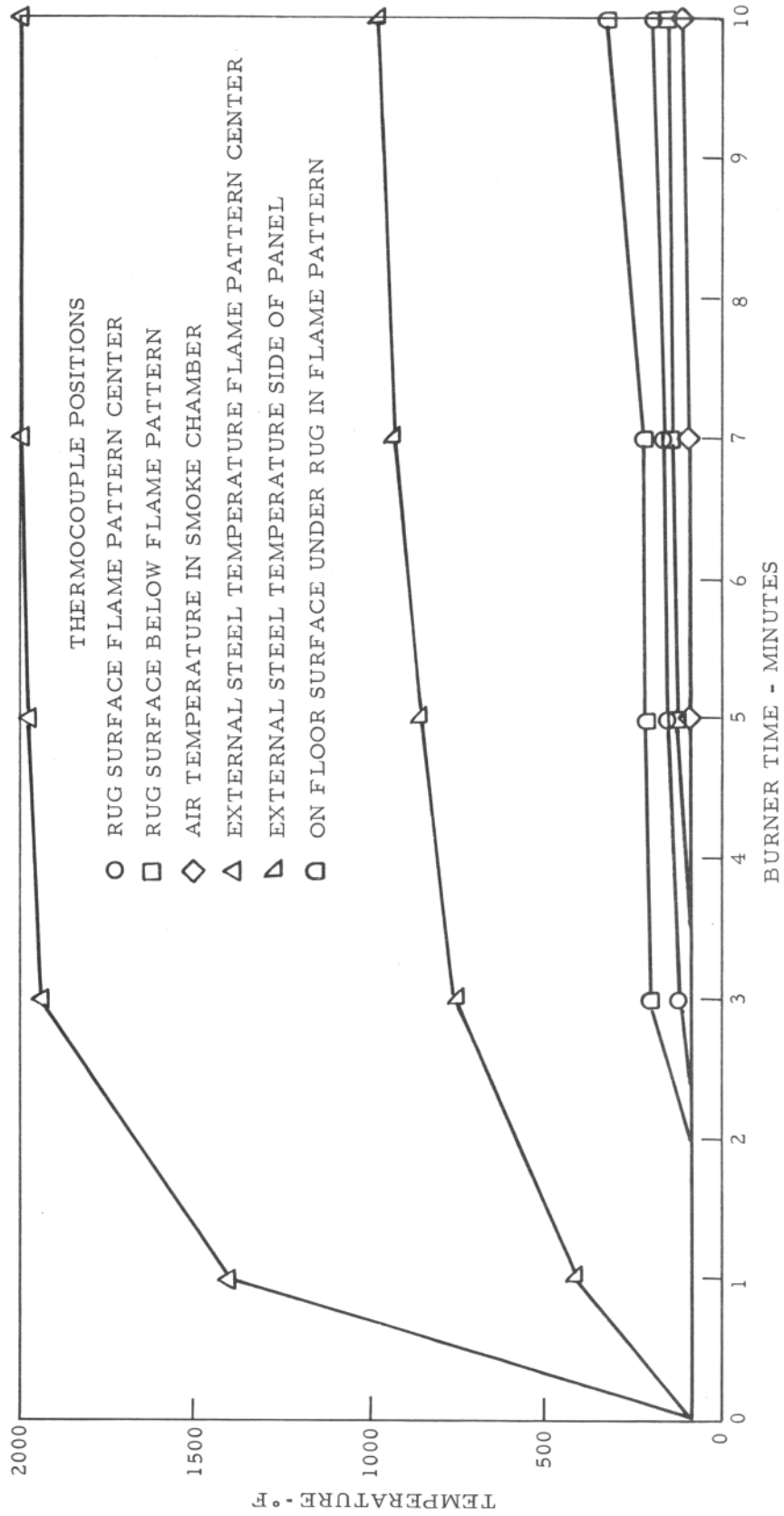


FIGURE F-4. TEST 4 - FLOOR PANEL CONFIGURATION AND THERMAL PROFILES